



国际木材解剖学家协会（IAWA）中国分会  
第八届学术研讨会

**The 8th IAWA China Group Annual Meeting**

**Meeting Agenda**

论  
文  
摘  
要

四川 成都

2021年11月13日-14日

Chengdu

November 13-14th, 2021

## 目 录

基于 <i>LaRAV1-LaCDKB1;3</i> 模块解析温度调控落叶松休眠解除的机制.....	4
Artificial wood cell wall as a valid tool to investigate wood formation and application.....	6
气候变暖正威胁高海拔喜马拉雅桦树林：来自木材解剖与形成层物候的证据.....	8
iWood：基于卷积神经网络的木材图像智能鉴定系统.....	10
Waste preserved wood derived biochar catalyst for promoted peroxymonosulfate activation towards bisphenol A degradation with low metal ion release: the insight into the mechanisms ....	12
方竹解剖构造与性能 .....	13
保青竹材耐老化性能研究.....	16
五个蓝莓品种枝条木质部结构及其栓塞脆弱性的差异.....	18
池杉形成层恢复活动期、活动期和休眠期 细胞超微结构变化.....	21
基于卷积神经网络对大果紫檀木材花纹识别研究.....	23
中山杉应压木管胞的微观物理力学特性研究.....	25
汉六朝遗址发掘木材的解剖构造和性能分析.....	28
TBAA/DMSO 共溶剂体系直接溶解微波液化竹材制备透明抗紫外纳米纤维素膜 .....	32
接骨木和西洋接骨木的构造对比.....	35
山桐子木材材性研究 .....	39
南京出土宋代棺木用材的树种鉴定及复原加固.....	41
水青树特殊管胞的分布位置及其形态特征的研究.....	44
淹水环境对中山杉管胞壁上纹孔形态特征的影响.....	46
钝叶黄檀木材 DNA 提取及条形码鉴定 .....	49
基于高分辨 X-ray 断层扫描的木材细胞结构分析方法 .....	51
人工倾斜处理对中山杉次生组织分生的影响.....	54
“鉴木”APP——海关木材监管的智能化应用 .....	59
Ultrastructure of parenchyma cell wall in bamboo ( <i>Phyllostachys edulis</i> ) culms .....	61
批量木材鉴别抽样检查中样本量的制定.....	62
木材标本采集与数字标本管理平台的研究.....	65
白果蒲桃木材基础材性研究.....	68
福建特有乡土树种突脉青冈和闽西青冈木材结构特征的分析.....	69

刚竹属竹材维管束特征结构研究.....	72
斜叶黄檀降真香的描述及其与海南黄檀木和降香黄檀木的区分.....	75
黄杨木特性及木雕应用.....	77
竹节维管束数量与形态特征研究.....	80
等离子体处理对热处理木材表面特性及渗透性能的影响.....	83
橡胶木菌纹薄板的制备.....	86
心材型花斑木解剖构造特征分析.....	88
人工林杨树吸收土壤中重金属 Cd 的累积规律研究.....	92
钝叶黄檀和斜叶黄檀新鲜叶片 DNA 提取方法的研究.....	94
碳酸钙原位增强热改性杨木热稳定性研究.....	99
毛白杨不同冠层枝条木质部水力功能性状对水氮添加的响应.....	101
基于 BP 神经网络的木材解剖特征的树种识别.....	104
苯丙素生物合成途径响应方竹茎秆变异的研究.....	106
Physical and mechanical properties of <i>Catalpa bungei</i> clones and estimation of the properties by near-infrared spectroscopy.....	108
在线测量木材颜色的智能传感检测系统设计.....	110
酚醛树脂浸渍-机械压缩处理对杉木木材细胞尺寸稳定性的影响.....	113
植物激素诱导杨树应拉木形成和负向地性生长的转录组分析.....	116
13 年生楸树无性系材性径向遗传变异研究.....	118
Comparison of vessel traits for plantation grown teak wood of different ages from the wet zone of Ghana. ....	120
From herbs to trees and back again: changes in the degree of woodiness among carrots .....	122
Stem anatomy of the South African genera of Gnaphalieae (Asteraceae) with emphasis on the evolution of interxylary phloem.....	123
Wood anatomy of the tribe Diosmeae, a large Cape lineage of Rutaceae .....	125
Adaptation of different tree species to increasing autumn temperatures .....	126
Addressing controversies in safety - vessel diameter relationships .....	127
Ontogeny of divided vascular cylinders in <i>Serjania</i> : the rise of a novel vascular architecture in Sapindaceae .....	128
An introduction to quantitative wood anatomy using ROXAS.....	129
Anatomical structure of three lesser-used wood species grown in Indonesia.....	130

Anatomical identification of charcoal and briquettes - developments in the international charcoal trade and the increasing use of substitutes from NTFPs.....	131
Anatomical wtructure of benuang ( <i>Octomeles sumatrana</i> ) wood and its fiber quality assessment for pulp and paper manufacturing .....	132
Wood species identification by using two-electrode capacitive-based spectroscopy错误!未定义书签。	
Spatial distribution of chemical components in the phellem of <i>Cerasus jamasakura</i> (Siebold ex Koidz.) H. Ohba.....	133
Blue intensity as climate proxy: Application on black spruce in the eastern Canadian taiga .....	135
Hygroscopic swelling of moso bamboo cells .....	136
Performance of low molecular weight of phenol formaldehyde-impregnated woods on dimensional stability and durability against termites.....	137

# 基于 *LaRAV1-LaCDKB1;3* 模块解析温度调控落叶松休眠解除的机制

李万峰<sup>1,\*</sup> 康岩慧<sup>1</sup> 张耀<sup>2</sup> 臧巧路<sup>1</sup> 齐力旺<sup>1</sup>

(1 林木遗传育种国家重点实验室, 国家林草局林木培育重点实验室, 中国林业科学研究院林业研究所, 北京 100091; 2 林木遗传育种国家重点实验室, 国家林草局林木培育重点实验室, 中国林业科学研究院森林生态环境与保护研究所, 北京 100091; \*通讯作者(liwf@caf.ac.cn))

**摘要:** 温带地区树木的休眠解除和恢复活动过程与细胞周期基因的表达调控密切相关。然而, 温度调控细胞周期基因表达的具体机制还不清楚。我们比较了落叶松活动期和休眠期的转录组, 着重分析了细胞周期基因和转录因子的表达、它们之间的关系以及对温度的响应。结果表明, 12 个细胞周期基因和 31 个转录因子 (17 个家族) 在活动期高表达, 说明它们之间可能存在调控关系; 启动子分析表明, 12 个细胞周期基因可能受到 10 个转录因子家族的调控; 综合分析显示, 来自 7 个家族的 16 个转录因子与 10 个细胞周期基因之间可能存在 73 个调控事件, 而酵母单杂交和双荧光素酶实验证实了其中的 2 个, 涉及到 2 个转录因子 (*LaMYB20* 和 *LaRAV1*) 和 2 个细胞周期基因 (*LaCDKB1;3* 和 *LaCYCB1;1*)。最后, 我们发现 *LaRAV1* 和 *LaCDKB1;3* 在休眠解除和恢复活动过程中具有相同的表达模式, 进一步表明它们参与落叶松的休眠解除和恢复活动过程。这些结果不仅有助于解析温度调控细胞周期基因表达的具体机制, 也有助于理解气候变化背景下温度调控树木生长发育的机理, 为林木培育提供理论基础。

**关键词:** 形成层; 细胞周期基因; 休眠解除; 落叶松; 恢复活动; 温度; 转录因子

# Concerted control of the *LaRAV1-LaCDKB1;3* module by temperature during dormancy release and reactivation of larch

Wan-Feng Li<sup>1,\*</sup>, Yanhui Kang<sup>1</sup>, Yao Zhang<sup>2</sup>, Qiao-Lu Zang<sup>1</sup>, and Li-Wang Qi<sup>1</sup>

(1 State Key Laboratory of Tree Genetics and Breeding, Key Laboratory of Tree Breeding and Cultivation, National Forestry and Grassland Administration, Research Institute of Forestry, Chinese Academy of Forestry, No. 1, Dongxiaofu, Xiangshan Road, Haidian District, Beijing 100091, People's Republic of China; 2 State Key Laboratory of Tree Genetics and Breeding, Key Laboratory of Tree Breeding and Cultivation, National Forestry and Grassland Administration, Research Institute of Forest Ecology, Environment and Protection, Chinese Academy of Forestry, No. 1, Dongxiaofu, Xiangshan Road, Haidian District, Beijing 100091, People's Republic of China; \*Corresponding author (liwf@caf.ac.cn))

**Abstract:** Dormancy release and reactivation of temperate-zone trees involve the temperature-modulated expression of cell-cycle genes. However, information on the detailed regulatory mechanism is limited. Here, we compared the transcriptomes of the stems of active and dormant larch trees, emphasizing the expression patterns of cell-cycle genes and transcription factors and assessed their relationships and responses to temperatures. Twelve cell-cycle genes and 31 transcription factors were strongly expressed in the active stage. Promoter analysis suggested that these 12 genes might be regulated by transcription factors from 10 families. Altogether, 73 cases of regulation between 16 transcription factors and 12 cell-cycle genes were predicted, while the regulatory interactions between *LaMYB20* and *LaCYCB1;1*, and *LaRAV1* and *LaCDKB1;3* were confirmed by yeast one-hybrid and dual-luciferase assays. Last, we found that *LaRAV1* and *LaCDKB1;3* had almost the same expression patterns during dormancy release and reactivation induced naturally or artificially by temperature, indicating that the *LaRAV1-LaCDKB1;3* module functions in the temperature-modulated dormancy release and reactivation of larch trees. These results provide new insights into the link between temperature and cell-cycle gene expression, helping to understand the temperature control of tree growth and development in the context of climate change.

**Keywords:** cambium; cell-cycle gene; dormancy release; larch; reactivation; temperature; transcription factor

# Artificial wood cell wall as a valid tool to investigate wood formation and application

Qiang Li<sup>1,2,\*</sup>, Youming Xu<sup>1,\*</sup>, Hongbo Yu<sup>3</sup>, Yasumitsu Uraki<sup>4</sup>

(1 College of Horticulture and Forestry Science, Huazhong Agricultural University, China; 2 College of Engineering, Huazhong Agricultural University, China; 3 College of Life Science and Technology, Huazhong University of Science and Technology, China; 4 Research Faculty of Agriculture, Hokkaido University, Kita-ku, Sapporo 060-8589, Japan)

**Abstracts:** Wood as the most abundant Natural resource on earth has built the foundation of our daily lives. Especially in recent years, wood has been significantly advanced as a feedstock for clean energy, versatile multifunctional materials, and renewable and green products, all of which have promoted the development of future sustainability. Even though these applications have been much sought after, many underlying science regarding wood cell wall formation and chemical relationships between their component polymers is still less-well understood. These elusive fundamentals have not only hindered our understanding of tree growth and wood formation, but also hampered the implementation of wood-based advanced manufacturing; for instance, modern biorefinery for advanced biofuels and bioproducts.

To address these challenges, we have developed an artificial wood cell wall model to understand the formation of polysaccharides matrix and the chemical relationship of lignin-polysacchride. A bacterial cellulose film with honeycomb patterns have been fabricated with controlled cell growth path, and the resultant bacterial cellulose film served as the scaffold of the wood cell wall. Afterwards, hemicellulose was deposited into cellulose matrix, which was followed by the in-vitro synthesis of lignin in this cellulose-hemicellulose matrix.

By using this artificial cell wall model, we elucidated 1) the hemicellulose role in regulating the deposition and formation of lignin structures, especially lignin distribution in polysaccharide matrix and lignin  $\beta$ -O-4 interunitary linkages formation; 2) the contribution of cellulose, hemicellulose, and lignin to the cell wall mechanical strength. Our artificial wood cell wall model has further unveiled its potential in elucidating hemicellulose and lignin function in cell wall deconstruction and valorization. We have elucidated the validity of wood cell wall deformation models and found the best fit of the two-phase model. Moreover, by using the artificial cell wall model, we clarified the roles of both hemicellulose and lignin in enzymatic deconstruction of cell wall for bioethanol production. Hemicellulose itself cannot inhibit enzymatic hydrolysis, but hemicellulose can enhance lignin formation to increase its recalcitrance to cellulose hydrolysis. Highlighted by above results, artificial wood cell wall has been proved as a valid tool to elucidate both wood formation and deconstruction, especially the relationship between cell wall components and their inhibition of

enzymatic hydrolysis for biofuel production.

**Keywords:** Artificial wood cell wall; cell wall formation; cell wall deconstruction



# 气候变暖正威胁高海拔喜马拉雅桦树林：来自木材解剖与形成层物候的证据

李晓霞<sup>1</sup> Sergio Rossi<sup>2,3</sup> Shalik Ram Sigdel<sup>1</sup> Binod Dawadi<sup>4</sup> 梁尔源<sup>1,\*</sup>

(1 中国科学院青藏高原研究所青藏高原地球系统科学国家重点实验室, 北京 100101; 2 University of Quebec in Chicoutimi, Département des Sciences Fondamentales, Laboratoire d'Écologie Végétale, 555, Boulevard de l'Université, Chicoutimi (QC) G7H2B1, Canada; 3 Key Laboratory of Vegetation Restoration and Management of Degraded Ecosystems, Guangdong Provincial Key Laboratory of Applied Botany, South China Botanical Garden, Chinese Academy of Sciences, Guangzhou 510650, China; 4 Central Department of Hydrology and Meteorology, Tribhuvan University, Kirtipur, Kathmandu, Nepal; \*Author for correspondence (e-mail: liangey@itpcas.ac.cn))

**摘要：**喜马拉雅山地区正在经历远高于全球平均水平的暖干气候，但目前我们仍不清楚该地区高海拔森林生态系统如何响应这种快速的气候变化。该研究通过将定量木材解剖与形成层物候相结合，旨在理解生长动态如何影响喜马拉雅森林水力安全与效率之间的权衡。该研究调查了喜马拉雅山中部两个海拔梯度的糙皮桦 (*Betula utilis* D. Don) 木质部分化时间及其与水力解剖性状之间的关系。在 2014 年 4 月至 2014 年 9 月期间，以每周通过采集微树芯的方式来监测木质部分化过程。测量了形成层组织切片上的导管面积，计算了水力直径，并评估了气候要素对木质部生长速率的影响。研究表明，两个研究样点的木质部分化发生于 6 月至 9 月期间。除热量条件外，水分获得对糙皮桦木质部生长速率具有显著的积极影响。导管扩大阶段的开始日期和持续时间与水力直径大小密切相关。导管扩大时间较早和持续时间较长的树木呈现出较大的水力直径。形成层物候与水力直径之间的这种密切关系表明，气候变暖引起的生长提前在促进木质部水分传输效率的同时，也加剧了干旱引起的木质部栓塞风险。这意味着持续的暖干气候将对喜马拉雅山高海拔糙皮桦森林生长和分布产生威胁。

**关键词：**树轮；木质部形成；形成层；木质部解剖；木质部分化；水力性状

# **Warming menaces high-altitude Himalayan birch forests: evidence from cambial phenology and wood anatomy**

Xiaoxia Li<sup>a</sup>, Sergio Rossib<sup>c</sup>, Shalik Ram Sigdel<sup>a</sup>, Binod Dawadi<sup>d</sup>, Eryuan Liang<sup>a,\*</sup>

(a State Key Laboratory of Tibetan Plateau Earth System, Resources and Environment (TPESRE), Institute of Tibetan Plateau Research, Chinese Academy of Sciences, Beijing 100101, China; b University of Quebec in Chicoutimi, Département des Sciences Fondamentales, Laboratoire d'Écologie Végétale, 555, Boulevard de l'Université, Chicoutimi (QC) G7H2B1, Canada; c Key Laboratory of Vegetation Restoration and Management of Degraded Ecosystems, Guangdong Provincial Key Laboratory of Applied Botany, South China Botanical Garden, Chinese Academy of Sciences, Guangzhou 510650, China; d Central Department of Hydrology and Meteorology, Tribhuvan University, Kirtipur, Kathmandu, Nepal; \*Author for correspondence (e-mail: liangey@itpcas.ac.cn))

**Abstract:** The Himalayas are experiencing dramatic warming and drought events, which occur at a faster rate than the global average. How will the high-elevation ecosystems cope with such changing conditions? This study aims to combine cambial phenology with quantitative wood anatomy to understand how the growth dynamics affect the trade-off between safety and efficiency of water transport in the Himalayan forests. We investigated the timing of xylogenesis and its relationship with hydraulic wood anatomical traits in Himalaya birch (*Betula utilis* D. Don) at two altitudes in the central Himalayas. Xylogenesis was monitored weekly from April to September 2014 by collecting microcores. We measured vessel area on histological sections, calculated the hydraulic diameter, and assessed the effects of climate on xylem production rate. Xylogenesis occurred from June to September in both study sites. Moisture availability influenced positively xylem growth besides thermal conditions. The onset and duration of enlargement were correlated with the hydraulic diameter. Trees with earlier onsets and longer durations of vessel enlargement exhibited larger hydraulic diameters. The close relationship between cambial phenology and hydraulic diameter suggests that earlier growth resumption induced by climate changes may result in larger vessels, which are more efficient in water transport, but vulnerable to drought-induced cavitation. The ongoing warming and drying climate conditions may menace the survival of birch forest in the central Himalayas.

**Keywords:** tree ring; xylem formation; cambium; xylem anatomy; xylogenesis; hydraulic traits

# iWood: 基于卷积神经网络的木材图像智能鉴定系统

何拓<sup>1,2</sup> 刘守佳<sup>1,2</sup> 陆杨<sup>1,2</sup> 张永刚<sup>1,2</sup> 焦立超<sup>1,2</sup> 殷亚方<sup>1,2,\*</sup>

(1 中国林业科学研究院木材工业研究所 北京 100091; 2 中国林业科学研究院木材标本馆 北京 100091)

## 摘要:

**【目的】**建立基于卷积神经网络的木材识别系统,实现木材树种在多场景条件下的自动精准识别。

**【方法】**从经正确定名的 15 种黄檀属和 11 种紫檀属木材标本横切面采集构造特征图像,并建立图像数据集 Rosewood-26;分别构建 AlexNet, VGG16, DenseNet-121 和 ResNet-50 等 4 个卷积神经网络模型,利用 ImageNet 图像数据集分别对以上 4 个模型进行迁移学习,进而采用 Rosewood-26 图像数据集分别对模型进行训练、测试和比较,优选识别性能较好的卷积神经网络模型,并进行木材树种分类;在此基础上,构建了包含 15 种黄檀属和 11 种紫檀属树种的木材自动识别系统 iWood,利用市场木材样品对该系统进行应用测试和评价。

**【结果】**在所构建的 4 个卷积神经网络模型中,ResNet-50 模型表现出最高的识别精度(98.3%)、最少的权重数量以及较低的模型复杂性,适用于木材树种准确快速识别;ResNet-50 模型对 9 种黄檀属和 3 种紫檀属木材的识别精度达到 100%,并成功鉴别构造特征极其相似的檀香紫檀和染料紫檀;基于 ResNet-50 模型构建的木材图像智能鉴定系统 iWood,在“属”和“种”水平的识别精度分别为 91.8%和 77.3%。**【结论】**本研究开发的基于卷积神经网络的木材图像智能鉴定系统 iWood 适用于海关执法、木材贸易和质量监督检验等多场景下的木材自动精准识别,为我国提升林产品产业链监管、增强 CITES 履约执法能力以及保护森林树种多样性提供科技支撑。

**关键词:** iWood; 木材构造特征; 图像数据集; 濒危树种; 黄檀属; 紫檀属; 木材自动识别

# **iWood: Automated and accurate wood identification system for endangered and precious tree species using convolutional neural networks**

## **Abstract:**

[Objective] An image recognition method based on convolutional neural networks (CNNs) for endangered and precious tree species is developed in this study to reach the automatic and accurate identification of timber at the species level in multi-scene conditions.

[Method] Images representing wood anatomical features were collected from transverse section of authentic wood specimens for 15 *Dalbergia* and 11 *Pterocarpus* species, and an image data set of Rosewood-26 was established. Four CNN models, i.e. AlexNet, VGG16, DenseNet-121 and ResNet-50 were constructed and pre-trained with ImageNet for transfer learning. And then the image data set Rosewood-26 was deployed to re-train and test these models, which were comparatively analyzed and evaluated to result in an optimal one for timber identification. A timber identification system was developed for identifying those samples collected from timber market for application test.

[Result] Among the four CNN models, ResNet-50 showed the highest identification accuracy (98.3%) and lower model complexity, which is suitable to timber identification accurately and rapidly. The ResNet-50 model achieved 100% accuracy when identifying 9 *Dalbergia* and 3 *Pterocarpus* species, and successfully discriminated *P. santalinus* from its anatomically similar species, *P. tinctorius*. The automated timber identification system based on ResNet-50 model exhibited an identification accuracy of 91.8% at the genus level and 77.3% at the species level.

[Conclusion] The timber identification system, iWood, developed in this study using CNNs is applicable in broad fields, i.e. customs enforcement, timber trade and quality inspection, and can reach automatic and accurate identification of wood species. This study will provide scientific support for promoting regulation of forest product industry chain, enhancing CITES enforcement capabilities and protecting forest species diversity.

**Keywords:** iWood, Wood anatomical features, Image data set, Endangered tree species, *Dalbergia*, *Pterocarpus*, Automated identification of wood

# Waste preserved wood derived biochar catalyst for promoted peroxymonosulfate activation towards bisphenol A degradation with low metal ion release: the insight into the mechanisms

Jiangtao Shi, Boren Dai, Xingyu Fang, Lijie Xu, Ying Wu, Haiqin Lu, Juqin Cui,  
Shuguang Han, Lu Gan

(Nanjing forestry university)

**Abstract:** The rational disposal of waste preserved wood is of great significance since its embedded metals (Cu, As and Cr) pose potential threat to environment and human health. In this study, a biochar catalyst derived from waste preserved wood (PWB) was prepared for the degradation of bisphenol A (BPA) via peroxymonosulfate (PMS) activation. The PWB exhibited prominent catalytic degradation capability towards BPA compared with common wood derived biochar (CWB). Further tests and analysis elucidated that both radical species ( $\bullet\text{OH}$ ) and non-radical species ( $^1\text{O}^2$ ) were generated by the PWB/PMS system, whereas only  $^1\text{O}^2$  was detected in CWB/PMS system. Specifically, the metal compounds, especially metallic Cu in the PWB activated PMS via radical pathway, and the C=O groups in the biochar generated the non-radical pathway, the coexistence of which resulted in higher BPA degradation efficiency in PWB/PMS system. It was also demonstrated that the heavy metal ion leaching (As and Cr) in PWB/PMS system was negligible. Furthermore, the As could effectively inhibit the leakage of oxidized  $\text{Cu}^{2+}$ . This study provides a novel approach to prepare high efficient carbocatalysts for organic pollutant degradation in water, which also enables the waste preserved wood with an environmental nondestructive mode of dispatch.

**Keywords:** Peroxymonosulfate; preserved wood; biochar catalyst; low metal leaching; radical/non-radical synergy

# 方竹解剖构造与性能

刘文娟 林剑\*

(北京林业大学材料科学与技术学院, 北京市海淀区, 100083)

**摘要:** 方竹因径小壁薄而受关注度低, 相关的基础构造与应用研究较少。为系统性掌握方竹解剖构造与性质, 本研究以遵义市桐梓县楚米镇 1-5 年生方竹为研究对象, 采用体式显微镜和生物显微镜观察方竹宏观切片形态和微观维管束与纤维形态, 依据国标测定方竹密度、干缩率等物理性质和化学成分含量, 在此基础上, 探究方竹竹龄、竹秆纵向部位在构造和性能方面的变化规律。结果表明: 方竹由皮层、基本薄壁组织、维管束和髓环组成; 其中, 维管束散生在基本组织之中, 并由纤维组织、输导组织以及少量薄壁细胞组成, 在横切面上, 略呈梅花形, 包含断腰型、双断腰型和紧腰型三种类型, 且不同部位维管束的形状、大小及密度均有较大差异性, 即: 靠近竹青一侧的维管束分布密集, 形状较小, 输导组织分化不完全, 几乎没有导管和筛管, 中间部位的维管束形态稳定, 排列分散有序, 大小几乎统一, 输导组织分化完全, 是方竹维管束主要类型的代表, 靠近竹黄一侧的维管束则排列混乱。方竹竹纤维长度属于长纤维等级, 不同竹龄与不同纵向部位的竹纤维长度、宽度和长宽比变化差异较小, 并无一定变化规律。方竹密度随竹龄增加呈现增大的趋势, 全干干缩率和气干干缩率随竹龄增加呈下降趋势, 且后者波动性相对较大。1-5 年生方竹中部冷水抽提物含量为 3.29%-4.89%, 平均含量为 4.02%, 热水抽提物含量为 4.61%-6.66%, 平均含量为 5.46%, 两者随竹龄增大呈先下降后上升趋势, 1%NaOH 抽提物含量为 24.61%-26.72%, 平均含量为 25.76%, 两者随竹龄增大呈先上升后下降趋势, 苯醇抽提物含量为 3.62%-5.40%, 平均含量为 4.22%, 随竹龄增大而增加, 综纤维素含量为 69.15%-70.95%, 平均含量为 70.33%,  $\alpha$ -纤维素含量为 45.01%-47.84%, 平均含量为 46.57%, 酸不溶木质素含量为 25.71%-26.50%, 平均含量为 26.02%, 三者随竹龄变化差异较小, 灰分含量为 0.91%-1.99%, 平均含量为 1.40%, 其中 1 年生含量最多, 3 年生含量最少。

**关键词:** 方竹; 维管束; 竹纤维; 物理性质; 化学成分

# Anatomical structure and properties of *Chimonobambusa quadrangularis Makino*

Wenjuan Liu, Jian Lin\*

(College of Materials Science and Technology Beijing Forestry University, Haidian Beijing, 100083)

**Abstract:** *Chimonobambusa quadrangularis Makino* attracts low attention due to its small diameter and thin wall, and the relevant basic structure and application research are less frequent. In order to systematically grasp the anatomical structure and properties of bamboo, 1-5 years old bamboo grown in chumi town tongzi county Zunyi city were selected as research materials. The macro slice morphology and micro vascular bundle morphology as well as fiber morphology were observed by using type microscopes and biological microscopes. The density, dry shrinkage rate physical properties and chemical content of bamboo were determined based on national standard respectively. Furthermore, the variation of structure and properties with age and longitudinal position of bamboo were also discussed. The results are as follows: *Chimonobambusa quadrangularis Makino* was composed of cortex, basic parenchyma tissue, vascular bundle and myelin ring. The vascular bundle was scattered in the basic tissue, and it was composed of fibrous tissue, conducting tissue and a few parenchyma cells. In the cross section, vascular bundle showed a quincunx shape including three types of broken waist type and double broken waist type as well as tight waist type. There were great differences in the shape, size and density among different parts of the same cross section. For the part near bamboo green, the vascular bundle distribution is dense, the shape is small, the conduction tissue differentiation is not complete, almost no vessels and sieve tube. In the case of middle part, it has stable shape and uniform size, the conduction tissue is completely differentiated, which is the representative of the main types of vascular bundle. For the part near bamboo yellow, the arrangement of vascular bundle were disordered. The length of bamboo fiber belongs to the long fiber grade. The variation of fiber length, width and length-width ratio among different ages and longitudinal positions of bamboo was small, and showing non-change regulation. The density of bamboo increased with the increase of bamboo age, and the oven-dried and air-dried shrinkage rate decreased with the increase of bamboo age, but the latter volatility is relatively large. The content of cold water extract in 1-5 years old bamboo was 3.29%-4.89%, and the average content was 4.02%, the content of hot water extract was 4.61%-6.66%, and the average content was 5.46%, both showed a decrease-increase trend with the increase of bamboo age, the content of 1%NaOH extract was 24.61%-26.72%, and the average content was 25.76%, it showed an increase-decrease trend with the increase of bamboo age, the content of phenol extract was 3.62%-5.40%, and the average content was 4.22%, it increased with the increase of bamboo age, the holocellulose content was 69.15%-70.95%, and the average content was 70.33%, the  $\alpha$ -cellulose content was 45.01%-47.84%,

and the average content was 46.57%, the acid-insoluble-lignin content was 25.71%-26.50%, and the average content was 26.02%, the three varied slightly with bamboo age increasing, the ash content was 0.91%-1.99%, and the average content was 1.40%, thereinto, one year had the maximum content and three year had the minimum content.

**Keywords:** Bamboo; Vascular bundles; Bamboo fiber; Physical properties; Chemical content



# 保青竹材耐老化性能研究

胡馨芸<sup>1</sup> 陈果希<sup>1</sup> 陈燕<sup>1</sup> 齐锦秋<sup>1</sup> 姜永泽<sup>1</sup> 黄兴彦<sup>1</sup> 谢九龙<sup>1</sup>

(四川农业大学, 林学院)

**摘要:** 为掌握保青毛竹竹材的适用范围, 用清漆、木蜡油、水性漆三种漆料涂饰保青竹材, 并通过紫外老化实验、人工加速老化实验、不同温度实验、不同酸碱度实验, 结合表色系统分析, 研究环境和漆饰对保青毛竹竹材的耐老化性能的影响。(1) 紫外老化试验中, 随着实验周期的不断增加, 四种保青竹材表面材色开始缓慢变黄, 其中无涂饰竹材的总色差 $\Delta E^*$ 变化量最大(8.59), 材色变化最显著; 木蜡油对竹材的保护效果较好,  $\Delta E^*$  (5.55) 变化量最小, 20 周期后红绿值  $a^*$  仍然保持原色的 57.27%。(2) 人工加速老化实验中, 95°C 高温高湿和 100°C 高温干燥的环境对保青竹材表面有着显著影响, 其中无涂饰竹材  $\Delta E^*$  变化量最大(11.58), 木蜡油对漆饰的竹材  $\Delta E^*$  (7.3) 变化量最小。(3) -80°C 至 200°C 的不同温度试验中, 保青竹材的材色在低温环境中均轻微变绿, 在 40-120°C 环境中材色变黄程度较小, 在 140-200°C 高温环境中材色变化剧烈, 尤其是在 180°C 和 200°C 极高温环境中, 保青竹材表面漆膜被烘烤后变至焦褐色。加热处理采用真空干燥箱和鼓风干燥箱进行对比, 真空干燥箱处理的保青竹材表面颜色保持优于鼓风干燥箱。不同温度实验中, 无涂饰竹材总色差  $\Delta E^*$  变化量最小。(4) 不同酸碱度处理结果, 酸碱环境对保青竹材颜色影响较小。在极酸、极碱环境中, 有漆饰的保青竹材表面漆膜发生龟裂、剥落, 影响了保青竹材表面颜色, 其中清漆竹材和水性漆竹材的  $\Delta E^*$  变化量明显高于木蜡油竹材和无涂饰竹材, 无涂饰竹材表面材色变化最小。

**关键词:** 毛竹; 耐老化; 颜色

# Study on the aging resistance of color-preserving of bamboo

Hu Xinyun<sup>1</sup>, ChenGuoxi<sup>1</sup>, Chenyan<sup>1</sup>, Qi Jinqiu<sup>1</sup>, Jiang Yongze<sup>1</sup>, Huang Xingyan<sup>1</sup>, Xie Jiulong<sup>1</sup>

(College of Forestry, Sichuan Agricultural University)

**Abstract:** In order to study the application range of color-preserving bamboo, three kinds of lacquer, wood wax oil and water paint were used to paint color-preserving bamboo. The effects of environment and paint on the aging resistance of color-preserving bamboo were studied by UV aging experiment, artificial accelerated aging experiment, different temperature experiment, different pH experiment and color system analysis. (1) In the UV aging test, the surface color of the four kinds of bamboo began to turn yellow slowly with increasing the experimental period, and the total color difference  $\Delta E^*$  of the bamboo without coating changed the most (8.59), and the color change was the most significant. Wood wax oil had a better protective effect on bamboo, and the change of  $\Delta E^*$  (5.55) was the smallest. After 20 cycles, the red-green value  $a^*$  still retained 57.27% of the original color. (2) In the artificial accelerated aging experiment, the environment of high temperature (95 °C) and high humidity and high temperature (100 °C) and dry had a significant effects on the surface of bamboo. The change of  $\Delta E^*$  of bamboo without coating was the largest (11.58), and the change of  $\Delta E^*$  of bamboo painted with wood wax oil was the smallest (7.3). (3) In different temperature tests from -80 °C to 200 °C, the color of color-preserving bamboo became slightly green in low temperature environment. The color of color-preserving bamboo became slightly yellow in the environment of 40-120 °C. The color of color-preserving bamboo changed dramatically in the high temperature environment of 140-200 °C, especially in the extremely high temperature environment of 180 and 200 °C. The paint film on the surface of color-preserving bamboo became brown after baking. The heating treatment was compared with the vacuum drying oven and the air blowing drying oven. The surface color of green bamboo treated by the vacuum drying oven was better than that of the air blowing drying oven. The variation of total color difference  $\Delta E^*$  of bamboo without coating was the smallest at different temperatures. (4) The acid-base environment had little effect on the color of bamboos. In the extremely acid and alkali environment, the surface paint film of lacquered bamboo cracked and peeled, which affected the surface color of lacquered bamboo. The  $\Delta E^*$  change of lacquered bamboo and waterborne lacquered bamboo was significantly higher than that of wood wax oil bamboo and bamboo without coating, and the change of surface color of bamboo without coating was the least.

**Keywords:** Moso Bamboo; Ageing resistance; color

# 五个蓝莓品种枝条木质部结构及其栓塞脆弱性的差异

刘家宝<sup>1</sup> 张亚<sup>2</sup>

(1 安徽师范大学生态与环境学院, 芜湖, 安徽 241000; 2 安徽省重要生物资源保护与利用研究重点实验室, 安徽师范大学生命科学学院, 芜湖, 安徽 241000)

**摘要:** 木本植物因干旱造成的木质部水力中断是许多森林衰退和死亡的重要原因之一。近年来, 因气候变化引起的极端干旱事件对蓝莓种植产业的影响日趋凸显, 研究蓝莓对环境干旱的响应对减轻蓝莓种植产业因干旱导致的减产等损失具有重要意义。以往有关蓝莓干旱适应性的研究多集中于叶片水平的光合和蒸腾作用以及干旱对蓝莓开花时间和果实品质的影响, 从枝条水力结构探究蓝莓的抗旱性少有报道。为了比较不同蓝莓品种之间的枝条木质部结构及其抗旱性的差异, 该研究以安徽省芜湖市徽王莓岭蓝莓园引种的两种蓝莓五个品种(即南高丛蓝莓: 奥尼尔、薄雾; 兔眼蓝莓: 灿烂、梯芙兰、顶峰)为实验材料, 进行了以下实验: 1) 运用光学显微镜和扫描电镜观察木质部的导管结构, 并计算导管直径、导管密度、导管壁厚度、导管群指数、导管壁加固系数、纹孔面积、纹孔密度、纹孔大小和边材密度等木质部结构参数; 2) 用自然干燥法测定蓝莓枝条的栓塞脆弱性曲线, 计算木质部导水能力丧失 12%、50%、88%时的木质部水势(P12、P50、P88), 并结合自然状态下枝条正午水势计算枝条的水力安全阈值。研究表明: 1) 南高丛蓝莓的导管直径、导管群指数和纹孔面积均小于兔眼蓝莓, 但南高丛蓝莓的导管壁加固系数和边材密度均大于兔眼蓝莓。2) 兔眼蓝莓枝条栓塞脆弱性大于南高丛蓝莓。五个蓝莓品种抗栓塞能力由强到弱依次排序为: 奥尼尔>薄雾>梯芙兰>灿烂>顶峰, 其中奥尼尔抗栓塞能力最强(P50 = -1.70 MPa), 顶峰抗栓塞能力最弱(P50 = -1.36 MPa)。五个蓝莓品种的水力安全阈值均为正值, 但其正午枝条水势均低于各自的 P12 值。3) 五种蓝莓品种的 P50 与导管直径和纹孔面积呈正相关关系, 与导管壁加固系数和边材密度呈负相关关系。该研究揭示了不同蓝莓品种的枝条木质部结构与其枝条栓塞脆弱性的相关性, 为阐明不同蓝莓品种之间抗旱性差异提供了新思路、新视野, 也为蓝莓种植产业的选种、引种、育种, 园林管理和水分灌溉等提供一定的科学依据。

**关键词:** 蓝莓; 木质部结构; 栓塞脆弱性; 抗旱性; 水分运输

# Differences in xylem structure and embolism vulnerability of branches of five blueberry cultivars

Liu Jiabao<sup>1</sup>, Zhang Ya<sup>2</sup>

(1 College of Ecology and Environment, Anhui Normal University, Wuhu 241000, Anhui; 2 Anhui Provincial Key Laboratory of the Conservation and Exploitation of Biological Resources, College of Life Sciences, Anhui Normal University, Wuhu 241000, Anhui)

**Abstract:** Xylem hydraulic disruption caused by drought is one of the main causes of forest decline and death. In recent years, the impact of extreme drought events caused by climate change on the blueberry plantation has become increasingly prominent. Studying the drought response of blueberry is very important to reduce the production losses caused by drought. Previous studies on drought adaptability of blueberry focused mainly on the drought effect on the photosynthesis and transpiration of leaves, or the flowering time and fruit quality, while researches on the drought resistance from a perspective of hydraulic structure of branches were poorly reported. In order to compare the differences of the xylem structure and drought resistance of branches among different blueberry cultivars, 5 blueberry cultivars from two species growing at Huiwang Meiling Plantation in Wuhu were selected in this study, which were *Vaccinium corymbosum* (i.e., Southern Highbush, including O'Neal and Misty) and *Vaccinium ashei* (i.e., Rabbit-eye, including Britewell, Tifblue and Climax). Experiments were carried out as follows: 1) The vessel structure of blueberry cultivars were observed and the vessel diameter, vessel density, vessel wall thickness, vessel group index, conduct wall reinforcement, pit area, pit density, pit size, and sapwood density were calculated; 2) The embolism vulnerability curves of blueberry branches were measured by the bench dehydration method to calculate the xylem water potential (P12, P50, P88) when the loss of xylem hydraulic conductivity was reached by 12%, 50% and 88%, and the safety margin of branches was calculated by combining the midday water potential of branches in natural state. The results were listed below: 1) The Southern Highbush showed lower vessel diameter, vessel group index and pit area, but higher vessel wall reinforcement and sapwood density than the Rabbit-eye. 2) The Rabbit-eye branches showed higher embolism vulnerability than the Southern Highbush. The order of the embolism resistance ability of the five blueberry cultivars was O'Neal > Misty > Tifblue > Britewell > Climax, where O'Neal showed the highest resistance (P50 = -1.70 MPa) and Climax the lowest (P50 = -1.36 MPa). The safety margins of five blueberry cultivars were all positive values, but the midday water potentials of branches were all lower than P12 values in five cultivars. 3) P50 values in five cultivars showed a positive correlation with the vessel diameter and the pit area, but a negative correlation with vessel wall reinforcement and sapwood density. This study revealed the correlation between the xylem structure of branches and the embolism vulnerability in five blueberry

cultivars, which provided a new scope for clarifying the difference of drought resistance among blueberry cultivars. This study also gave a scientific basis for seed selection, introduction, breeding, landscape management and water irrigation of blueberry plantation.

**Keywords:** blueberry; xylem structure; embolism vulnerability; drought resistance; water transport

# 池杉形成层恢复活动期、活动期和休眠期 细胞超微结构变化

陶洁云<sup>1,2</sup> 徐有明<sup>1</sup> 李强<sup>1</sup> 孙小苗<sup>2</sup> 金凯<sup>2</sup>

(1 华中农业大学园艺林学学院, 武汉; 2 上海木材工业研究所, 上海)

**摘要:** 研究形成层分生活动细胞超微构造变化, 理解木材形成机理, 指导林业材质改良。本文以池杉为研究材料, 通过制作超薄切片, 利用透射电镜, 从超微结构层面深入了解池杉木材形成过程。3月中旬至4月上旬, 形成层活动处于恢复活动期, 细胞中可见细胞器为高尔基体与小液泡, 形成层带开始分化出韧皮部细胞。4月中旬形成层处于活动期前期, 细胞内液泡融合, 细胞内含物开始逐渐增多, 形成带细胞开始沉积次生壁。4月中旬至5月底形成层处于活动期, 形成层带细胞小幅度径向伸展, 在4月下旬观察到形成层带分化出木质部细胞。6月初至8月底形成层处于活跃期, 形成层带细胞中细胞器发育成熟, 细胞核明显可见, 形成层分生活动处在当年巅峰期。9月初形成层处于活跃期末期, 溶酶体伴随内质网同时出现。11月上旬形成层处于休眠期初期, 形成层细胞壁已经完成沉积。11月中旬即休眠期初期, 部分形成层带细胞液泡膜破裂, 释放出大量水解酶, 引起核变形与解体, 木质部完全停止分化, 但仍可见少量幼嫩韧皮部细胞。已经死亡的形成层带细胞其细胞核内凋亡小体溢出, 细胞内分散的核质呈现异常的染色。

**关键词:** 池杉; 形成层; 超微结构; 分生活动; 细胞壁

# The cambium cell ultrastructural changes of *Taxodium ascendens* in its recovery activity, active period and dormant periods

Tao Jieyun<sup>1,2</sup>, Xu Youming<sup>1,\*</sup>, Li Qiang<sup>1</sup>, Sun Xiaomiao<sup>2</sup>, Jin Kai<sup>2</sup>

(1 College of Horticulture and Forestry Science, Huazhong Agricultural University; 2 Shanghai Wood Industry Insititue )

**Abstract:** To study the ultrastructural changes of cambium meristematic active cells, can deeply understand the formation mechanism of wood and improve wood quality. In this paper, the wood formation process of *Taxodium ascendens* was studied in ultrastructural level by making ultrathin sections and using transmission electron microscope (TEM). From mid-March to early April, cambium activity recovered. Golgi apparatus and vacuoles were seen in the cells, and the cambium zone began to differentiate into phloem cells. In mid-April, the cambium is in the early stage of activity. Intracellular vacuoles fuse and cell inclusions gradually increase, forming secondary walls with cells beginning to deposit. The cambium was active from mid-April to the end of May, and cells in the cambium zone extended radially with small amplitude. Xylem cells differentiated from the cambium zone were observed in late April. Cambium was active from early June to the end of August, organelles in cambium zone cells were mature, nuclei were visible, and cambium meristem activity was at the peak of that year. In early September, the cambium was at the end of its active phase, and lysosomes appeared with the endoplasmic reticulum. In early November, cambium was in the early resting stage, and the cambium cell wall had been deposited. In mid-November, at the beginning of dormancy, part of cambium zone cell vacuole membrane ruptured, releasing a large number of hydrolases, resulting in nuclear deformation and disintegration. Xylem differentiation stopped completely, but a small number of young phloem cells were still visible. The dead cambium zone cells are overflowing with apoptotic bodies and abnormal staining of dispersed cytoplasm.

**Keywords:** *Taxodium ascendens*; Cambium; Ultrastructure; eristem activity; The cell wall; Wood formation

# 基于卷积神经网络对大果紫檀木材花纹识别研究

田朔 蒋彤 (BANDA CHARITY) 李文珠\*

(浙江农林大学 化学与材料工程学院, 杭州, 临安 311300)

**摘要:** 对大果紫檀木材花纹图像采集和分类, 采用 Faster RCNN (Faster Region Based Convolutional Neural Networks) 神经网络作为识别检测算法, 通过特征提取模块改进和图像增强, 构建大果紫檀木材花纹数据集。在模型设计中对神经网络架构和卷积核进行改进, 引入随机正则化函数, 弱化过拟合现象和减少特征维度。在神经网络中加入训练集进行模型训练, 将得到的模型进行数据迁移, 应用到图像测试集上进行反演, 最后将模型的输出结果与大果紫檀木材花纹进行关联, 实现木材花纹识别检测。结果表明: 木材花纹识别准确率为 96%, 基本达到了预期结果, 本次研究设计具有一定的应用价值, 与传统方法相比进一步提高了识别速率, 但也存在一些问题, 比如在完成度上缺少大量的训练, 因此造成了一些误差, 这也是以后需要重视并攻克的问题。通过对大果紫檀木材花纹识别算法的研究, 在多学科融合背景下加强木材学科和计算机学科的联系, 探索木材识别与鉴定的新思路和新方法。

**关键词:** 大果紫檀; 卷积神经网络; 木材花纹; 特征提取; 过拟合



# Research on woodgraining recognition of *pterocarpus macrocarpus* based on convolutional neural network

**Abstract:** For the collection and classification of *Pterocarpus macrocarpus* wood pattern images, the Faster RCNN (Faster Region Based Convolutional Neural Networks) neural network is used as the recognition and detection algorithm, and the improvement of the feature extraction module and image enhancement are used to construct the *Pterocarpus macrocarpus* wood pattern data set. In the model design, the neural network architecture and convolution kernel are improved, and the random regularization function is introduced to weaken the over-fitting phenomenon and reduce the feature dimension. The training set is added to the neural network for model training, the obtained model is transferred and applied to the image test set for inversion, and finally the output result of the model is associated with the wood pattern of *Pterocarpus macrocarpus* to realize wood pattern recognition and detection. The results show that the accuracy of wood pattern recognition is 96%, which basically achieves the expected results. This research design has certain application value. Compared with traditional methods, the recognition rate is further improved, but there are some problems, such as the degree of completion. The lack of a lot of training has caused some errors. This is also a problem that needs to be addressed and overcome in the future. Through the research on the wood pattern recognition algorithm of *Pterocarpus macrocarpus*, strengthen the connection between the wood discipline and the computer discipline under the background of multidisciplinary integration, and explore new ideas and new methods for wood recognition and identification.

**Keywords:** *Pterocarpus macrocarpa*; convolutional neural network; wood pattern; feature extraction; over-fitting

# 中山杉应压木管胞的微观物理力学特性研究

杨季雨<sup>1</sup> 毕玉金<sup>1</sup> 潘彪<sup>1,\*</sup>

(1 南京林业大学材料科学与工程学院, 南京 210037)

**摘要:** 中山杉 (*Taxodium hybrid* 'Zhongshanshan') 作为速生材种, 在生长过程中易受到环境影响而产生应压木, 降低木材质量。管胞是构成针叶木材最主要的细胞, 对中山杉应压木管胞的微观物理力学性能进行系统研究有助于对中山杉应压木的合理利用。

取 14 年生的弯曲的中山杉的弯曲处作为研究对象。由于径向方向上的应压木宽度有限, 故将试样尺寸调整为 5 mm×5 mm×20 mm (轴向), 其余按照标准测量饱水、气干和绝干三种状态下试样的径向、弦向和轴向尺寸, 排水法测量体积并称重; 分别计算中山杉试样的气干密度、全干密度、基本密度、气干干缩率和全干干缩率, 对实验数据进行统计分析; 再利用 XRD 测定了应压区和对应区木材的微纤丝角和纤维素相对结晶度并进行相关性分析和线性拟合分析。采用富兰克林离析法分离管胞, 将管胞固定在自制仪器上进行单根管胞拉伸性能的测定, 根据公式  $\sigma = P_{\max}/S$  计算单根管胞抗拉强度, 其中 S 为管胞横截面积。取 100  $\mu\text{m}$  厚度的木薄片, 使用万能力学实验机测试薄片的顺纹拉伸性能。

结果表明: 中山杉应压木的密度显著大于对应木: 应压木的气干密度、全干密度和基本密度分别为 0.662 g/cm<sup>3</sup>、0.603 g/cm<sup>3</sup> 和 0.528 g/cm<sup>3</sup>, 对应木的气干密度、全干密度和基本密度分别为 0.430 g/cm<sup>3</sup>、0.379 g/cm<sup>3</sup> 和 0.326 g/cm<sup>3</sup>, 中山杉应压木的轴向气干和全干干缩率分别为 1.801% 和 5.973%, 分别是对应木的 2.9 倍和 5.9 倍; 而应压木的横向干缩率和体积干缩率均显著小于对应木。相关性分析表明应压木的纵向气干和全干干缩率均与微纤丝角呈极显著正相关关系, 线性拟合方程分别为  $Y=0.1759X-5.0717$  和  $Y=0.5526X-16.4590$ , R<sup>2</sup> 分别为 0.3581 和 0.4315。应压木单根管胞的拉伸断裂载荷为 12.91 mN, 较对应木减小了约 64%; 抗拉强度为 64.59 MPa, 较对应木减小了约 40%。应压木 100  $\mu\text{m}$  木薄片的顺纹拉伸断裂载荷为 16.89 N, 较对应木减小了约 37%; 木薄片抗拉强度为 16.86 MPa, 较对应木减小了约 38%。应压木单根管胞以及应压木木薄片的拉伸断裂载荷、抗拉强度较对应木均显著减小。木薄片的顺纹拉伸断裂载荷、顺纹抗拉强度与微纤丝角均呈负相关; 线性拟合方程分别为  $Y=-1.721X+85.205$   $Y=-2.026 X+97.297$ , 对应 R<sup>2</sup> 分别为 0.3931 和 0.4421。

结论: (1) 中山杉应压木的密度大于中山杉对应木; (2) 中山杉应压木的拉伸性能显著低于对应木, 木薄片的顺纹拉伸断裂载荷、顺纹抗拉强度与微纤丝角均呈负相关, 单根管胞的拉伸性能与微纤丝角不呈现相关关系; (3) 中山杉应压木的横向和体积干缩率小于中山杉对应木, 受微纤丝角和结晶度变化影响, 中山杉应压木的纵向气干和全干干缩率均明显增加。

**关键词:** 中山杉; 应压木; 物理性质; 拉伸性能

# Study on microscopic physical and mechanical properties of compression wood tracheids of *Taxodium* hybrid 'Zhongshanshan'

Yang Jiyu<sup>1</sup>, Bi Yujing<sup>1</sup>, Pan Biao<sup>1,\*</sup>

(1 Nanjing Forestry University Materials Science and Engineering )

**Abstract:** As a fast-growing species, *Taxodium* hybrid 'Zhongshanshan' was susceptible to the environment and gravity, and thus formed compression wood which reduces the quality of timber. Therefore, a systematic study of the physical and mechanical properties of the compression wood of *Taxodium* hybrid 'Zhongshanshan' can help the rational utilization of the compression wood of *Taxodium* hybrid 'Zhongshanshan'. Tracheids are the most important cells that make up coniferous wood. A systematic study of the microphysical and mechanical properties of the tracheids of *Taxodium* hybrid 'Zhongshanshan' would help to make rational use of compression wood of *Taxodium* hybrid 'Zhongshanshan'.

The bends of 14-year-old bent *Taxodium* hybrid 'Zhongshanshan' were taken as the object of study. Due to the limited width of the pressed wood in the radial direction, the size of the sample is adjusted to 5 mm×5 mm×20 mm (axial), and the rest are measured in accordance with the standard under three conditions: saturated, air-dried and absolutely dry. The radial, chordal and axial dimensions of the shaft are measured by the drainage method and weighed. The radial, chordal, and axial dimensions of the specimens were measured in three states: waterlogged, air-dried, and total dry, and the volume was measured and weighed by the drainage method; the air-dry density, full-dry density, basic density, air-dry shrinkage rate, and full-dry shrinkage rate of the specimens were calculated, and the experimental data were statistically analyzed; then the microfibril angle was measured and correlation and linear fit analyses were performed. The tracheid were separated by the Franklin separation method, and the tracheid were fixed on a self-made instrument to determine the tensile properties of a single tracheid. The tensile strength of single tracheid was calculated according to the formula  $\sigma = P_{\max}/S$ , which S is the cross-sectional area of the tracheid. The wood thin slices of 100  $\mu\text{m}$  thickness were taken and the tensile properties of the thin slices were tested by using a universal mechanical testing machine.

The results showed that the densities of the compression wood were significantly higher than those of the opposite wood: 0.662 g/cm<sup>3</sup>, 0.603 g/cm<sup>3</sup> and 0.528 g/cm<sup>3</sup> for the compression wood, and 0.430 g/cm<sup>3</sup>, 0.379 g/cm<sup>3</sup> and 0.326 g/cm<sup>3</sup> for the opposite wood, respectively. The axial air-dry and full-dry shrinkage of the compression wood were 1.801% and 5.973%, respectively, which were 2.9 and 5.9 times higher than those of the opposite wood; while the lateral and volumetric shrinkage

of the compression wood were significantly smaller than those of the opposite wood. The correlation analysis showed that the longitudinal air-dry and full-dry shrinkage rates of compression wood were highly significant and positively correlated with the microfibril angle, and the linear fitting equations were  $Y=0.1759X-5.0717$  and  $Y=0.5526X-16.4590$ , respectively. the tensile fracture load of single tracheid of compression wood was 12.91 mN, which was about 64% less than that of the opposite wood; the tensile strength was 64.59 MPa, which was about 40% less than that of the opposite wood. The tensile strength was 64.59 MPa, which was about 40% less than that of the opposite wood. The tensile fracture load of the 100  $\mu\text{m}$  wood sheet was 16.89 N, about 37% less than that of the opposite wood, and the tensile strength of the wood sheet was 16.86 MPa, about 38% less than that of the opposite wood. The tensile fracture load and tensile strength of the single tracheid of the compression wood and the compression wood flakes were significantly reduced compared with those of the opposite wood. The tensile fracture load and tensile properties of the wood sheet were negatively correlated with the microfibril angle; the linear fitting equations were  $Y=-1.721X+85.205$   $Y=-2.026X+97.297$ .

Conclusions: (1) The density of the compression wood of *Taxodium* hybrid ‘Zhongshanshan’ is greater than that of the opposite wood of *Taxodium* hybrid ‘Zhongshanshan’; (2) the tensile properties of *Taxodium* hybrid ‘Zhongshanshan’ compression wood were significantly lower than those of the opposite wood. (2) The tensile properties of the compression wood were significantly lower than those of the opposite wood, and the tensile fracture load and tensile properties of the wood thin section in smooth grain were negatively correlated with the microfibril angle, and the tensile properties of the single tracheids were not correlated with the microfibril angle; (3) The transverse and volumetric dry shrinkage of *Taxodium* hybrid ‘Zhongshanshan’ opposite wood is greater than that of *Taxodium* hybrid ‘Zhongshanshan’ compression wood, the longitudinal air-dry and full-dry shrinkage rates were significantly increased by the change of the microfibril angle.

**Keywords:** *Taxodium* hybrid ‘Zhongshanshan’; compression wood; physical properties; stretch properties

# 汉六朝遗址发掘木材的解剖构造和性能分析

尹宁宁 李文珠\* 李小晴

(浙江农林大学 化学与材料工程学院 杭州临安 311300)

**摘要:**【目的】余姚市花园新村汉六朝遗址是一处典型的汉文化遗址，本文在遗址发掘现场的四个护岸处采集木构设施中的木桩和横板，进行木材解剖特征观察、最大含水率(WMC)、基本密度和热重曲线(TG)的测试，判别木材样品的材种、试样的腐朽和降解情况。为推断汉六朝时期余姚当地的林木分布和木材选用提供理论基础和参考数据。

【材料与方法】在遗址挖掘现场的四个护岸处分别采集木桩试样(编号为Z-1、Z-2、Z-3、Z-4)和横板试样(编号为B-1、B-2)。(取样标示见图)



- 1、针对试样的实际情况，分别进行直接切片和冷冻后切片，然后用体视显微镜和生物显微镜观察木材的解剖构造特征。
- 2、取不规则试样，放入水中使试样吸水饱和后取出称量重，然后再把试样放入电热鼓风干燥箱中，在 $105\pm 3^{\circ}\text{C}$ 温度下烘至绝干后取出冷却至室温后称重，计算试样的最大含水率值。
- 3、由于试样的形状不规则，无法依据相关标准进行测试，故选用固体密度计，应用液体石蜡作为介质，运用阿基米德定律，进行密度测试。
- 4、采用综合热分析仪进行热重分析(TGA)，温度为室温到 $800^{\circ}\text{C}$ ，高纯氮气流速为 $50\text{ml}/\text{min}$ ，升温速度为 $20^{\circ}\text{C}/\text{min}$ ，得到热重曲线和样品的热稳定性、热分解情况及残炭量等信息。

【结果与分析】1、所采集的试样表面有泥沙附着，木桩试样基本为木段形，横板试样尺寸和形状不规则，有一定的腐烂和降解情况；通过木材切片和解剖构造特征观察，查阅相关资料判别试样的木材类别分别为：

Z-1——栗木；Z-2——白青冈；Z-3——乌桕；Z-4——马尾松；B-1——黄杞；B-2——檫木

2、对试样的最大含水率(WMC)、基本密度和热重曲线的测试结果表明，木材腐朽程度不仅与树种本身的性能有关系，与所处的地理环境和用途也有一定关系。

(1) 试样的最大含水率分别为 $204.41\%$ 、 $184.34\%$ 、 $771.62\%$ 、 $215.52\%$ 、 $906.03\%$ 、 $105.05\%$ ，均存在一定程度的腐朽和降解情况；其中乌桕和黄杞的最大含水率较高，达到了四级。

(2) 试样的残留基本密度分别为 $66\%$ 、 $56\%$ 、 $26\%$ 、 $82\%$ 、 $22\%$ 、 $85\%$ ，残留基本密度值越小，降解程度越大，残留基本密度得到的结果与最大含水率一致，不同程度上都有降解和腐朽。

(3) 试样热解后的残炭量均较高，相比正常木材快速热解温度范围有所扩大，其中起始温度较低，而热解趋稳温度则较高，这都说明了试样有一定程度的降解，产生了热稳定性差的成分。

子和化学结构。

**关键词：**木材解剖；木材降解；最大含水率；残留基本密度

# Analysis of anatomical structure and properties of wood excavated from han and six dynasties sites

Ningning Yin, Wenzhu Li\*, Xiaoqing Li

(College of Chemical and Material Engineering, Zhejiang A&F University, Hangzhou Lin 'an 311300)

**Abstract:** [objective] Yuyao garden new village ruins of the han dynasties is a site of the typical Chinese culture, this article on the site excavation site of the four revetment collected wooden piles and the rung of facilities, wood anatomical characteristics observed, maximum moisture content (WMC), basic density and thermogravimetric curve (TG) test, discriminant wood decay and degradation of the material of the sample, the sample. It provides theoretical basis and reference data for inferring local forest distribution and wood selection in Yuyao during Han and Six Dynasties.

[Materials and Methods] Wooden pile samples (numbered Z-1, Z-2, Z-3, Z-4) and horizontal plate samples (numbered B-1, B-2) were collected from the four revetment sites of the excavation site.(See figure for sampling label)



1. According to the actual situation of the samples, direct section and frozen section were conducted respectively, and then the anatomical structure characteristics of wood were observed with stereomicroscope and biological microscope.
2. Take irregular samples, put them into water to make them saturated with water and then weigh them. Then put the samples into the electric blast drying oven, bake until completely dry at  $105\pm 3^{\circ}\text{C}$ , take them out and weigh them after cooling to room temperature, and calculate the maximum moisture content of the samples.
3. Due to the irregular shape of the sample, it is impossible to test it according to relevant standards, so a solid densitometer is selected, liquid paraffin is used as the medium, and Archimedes' law is applied to test the density.
4. Thermogravimetric analysis (TGA) was carried out by comprehensive thermal analyzer at room temperature to  $800^{\circ}\text{C}$ , high purity nitrogen flow rate of  $50\text{mL}/\text{min}$ , and heating rate of  $20^{\circ}\text{C}/\text{min}$ . Thermogravimetric curves and thermal stability, thermal decomposition and carbon residue of samples were obtained.

[Results and Analysis] 1. There is sediment attached on the surface of the sample collected. The wooden pile sample is basically in the shape of wood segments, and the size and shape of the transverse plate sample are irregular, and there is some decay and degradation. Through the observation of wood section and anatomical structure characteristics, the classification of wood samples determined by referring to relevant data is as follows:

Z - 1 - chestnut; Z-2 -- White Cypress; Z - 3 - tallow; Z-4 -- Masson pine; B - 1 - huang qi. B - 2 - polishing the wood

2. The test results of maximum moisture content (WMC), basic density and thermogravimetric curve showed that the degree of wood decay was not only related to the properties of the tree species, but also to the geographical environment and use.

(1) The maximum water content of the samples were 204.41%, 184.34%, 771.62%, 215.52%, 906.03% and 105.05%, respectively, which were all decayed and degraded to a certain extent. The maximum water content of Tallow and yellow berry is higher, reaching 4.

(2) The residual basic density of samples were 66%, 56%, 26%, 82%, 22% and 85%, respectively. The smaller the residual basic density value was, the greater the degree of degradation was. The results of residual basic density were consistent with the maximum water content, and there were degradation and decay in different degrees.

(3) The amount of carbon residue in the samples after pyrolysis is higher, and the temperature range of rapid pyrolysis is wider than that of normal wood. The initial temperature is lower, while the pyrolysis stability temperature is higher, which indicates that the samples have a certain degree of degradation, resulting in poor thermal stability of molecular and chemical structures.

**Keywords:** wood anatomy; wood degradation; maximum moisture content; residual basic density



# TBAA/DMSO 共溶剂体系直接溶解微波液化竹材制备透明抗紫外纳米纤维素膜

邵慧娟 谢九龙

(四川农业大学林学院)

## 摘要:

1) 研究目的: 抗紫外塑料薄膜具有难降解、不可再生的缺点, 使用后难以回收, 对环境污染严重; 随着人们对环境保护意识的增强, 利用可再生、绿色环保、来源广泛的木质生物资源制备生物基抗紫外膜获得广大研究者广泛的关注和研究。

2) 研究方法: 利用高功率微波选择液化竹材加工剩余物, 主要是富含纤维细胞组织的竹青和富含薄壁细胞组织的竹黄, 制备含有木质素的竹材细胞, 随后, 将上述未经处理的液化竹材纤维细胞和液化竹材薄壁细胞在常温条件下溶解在 TBAA (四丁基乙酸铵) /DMSO (二甲亚砜) (15/85,wt.%) 共溶体系中以获取纳米纤维素溶液, 最后通过溶剂浇筑法制备透明抗紫外纳米纤维素膜。

3) 研究结果: 傅里叶红外光谱分析 (FTIR) 结果显示, 高功率微波液化后的竹材细胞在  $1735\text{ cm}^{-1}$  处的红外峰消失, 表明微波液化竹材细胞的大部分半纤维素被去除; 液化竹材纤维细胞的木质素含量高于液化竹材薄壁细胞, 分别为 9.77% 和 4.62%; 透射电镜 (TEM) 结果显示, 溶解后的竹材纤维细胞和竹材薄壁细胞的直径分别为 3.7 nm 和 4.2 nm; X 射线衍射 (XRD) 结果表明, 液化竹材纤维细胞和液化竹材薄壁细胞的结晶度分别为 72.68% 和 64.06%, 高于未微波液化的纤维细胞 (61.97%) 和薄壁细胞 (48.52%), 且再生后的纳米纤维素由纤维素 I 晶型转变到了纤维素 II 型; 紫外-可见光分析表明, 液化纤维素细胞纳米纤维素膜和液化薄壁细胞纳米纤维素膜在 800 nm 处的透光率分别为 73.56% 和 78.52%, 且液化纤维细胞纳米纤维素膜的紫外屏蔽性能优于液化薄壁细胞纳米纤维素膜, 其对 UVA 波段和 UVB 波段的吸收率分别达 82% 和 99% 以上; 除此之外, 抗紫外纳米纤维素膜也具有较好的拉伸强度 (15-25 MPa) 和热稳定性。

4) 研究结论: 高功率微波选择性液化可快速获得木质素含量在 4-10% 的竹材细胞, 通过 TBAA/DMSO 共溶体系可获得直径  $<10\text{ nm}$  的纳米纤维素, 同时微波选择性液化竹细胞中含有的木质素能较均匀的分散在纳米纤维素膜中, 所制备的纳米纤维素膜具有优异的紫外线屏蔽性能, 同时也保持了较高的透明度; 除此之外, 原料中的木质素含量也会对其成膜状态、紫外吸收性能以及力学性能产生影响; 微波选择性液化与 TBAA/DMSO 共溶体系相结合可作为一种简单易行的方法制备透明抗紫外纳米纤维素膜。

**关键词:** 竹材; 紫外线屏蔽; 纳米纤维素膜; 微波液化; 四丁基醋酸铵

# Transparent and UV-absorbing nanocellulose films prepared by directly dissolving microwave liquefied bamboo in TBAA/DMSO co-solvent system

Huijuan Shao, Jiulong Xie

(College of Forestry, Sichuan Agricultural University, Chengdu, Sichuan)

## Abstract:

1) Research objective: UV-blocking plastic film is non-renewable, difficult to degrade and recycle after using, causing serious environmental pollution. With the enhancement of people's awareness of environmental protection. The preparation of bio-based UV-blocking films using renewable, green and widely sourced lignocellulosic biomass has attracted much attention and research.

2) Research method: High power microwave was used to selectively liquefy the residues of bamboo processing, most of these residues are the inner bamboo portions that are rich in parenchyma cells and the outer portions that are rich in vascular bundles. Then, the above-mentioned liquefied bamboo parenchyma cells and liquefied bamboo vascular bundles were dissolved in TBAA (tetrabutylammonium acetate)/DMSO (dimethyl sulfoxide) (15/85, wt.%) co-solvent at room temperature without other treatment to obtain nanocellulose solution. Finally, transparent and UV-blocking nanocellulose films were prepared by solvent-casting.

3) Research results: The results of FTIR showed that the peak at 1735  $\text{cm}^{-1}$  assigned to C=O stretching vibration of carboxyl and acetyl groups in hemicellulose disappeared, indicating the removal of a large part of hemicellulose in liquefied bamboo cells. The lignin content of liquefied bamboo vascular bundles was higher than that of liquefied bamboo parenchyma cells, which were 9.77% and 4.62%, respectively. TEM showed the diameter of liquefied bamboo cells was small, 4.62% and 9.77% for liquefied bamboo parenchyma cells and liquefied bamboo vascular bundles, respectively. The results of XRD showed that the crystallinity of liquefied bamboo vascular bundles and liquefied bamboo parenchyma cells were 72.68% and 64.06% respectively, which were higher than that of non-microwave liquefied vascular bundles (61.97%) and parenchyma cells (48.52%), and the regenerated nanocellulose crystallinity structure changed from cellulose I structure to cellulose II structure. UV-vis analysis showed that the transmittance of liquefied vascular bundles nanocellulose films and liquefied parenchyma cell nanocellulose films at 800 nm were 73.56% and 78.52% respectively, and the UV-blocking performance of liquefied vascular bundles nanocellulose film was better than that of liquefied parenchyma cell nanocellulose film, and its UVA and UVB blocking efficiency were more than 82% and 99%, respectively. In addition, the UV-blocking

nanocellulose film also had good tensile strength (15-25 MPa) and thermal stability.

4) Research conclusion: High power microwave selectively liquefaction can quickly obtain bamboo cells with lignin content of 4-10%. Nanocellulose with diameter less than 10 nm can be obtained through TBAA/DMSO co-solvent dissolution system, and lignin retained in the bamboo cells can be evenly dispersed in nanocellulose film. The prepared nanocellulose film had excellent UV-blocking performance. Meanwhile, it also maintained high transparency. In addition, the lignin retained in the bamboo cells will also affect its film-forming, UV absorption properties and mechanical properties. In conclusion, microwave selective liquefaction combined with TBAA/DMSO co-solvent system can be used as a simple method to prepare transparent and UV-blocking nanocellulose films.

**Keywords:** Bamboo; UV-shielding properties; Nanocellulose film; Microwave liquefaction; Tetrabutylammonium acetate

# 接骨木和西洋接骨木的构造对比

张静涵 骆嘉言\*

(张静涵, 南京林业大学材料科学与工程学院; 骆嘉言, 南京林业大学材料科学与工程学院)

**摘要:** 接骨木 (*Sambucus williamsii* Hance)、西洋接骨木 (*Sambucus nigra* Linn) 都是五福花科 (ADOXACEAE) 接骨木属 (*Sambucus*) 树种。接骨木产于中国黑龙江、吉林、辽宁、河北、山西、陕西、甘肃、山东、江苏、安徽、浙江、福建、河南、湖北、湖南、广东、广西、四川、贵州及云南等省区。西洋接骨木分布在欧洲以及中国的山东、上海、江苏等地。本文以生长在南京林业大学内的接骨木和产自捷克的西洋接骨木为研究对象, 对比二者的构造区别。

接骨木生长轮明显, 环孔材且有半环孔材的趋势; 导管呈椭圆形和多角形; 管孔组合有单管孔、径列复管孔、管孔团, 径列复管孔 2-6 个管孔。管孔最大弦向直径可达 77 $\mu\text{m}$ , 平均 51 $\mu\text{m}$ , 导管平均长度 400 $\mu\text{m}$ 。单穿孔, 穿孔板甚倾斜, 导管间纹孔互列式, 纹孔呈多角形, 不具有附物纹孔。导管—射线间纹孔为同管间纹孔式。木纤维细胞壁薄至厚, 平均木纤维长度 986 $\mu\text{m}$ , 纤维具有螺纹加厚(解离后可见)。轴向薄壁组织很少, 轮界状(带宽 2~3 个细胞), 轴向薄壁细胞束由 3-4 个细胞组成。具有多列木射线, 射线宽 2-6 个细胞, 射线高度 6-26 个细胞, 最高可达 28 个细胞; 部分木射线全部由横卧细胞组成, 部分由横卧细胞和一排直立细胞组成。木射线水平端壁有大量纹孔存在。横切面可见射线内有内含物存在。未见叠生构造和胞间道。晶体未见。

西洋接骨木生长轮明显, 半环孔材。管孔组合形式有单管孔、复管孔、管孔团, 其中径列复管孔由 2-4 个管孔组成; 管孔呈径向排列、斜列。管孔数最大弦向直径可达 50 $\mu\text{m}$ , 平均 31 $\mu\text{m}$ , 管孔长度平均 427 $\mu\text{m}$ 。单穿孔, 穿孔板甚倾斜。管间纹孔互列式, 纹孔呈多角形, 中等大小, 未见附物纹孔。射线—导管间纹孔为同管间纹孔式。木纤维细胞壁薄至厚, 平均纤维长度 994 $\mu\text{m}$ 。轴向薄壁组织不发达, 轮界状, 轴向薄壁细胞束由 2-5 个细胞组成。具多列木射线, 射线宽度 2-3 个细胞, 高度 5-20 个细胞, 最高可达 37 个细胞; 射线由横卧细胞和 2 排直立细胞组成, 射线水平壁存在有大量纹孔。未见叠生构造。导管和射线内偶见黄色树胶。晶体未见。

通过对比可知, 接骨木与西洋接骨木在构造上略有差别: 接骨木径列复管孔居多, 而西洋接骨木则是管孔团居多; 接骨木管孔的弦向直径(平均 51 $\mu\text{m}$ )与西洋接骨木(平均 50 $\mu\text{m}$ )差异不大; 在纤维长度和导管长度上, 则是西洋接骨木(平均 994 $\mu\text{m}$ ; 平均 427 $\mu\text{m}$ )略长于接骨木(平均 986 $\mu\text{m}$ ; 平均 400 $\mu\text{m}$ ), 接骨木的纤维具有螺纹加厚, 而在西洋接骨木中并未发现; 接骨木的木射线相较于西洋接骨木来说, 略宽一点, 西洋接骨木的木射线更为细长些。

**关键词:** 接骨木; 西洋接骨木; 木材构造

# Structural comparison of *Sambucus Williamsii* Hance and *Sambucus nigra* L.

Zhang Jinghan, Luo Jiayan\*

(Zhang Jinghan, college of Materials Science and Engineering, Nanjing Forestry University; Luo Jiayan, college of Materials Science and Engineering, Nanjing Forestry University)

**Abstract:** *Sambucus Williamsii* Hance and *Sambucus nigra* L. are species of *Sambucus* belonging to ADOXACEAE. *Sambucus Williamsii* is produced in Heilongjiang, Jilin, Liaoning, Hebei, Shanxi, Shaanxi, Gansu, Shandong, Jiangsu, Anhui, Zhejiang, Fujian, Henan, Hubei, Hunan, Guangdong, Guangxi, Sichuan, Guizhou, Yunnan and other provinces in China. *Sambucus nigra* L. is distributed in Europe and Shandong, Shanghai, Jiangsu and other places in China. This paper takes the *Sambucus Williamsii* grown in Nanjing Forestry University and the *Sambucus nigra* grown in the Czech Republic as the research object to compare their structural differences.

*Sambucus Williamsii*: Growth ring boundaries distinct. Vessels porosity is ring-porous or semi-ring-porous. The shapes of vessels in the cross section are ovoid or angular. Vessel groupings include solitary, vessels in radial multiples of 2~6 and vessels clusters. The maximum tangential diameter of vessel lumina is 77 $\mu\text{m}$ , average 51 $\mu\text{m}$  and the average length is 400 $\mu\text{m}$ . The perforation plates are simple and parallel or extraordinary inclined. The arrangement of intervessel pits is alternate and the shape of pits is polygonal without vestured pits. The vessels-ray pits with distinct borders, similar to intervessels pits in size and shape throughout the ray cell. Fibers with thin to thick walls and the average length of fibers is 986 $\mu\text{m}$ . Helical thickenings in fiber elements can be found. *Sambucus Williamsii* have rare axial parenchyma. The arrangement of axial parenchyma are marginal bands with 2-3 cells wide. It has multiple rows of wood rays, the width of the rays is 2-6 cells and the height of the rays is 6-26 cells, up to 28 cells. Part of the wood ray is entirely composed of procumbent cells, and part of it is with one row of upright cells. Storied structure and intercellular canals were not found.

*Sambucus nigra* L.: Growth ring boundaries distinct and wood semi-ring-porous. Vessel groupings include solitary, vessels in radial multiples of 2~4 and vessels clusters. Vessels in diagonal and radial pattern. The maximum tangential diameter of vessel lumina is 50 $\mu\text{m}$ , average 31 $\mu\text{m}$  and the average length is 427 $\mu\text{m}$ . The perforation plates are simple and parallel or extraordinary inclined. The arrangement of intervessel pits is alternate and the shape of pits is polygonal without vestured pits. The vessels-ray pits with distinct borders, similar to intervessels pits in size and shape throughout the ray cell. Fibers with thin to thick walls and the average length of fibers is 994 $\mu\text{m}$ . It has rare axial parenchyma. The arrangement of axial parenchyma are marginal bands and axial parenchyma cell bundle consists of 2-5 cells. *Sambucus nigra* has multiple rows of

wood rays, the width of the rays is 2-3 cells and the height of the rays is 5-20 cells, up to 37 cells. Part of the wood ray is entirely composed of procumbent cells, and part of it is with two rows of upright cells. Storied structure and intercellular canals were not found.

By comparison, *Sambucus Williamsii* and *Sambucus nigra* are slightly different in structure. *Sambucus Williamsii* has the majority of vessels in radial multiples, while *Sambucus nigra* has mostly vessels clusters; the tangential diameter of the *Sambucus Williamsii* vessels (average 51 $\mu$ m) is not much different from that of *Sambucus nigra* (average 50 $\mu$ m). In terms of fiber and vessel length, *Sambucus nigra* (average 994 $\mu$ m; average 427 $\mu$ m) is slightly longer than *Sambucus Williamsii* (average 986 $\mu$ m; average 400 $\mu$ m). *Sambucus Williamsii* has helical thickenings in fiber elements, which is not found in *Sambucus nigra*. It was found that the wood rays of *Sambucus Williamsii* are slightly wider than that of *Sambucus nigra*, and the wood rays of *Sambucus nigra* are more slender.

**Keywords:** *Sambucus Williamsii*; *Sambucus nigra*; wood features

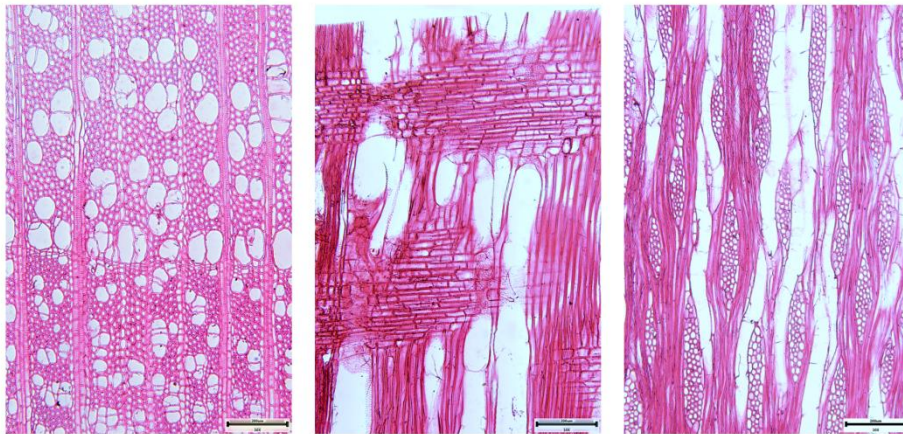


图 1 接骨木三切面

Figure1 Tri-section of *Sambucus williamsii*

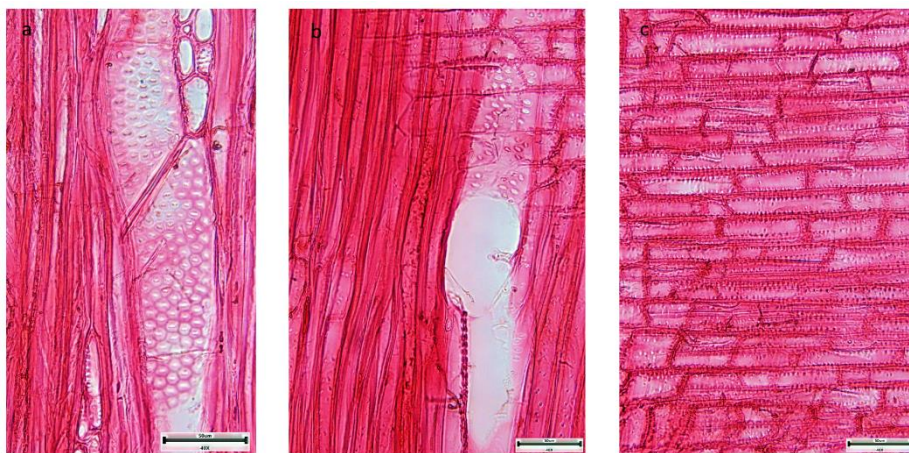


图 2 接骨木纹孔 (a:管间纹孔 b:射线-导管间纹孔 c:射线水平壁纹孔)

Figure2 Pits of *Sambucus williamsii* (a: Intervessel pits b: Vessel-ray pits c: Ray horizontal wall pits)





图3 接骨木纤维螺旋纹加厚

Figure3 Helical thickenings in fiber of *Sambucus williamsii*

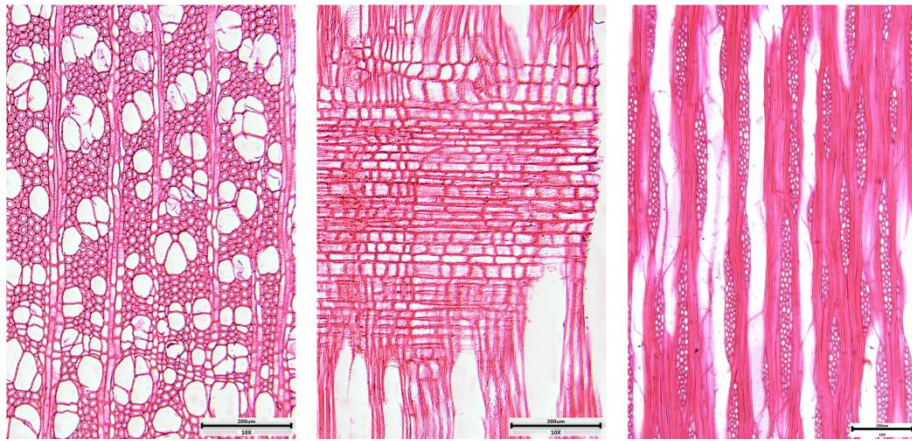


图4 西洋接骨木三切面

Figure4 Tri-section of *Sambucus nigra*

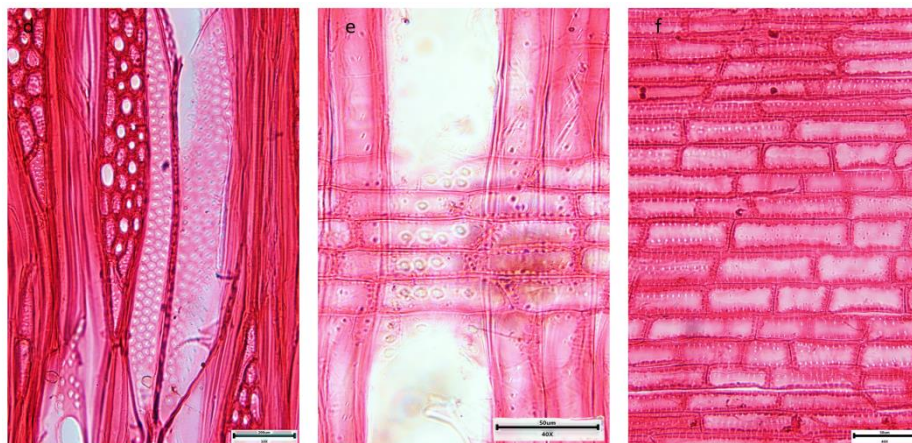


图5 西洋接骨木纹孔 (d:管间纹孔 e:射线-导管间纹孔 f:射线水平壁纹孔)

Figure5 Pits of *Sambucus nigra* (d: Intervessel pits e: Vessel-ray pits f: Ray horizontal wall pits)

# 山桐子木材材性研究

陈燕<sup>1</sup> 胡馨芸<sup>1</sup> 陈果希<sup>1</sup> 齐锦秋<sup>1</sup> 谢九龙<sup>1</sup> 姜永泽<sup>1</sup> 罗建勋<sup>2</sup>

(1 四川农业大学林学院; 2 四川省林业科学研究院)

**摘要:** 为了全面了解山桐子木材的材性状况, 对四川省 35 年生山桐木材的解剖性质、物理力学性质及抽提物进行了较为系统的研究。实验材料采集方法和主要物理力学性质测定方法按照相关国家标准进行; 采用永久切片法和离析法进行山桐子解剖性质的测定和分析; 利用乙酸乙酯和无水乙醇对山桐子试样进行溶剂抽提, 对抽提物进行成分分析。结果显示: 山桐子平均年轮宽度为 3.94mm, 最大宽度可达 13.0mm, 达到国家速生材生长标准, 属于优质速生用材树种。山桐子纤维形态指标平均值分别为: 长度 1398.77 $\mu\text{m}$ , 宽度 32.56 $\mu\text{m}$ , 双壁厚 5.83 $\mu\text{m}$ , 纤维腔径 14.21 $\mu\text{m}$ ; 导管形态指标平均值分别为: 长度 633.55 $\mu\text{m}$ , 宽度 90.28 $\mu\text{m}$ , 双壁厚 7.26 $\mu\text{m}$ , 导管腔径 75.15 $\mu\text{m}$ 。山桐子木材在含水率为 11.03% 时, 气干密度均值为 0.44g/cm<sup>3</sup>, 变化范围为 0.35~0.51g/cm<sup>3</sup>, 山桐子木材顺纹抗压强度 35.07MPa, 抗弯强度 65.09MPa, 从髓心到树皮方向, 山桐子力学强度逐渐增大。从气干到绝干, 其径向、弦向、轴向、体积干缩率分别为 1.61%、3.52%、0.44%、4.15%; 从湿材到绝干, 其径向、弦向、轴向干缩率分别为 3.29%、6.91%、0.89%。干缩率较小, 表明山桐子木材尺寸稳定性较好。山桐子耐腐, 山桐子木材心材、过渡层、边材的乙醇抽提物质量分数分别为 0.25%、0.75%、1.15%, 含量较低, 但成份组成中 2, 2'-亚甲基双-(4-甲基-6-叔丁基苯酚) 为应用极广泛的酚类抗氧化剂。乙酸乙酯抽提物主要成分为 2, 4-二叔丁基苯酚, 可用于制造天然橡胶及合成胶防老剂。基于以上结论, 质地轻软的山桐子, 易干燥, 稳定性好, 耐腐蚀, 可用于一次性可回收木制品及纸浆制作, 同时也是良好的家具用材。

**关键词:** 山桐子; 解剖性质; 物理性质; 力学性质; 抽提物



## Study on wood properties of *Idesia polycarpa*

Chenyan<sup>1</sup>, HuXinyun<sup>1</sup>, ChenGuoxi<sup>1</sup>, QiJinjiu<sup>1</sup>, XieJiulong<sup>1</sup>, JiangYongze<sup>1</sup>, LuoJianxun<sup>2</sup>

(1 The college of forestry, Sichuan agricultural university; 2 Sichuan Academy of Forestry)

**Abstract:** In order to comprehensively understand the wood properties of the wood of *Idesia polycarpa*, the anatomical properties, physical and mechanical properties and extracts of the 35-year-old *Idesia polycarpa* wood in Sichuan Province were systematically studied. The collection methods of the experimental materials and the main physical and mechanical properties determination methods are carried out in accordance with the relevant national standards; the permanent section method and the isolation method are used for the determination and analysis of the anatomical properties of *Idesia polycarpa*; The components of the ethyl acetate and absolute ethanol extract were analyzed. The results showed that the average annual ring width of *Idesia polycarpa* was 3.94mm with maximum width of 13.0mm, which reached the national fast-growing timber growth standard, which meet with requirements for the high-quality fast-growing timber species. The average fiber length, width, wall thickness, lumen diameter were 1398.77 $\mu$ m, 32.56 $\mu$ m, 5.83 $\mu$ m, 14.21 $\mu$ m, respectively; while those mean values for catheter were 633.55 $\mu$ m, 90.28 $\mu$ m, 7.26 $\mu$ m, 75.15 $\mu$ m, respectively. The average air-dry density of *Idesia polycarpa* wood is 0.44g/cm<sup>3</sup> with the variation range of 0.35~0.51g/cm<sup>3</sup>. The compressive strength along the grain and the bending strength is 35.07MPa and 65.09MPa, respectively. From the center to the bark, the mechanical strength of *Idesia polycarpa* gradually increases. From air-dry to absolutely dry, the radial, tangential, axial, and volume shrinkage rates are 1.61%, 3.52%, 0.44%, 4.15%, respectively; while from wet to absolutely dry, the radial, tangential, axial, and volume shrinkage rates were 3.29%, 6.91%, and 0.89%, respectively. The low shrinkage rate indicated that the better dimensional stability of the *Idesia polycarpa* wood. *Idesia polycarpa* is resistant to decay, and the content of ethanol extracts of *Idesia polycarpa* heartwood, transition layer and sapwood are 0.25%, 0.75% and 1.15% respectively. 2,2'-methylenebis-(4-methyl-6-tert-butylphenol) and 2,4-di-tert-butylphenol were the main components in the ethanol extract, which is widely used as phenolic antioxidant rubber antioxidant, respectively. Based on the above conclusions, the light and soft *Idesia polycarpa* wood, with good dimensional stability, decay resistance were ideal resources for recyclable wood products, pulp production as well as furniture.

**Keywords:** *Idesia polycarpa*; anatomical properties; Physical properties; Mechanical properties; Extracts

# 南京出土宋代棺木用材的树种鉴定及复原加固

吕偲琪<sup>1</sup> 翟胜丞<sup>1,\*</sup> 潘彪<sup>1</sup> 王军<sup>2</sup>

(1 南京林业大学材料科学与工程学院, 南京, 210037; 2 南京市考古研究院, 南京, 210004)

**摘要:** 考古木材所用材树种鉴定对于了解我国各各历史时期不同树种的生长、分布及利用情况, 对于研究当地历史、社会经济、不同历史时期气候情况以及探讨古人选材用材的智慧具有重要意义。本文通过对南京出土的宋代墓葬群十余个棺木用材进行取样和三切面切片观察, 根据三切面显微构造特征对样品进行树种鉴定。使用荧光显微镜观察古木细胞壁木质素自发荧光现象, 以定性判断木材的降解情况, 为木质文物的修复及保护提供理论依据。出土古木的润胀复原及加固一直是古木保护研究的热点, 本研究使用不同浓度的氯化胆碱溶液及 18wt% NaOH 溶液对 40 $\mu\text{m}$  厚度的干缩古木横切面切片和 5mm x 5mm x 5mm (T\*R\*L) 的木块进行浸渍处理, 观察浸渍前后横切面管胞润胀程度及管胞形态变化, 测量浸渍前后平均管胞面积变化, 计算其润胀度; 并进一步使用辛二酸复合溶液对复原后的木块进行加固处理, 测量木块处理前后增重率及加固收缩率。使用傅里叶变换红外光谱仪 (FTIR) 分析干缩木块、复原木块及加固木块细胞壁化学成分变化。研究表明: (1) 该墓葬群出土棺木用材均为硬松 (*Pinus subgenus Diploxylon*)。与正常材相比, 棺木用材细胞壁主要化学组分木质素所产生的自发荧光效应有所减弱, 表明木质素发生了降解。(2) 氯化胆碱浸渍后处理液的颜色基本无变化, 而 NaOH 浸渍液呈现棕色, 表明 NaOH 浸渍处理后样品木质素析出。50 $^{\circ}\text{C}$  时, 5% 的氯化胆碱溶液浸渍处理的切片管胞润胀效果最好, 平均管胞面积增大了 32.8%。(3) 使用 2%~25% 的辛二酸复合溶液加固木块, 结果显示, 当加固液浓度达到 20% 时, 古木试样的增重率达到峰值, 为 108.64%, 且试样加固收缩率最小, 为 0.34%, 该浓度加固液对古木加固的效果最佳。(4) 红外光谱图各主要化学组分特征峰显示在长期的埋藏环境中, 木材的主要化学组分发生了变化, 纤维素、半纤维素的降解严重, 不同溶液处理后木材试样的化学组分发生了不同变化。

**关键词:** 考古木材; 树种鉴定; 润胀复原; 加固

# Tree species identification, restoration and reinforcement of coffins of Song Dynasty unearthed in Nanjing

Lv Siqi<sup>1</sup>, Zhai Shengcheng<sup>1,\*</sup>, Pan Biao<sup>1</sup>, Wang Jun<sup>2</sup>

(1 College of Materials Science and Engineering, Nanjing Forestry University, Nanjing 210037; 2 Nanjing Institute of Archaeology, Nanjing Forestry University, Nanjing 210004)

**Abstract:** Wood identification, especially in archaeological wood, is of great significance to get to know the growth, distribution and utilization of different species, which were from different historical periods, and it is vital to reflect local history, social economy, climate conditions and the wisdom of ancient people in selecting materials and materials. In this paper, the samples were identified by three-section microstructure characteristics after sampling more than ten coffins from the Song Dynasty tombs unearthed in Nanjing and observing three-section sections. The fluorescence microscope was used to observe the auto-fluorescence phenomenon of lignin in ancient wood cell walls, which was quantitative researched through the degradation of wood and provided a theoretical basis for the restoration and protection of wood cultural relics. The swelling restoration and reinforcement of unearthed ancient woods has always been a hotspot, this paper used different concentrations of choline chloride (CHCINO) solution and NaOH (18wt%) to impregnate ancient wood cross-section slices (40 $\mu$ m) and 5mm x 5mm x 5mm (T\*R\*L) wood blocks, then observe the tracheid swelling degree and tracheid morphology change of the transverse section before and after immersion, and measure the average tracheid area change before and after immersion, then calculated the swelling degree, after then the suberic acid composite solution was used to strengthen the restored wood block, and measure the weight gain rate and reinforcement shrinkage rate of the wood block before and after treatment. Fourier Transform Infrared Spectrometer (FTIR) was used to analyze the chemical composition change of the cell walls of the shrunken wood, restored wood and reinforced wood blocks. The results of study showed that: (1) The coffins unearthed from the tombs are hard pine (*Pinus* subgenus *Diploxylon*). Compared with normal wood, the autofluorescence effect of lignin declined and indicated the degradation of lignin, which is the main chemical component of the cell wall of coffin wood. (2) The color of the treatment solution was basically unchanged after the choline chloride dipping, while the NaOH dipping solution was brown, indicating that the sample lignin precipitated after the NaOH dipping treatment. At 50°C, the slice immersed in 5% choline chloride solution had the best swelling effect, and the average tracheid area increased by 32.8%. (3) Using 2%~25% suberic acid composite solution to reinforce the wood block. The results showed that the best effect on ancient wood reinforcement was at the concentration of 20%, the weight gain of the ancient wood sample reached the peak value (108.64%), and the specimen reinforcement shrinkage is the smallest (0.34%). (4) The main peaks in the infrared

spectrum showed that the main chemical components had changed in the long-term buried environment, and the degradation of cellulose and hemicellulose was serious. After treatment with different solutions, the chemical composition of the wood sample has undergone different changes.

**Keywords:** Archaeological wood; tree species identification; swelling and recovery; reinforcement

# 水青树特殊管胞的分布位置及其形态特征的研究

任安捷 李茜然 李婷 勇璐 潘彪\*

(南京林业大学材料科学与工程学院, 南京 210037)

**摘要:** 水青树 (*Tetracentron sinense*) 为单种属落叶乔木, 是第三纪古老孑遗珍稀植物。在较早的研究中, 水青树被描述为次生木质部缺乏导管分子。后有学者发现水青树中存在具有导管基因的一类特殊管胞, 是存在于针叶树向阔叶树演化过程中的一种特征。研究特殊管胞的形态及分布有助于解释维管组织输导机理及树木细胞的演化规律。为了解水青树特殊管胞形态及分布, 探究导管分子演化过程, 通过切片和解离技术, 借助光学和电子显微镜对 34 年生水青树进行显微观察。

结果表明: 1.横切面上, 特殊管胞紧邻木射线, 沿径向整齐且连续排列并贯穿年轮界限, 排列方式多为一列, 偶见两列。纵切面上, 特殊管胞单独或纵向端接, 排列方式多为单列, 偶见两列 (如图 1)。2.特殊管胞平均长度为  $286.44 \pm 41.47 \mu\text{m}$ , 平均宽度为  $55.22 \pm 9.14 \mu\text{m}$ , 主要存在三种类型: 两头尖削的纺锤形无端壁, 有一个或两个倾斜侧面壁 (如图 2)。3. 弦面壁上布满特殊管胞之间的具缘纹孔, 呈对列、互列偶见梯状排列; 径面壁上存在与射线细胞间的单纹孔, 呈大圆形至椭圆形, 每区域 1-4 横列, 2-10 个纹孔 (如图 3); 径面壁上与正常管胞间无纹孔。水青树特殊管胞分布有一定规律, 其长度远小于水青树正常管胞, 弦向宽度略大于正常管胞。其纹孔类型和排布规律与一般阔叶材树种的导管壁上纹孔的类型和排布规律相似。特殊管胞形状不同于一般导管, 处于由管胞向导管进化的一种中间状态, 标志着该类细胞的一定演化水平。

**关键词:** 水青树; 木材解剖; 管胞形态

# Study on the formation position and morphological characteristics of special tracheid in *Tetracentron sinense*

Anjie Ren, Xiran Li, Ting Li, Lu Yong, Biao Pan\*

(College of Materials Science and Engineering, Nanjing Forestry University, Nanjing 210037)

**Abstract:** *Tetracentron sinense*, a single deciduous tree, is a rare and ancient relict plant of Tertiary. In earlier studies, it was described as secondary xylem lacking vessel. Some scholars have found that there is a special tracheid with the gene of vessel in the *Tetracentron sinense*. It is a feature of the evolution process of hardwood and softwood. The study of the morphology and distribution of special tracheid is helpful to explain the mechanism of vascular tissue transport and the evolution of special cells of *Tetracentron sinense*. In order to understand the morphology and distribution of special tracheid and explore the changes in its evolution process, the 34-year-old *Tetracentron* was anatomically analyzed with optical and electron microscopes through slicing and dissociation techniques.

The results showed that: 1. on the cross section, the special tracheid neatly and continuously arranged along the radial direction and run through the growth ring boundaries, mostly one column and occasionally two columns. On the longitudinal section, special tracheids are isolated or longitudinally terminated, mostly single columns, and occasionally two columns (Figure 1). 2. There are three types of special tracheids: fusiform without end wall, rhombic with one or two sidewalls (Figure 2), with an average length of  $286.44 \pm 41.47 \mu\text{m}$  and an average width of  $55.22 \pm 9.14 \mu\text{m}$ . 3. There were a large number of bordered pits on the wall in tangential section, which were arranged in opposite, alternate and scalariform pitting. The single pits on the radial wall were rounded or ellipse. There were 2-10 pits, arranged in 1-4 rows in per region. There were no pits between special tracheid and tracheid (Figure 3). The distribution of special tracheids has certain regularity. Compared with normal tracheids, the special tracheids are much shorter in length, and the tangential width are slightly larger. The type and arrangement of the pits are similar to those of the pits on the wall of general hardwood species. The shape of the special tracheid is different from the normal vessel in the hardwood, and it is in an intermediate state of the evolution from tracheid to vessel, marking a certain level of evolution of this type of cell.

**Keywords:** *Tetracentron sinense*; Wood anatomy; Tracheid morphology

# 淹水环境对中山杉管胞壁上纹孔形态特征的影响

赵欣然 郑欣欣<sup>1</sup> 潘彪<sup>1,\*</sup>

(1 南京林业大学材料科学与工程学院, 南京 210037)

**摘要:** 中山杉 (*Taxodium hybrid* 'Zhongshanshan') 中山杉是落羽杉属 (*Taxodium*) 杂交选育出的优良无性系品种, 适应生境广, 这与它的构造存在相关性。纹孔在树木生长过程中纹孔起到疏通和相邻细胞间水分和养分的生理作用, 纹孔的形态、数量和排列类型对水分和液体的渗透具有很大影响。为探究淹水对中山杉纹孔数目尺寸和超微构造的影响, 比较研究了淹水4年中山杉基部(离地高度约0.3 m)、和胸高处(离地高度1.3m)、无淹水胸高处的中山杉木芯在光学显微镜下纹孔数量及纹孔尺寸的差异, 扫描电镜下纹孔膜形态的变化。

结果显示:

1. 纹孔数量: 淹水后中山杉基部早材管胞单位长度上具缘纹孔对数量为137个/mm 胸高处早材管胞壁单位长度上具缘纹孔对数量平均为136个/mm, 两者较为接近, 无显著差异; 正常生境下胸高处早材管胞壁单位长度具缘纹孔对数量平均为105个/mm, 与淹水胸高处纹孔密度存在极显著差异 ( $p < 0.01$ )。

2. 纹孔尺寸: 淹水后中山杉基部及胸高处早晚材管胞壁具缘纹孔膜直径的均值分别为14.44 $\mu\text{m}$ 和12.21 $\mu\text{m}$ 以及14.95 $\mu\text{m}$ 和10.37 $\mu\text{m}$ 。淹水后基部早材管胞壁具缘纹孔膜直径小于胸高处, 但无显著差异; 晚材管胞壁具缘纹孔膜直径大于胸高处, 且两者存在显著差异 ( $p < 0.01$ )。正常生境下中山杉胸高处早晚材管胞壁具缘纹孔膜直径均值分别为13.73 $\mu\text{m}$ 和7.69 $\mu\text{m}$ , 均小于淹水环境下中山杉胸高处早晚材管胞壁具缘纹孔膜直径, 且存在极显著差异 ( $p < 0.01$ )。

3. 纹孔超微构造: 淹水环境与正常生境下中山杉管胞壁具缘纹孔膜形态无显著差异, 根据观察结果, 可以将中山杉纹孔膜形态分为三类: (1) 完全封闭: 在纹孔塞边缘无肉眼可见微孔。(2) 有均匀微孔: 塞缘微纤丝由纹孔塞发射而出彼此之间形成水滴状或长圆形微孔。(3) 开放: 纹孔塞出现偏移现象, 纹孔膜出现大面积孔洞。

结论:

淹水环境下中山杉胸高处管胞单位长度上具缘纹孔对数量增加, 具缘纹孔膜直径显著增大。这些变化更利于水分疏导, 提高了树木横向输水效率。

**关键词:** 中山杉; 淹水环境; 木材解剖构造; 纹孔形态

# Effects of flooding environment on morphological characteristics of pit on tracheid wall of *Taxodium* hybrid

Zhao Xinran<sup>1</sup>, Zheng Xinxin<sup>1</sup>, Pan Biao<sup>1,\*</sup>

**Abstract:** *Taxodium* hybrid 'Zhongshanshan' is an excellent clonal variety bred by hybridization of the genus *Taxodium* and adapted to a wide range of habitats, which is related to its structure. In the process of tree growth, pit plays a physiological role in dredging and water and nutrients between adjacent cells. The morphology, number and arrangement type of pit have a great influence on the permeability of water and liquid. In order to study the effect of waterlogging on the pit number, size and ultrastructure of *Taxodium* hybrid, the differences of pit number and size under optical microscope and the changes of pit membrane morphology under scanning electron microscope were compared among *Taxodium* hybrid cores at the base (about 0.3 m above the ground), chest height (1.3 m above the ground) and no waterlogging chest height after 4 years of waterlogging.

## RESULTS:

1. Number of pits: after flooding, the number of pit pairs with edge on the unit length of tracheid cells in the base of *Taxodium* hybrid was 137 / mm, and the average number of pits with edge on the unit length of tracheid cell wall in the chest height of *Taxodium* hybrid was 136 / mm, which were close to each other and had no significant difference. In normal habitat, the average number of pits per unit length of earlywood tracheid cell wall was 105 / mm, which was significantly different from that of flooded chest height ( $p < 0.01$ ).

2. Pit size: After flooding, the mean values of the pith membrane diameter of the basal and thoracic cell walls were 14.44 $\mu\text{m}$  and 12.21 $\mu\text{m}$ , and 14.95 $\mu\text{m}$  and 10.37 $\mu\text{m}$ , respectively. After flooding, the diameter of marginal pit membrane on the cell wall of basal earlywood was smaller than that at chest height, but there was no significant difference. The diameter of marginal pore membrane on the cell wall of latewood was larger than that at chest height, and there was a significant difference between the two ( $p < 0.01$ ). In the normal habitat, the mean diameter of the pit membrane of the early and late woods at the chest height of *Taxodium* hybrid was 13.73 $\mu\text{m}$  and 7.69 $\mu\text{m}$ , respectively, which was smaller than that of the cell wall of the early and late woods at the chest height of *Taxodium* hybrid in the flooded environment, and there was a significant difference ( $p < 0.01$ ).

3. Ultrastructure of the pit: There is no significant difference in the morphology of the pit membrane between the waterlogged environment and the normal habitat. According to the observation results, the pit membrane morphology can be divided into three categories: (1) Complete closure: there is no visible micro pores in the pit plug margin. (2) There are uniform micropores: the microfibrils on the torus edge emit from the groove plug to form water droplets or long circular



micropores. (3) Opening: the torus appears offset phenomenon, large area holes appear in the pit membrane.

#### CONCLUSION:

Under the flooding environment, the number of ciliated pit pairs per unit length of tracheid at the breast height of *T. chinensis* increased, and the diameter of ciliated pit membrane increased significantly. These changes are more conducive to water diversion and improve the lateral water conveyance efficiency of trees.

**Keywords:** *Taxodium* hybrid; flooded environment; Wood Anatomy; pit morphology

# 钝叶黄檀木材 DNA 提取及条形码鉴定

甘昌涛<sup>1,3</sup> 曹秀龙<sup>2,3</sup> 邱坚<sup>2,3,\*</sup>

(1 西南林业大学艺术与设计学院, 云南 昆明 650224; 2 西南林业大学材料科学与工程学院, 云南 昆明 650224; 3 西南林业大学云南省木材胶黏剂及胶合制品重点实验室)

**摘要:** 为了以 DNA 条形码鉴定珍稀保护钝叶黄檀树种, 以 CTAB 试剂盒法和 CTAB-SDS 法提取新鲜木材总 DNA, 针对 5 个条形码设计出 15 对引物, 分别进行 PCR 扩增, 并对 PCR 产物进行测序和序列比对分析。结果表明: 2 种方法均能从新鲜木材中提取优质 DNA, CTAB 试剂盒法提取的 DNA 纯度高但浓度低, CTAB-SDS 法提取的 DNA 浓度高但有少量蛋白残留, 但 2 种方法提取的 DNA 均能满足 PCR 扩增的需要。15 条引物中有 13 条被成功扩增, 其中只有 10 条成功测序, 10 条序列中只有 6 条可以通过在线比对工具 BLAST 鉴定到种。基于 *trnL*、*psbA-trnH*、*matK*、*rbcL* 序列构建的系统发育树表明 *D. obtusifolia*、*D. hupeana*、*D. cochinchinensis* 和 *D. sissoo* 亲缘关系较为接近 (图 1)。

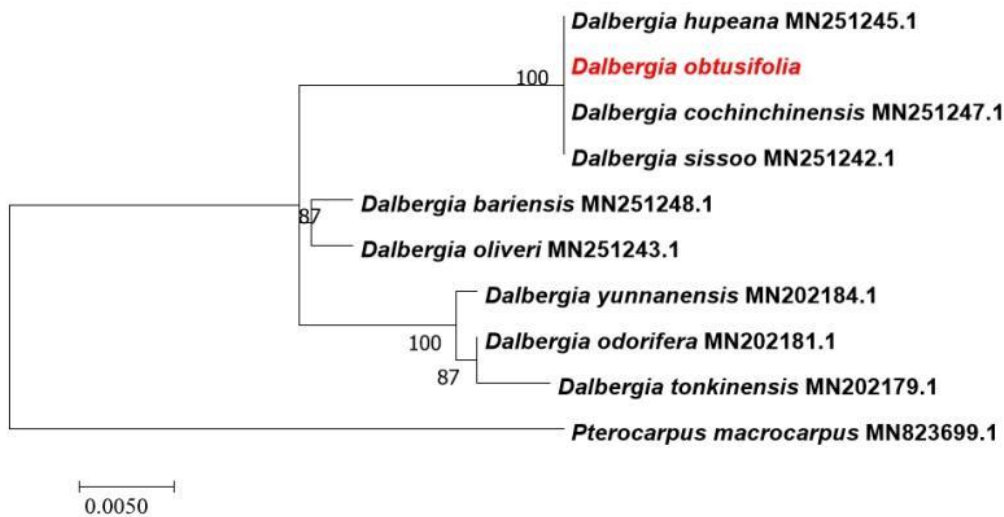


图 1 基于 *trnL*、*psbA-trnH*、*matK*、*rbcL* 序列构建的系统发育树

Fig.1 The phylogenetic tree obtained by maximum likelihood method based on the *trnL*, *psbA-trnH*, *matK*, *rbcL* sequence

**关键词:** 钝叶黄檀; DNA 提取; DNA 条形码; 木材鉴定

# DNA extraction and DNA barcoding identification of *Dalbergia obtusifolia*

Gan Chang-tao<sup>1</sup>, Cao Xiu-long<sup>2</sup>, Qiu Jian<sup>3</sup>

(1 of Art and Design, Southwest Forestry University, Kunming 650224, Yunnan, P.R. China; 2 College of Materials Science and Engineering, Southwest Forestry University, Kunming 650224, Yunnan, P.R. China; Yunnan Provincial Key Laboratory of Wood Adhesives and Glued; 3 Products, Southwest Forestry University, Kunming 650224, Yunnan, P.R. China)

**Abstract:** In order to identify rare and protected *Dalbergia obtusifolia* with DNA barcoding, wood DNA was extracted by CTAB kit method and CTAB-SDS method, fifteen pairs of primers were designed based on five barcodes, and PCR products were sequenced and analyzed. Results showed that good quality DNA from fresh wood could be extracted by the both 2 methods, the DNA extracted by CTAB has high purity but low concentration, the DNA extracted by CTAB-SDS has high concentration but small amount of protein residue. The DNA extracted by the 2 methods both could meet the needs of PCR amplification. Thirteen of fifteen primers were amplified, but only ten were sequenced successfully. Only six of ten sequences confirmed the species identity. According to the phylogenetic tree obtained by Maximum Likelihood method based on the *trnL*, *psbA-trnH*, *matK*, *rbcL* sequence, a sister relationship between the clade of *D. obtusifolia*–*D. hupeana* and *D. cochinchinensis*–*D. sissou* showed that the latter three species are most comparable to *D. obtusifolia* in the genus. (Fig.1).

**Keywords:** *D. obtusifolia*; DNA extraction; DNA barcoding; wood identification

# 基于高分辨 X-ray 断层扫描的木材细胞结构分析方法

刘星 夏重阳 石江涛\*

(南京林业大学材料科学与工程学院, 江苏 南京 210037)

**摘要:** 树木的生长不仅受遗传因素的影响,也受环境因子的影响。这就使得木材含有多细胞种类、复杂的三维结构、以及多尺度上的结构特征。这些复杂的结构与木材的物理力学性能密切相关。研究木材内部结构与其材性之间的关系可以为木材加工、木材保护、木材鉴定、木结构建筑等领域提供理论支撑。现今,对木材细胞的研究主要依靠显微切片与化学分析的技术,在显微镜下进行观察。但是,切片技术获取的多是二维图片,无法直接得到木材细胞在长度方向上的信息,而且操作中耗时较长、测量精度较低,对于处理过或易碎样品更是难以实现。这也限制了从更深层次对于细胞结构与木材性质间关系的理解。X 射线断层扫描技术(X-ray CT)是以非破坏性 X 射线透视技术,将待测物体做 360°自转,通过单一轴面的射线穿透被测物体,根据被测物体各部分对射线的吸收和透射率不同,收集每个角度的穿透图像,之后利用电脑运算重构出被测物体的实体图像。X-ray CT 不局限于二维尺度,既具有扫描电镜的特点,即表征木材内部结构,又具有 X 射线对不同物质的衰减率各异,且不破坏试件的特点。本实验旨在探究非粉末状木材在 X-ray 断层扫描处理下如何对细胞结构进行分析,提取想要的数据并进行量化。直接选择木材组织,自上而下化学处理,建立了基于同步辐射 X 射线  $\mu$ -CT (断层扫描)技术的木材组织三维结构数据采集方法。首次在 0.3 $\mu$ m 高分辨率上重构了木材组织三维可视化模型。木质素三维可视化模型构建有三个步骤:三维数据采集、图像量化处理和可视化。1) 采用 X 射线  $\mu$ -CT 技术直接采集了木质纤维素三维结构数据(原理如图 2.4 所示),解决了传统二维观察制样中造成的结构变形或破坏,也弥补了基于模型预测的不足。数据采集方法的主要参数有:加速电压为 50KV~60KV,体素分辨率 0.3 $\mu$ m,扫描区域 360°,曝光 2-3 秒,耗时 3.5-6 小时。单个样品约 1000 张二维图。2) 在二维界面上结合灰度级阈值化、直方图和形态学变换、分水岭算法分析、6 连通性分析、Soble 算子边缘检测算法分析等得到优化的二维图。实验结果表明,在三维空间中可以展示木材部分或整体结构和细胞之间的连接关系,如管胞,导管,木射线的连接方式、具缘纹孔的空间分布和形态等并获得其相关数据,如体积,占比,孔隙率,表面积等相关数据。实现从平面到立体,从静态到动态,从部分到整体的研究木材。

**关键词:** 木材; 细胞; 结构; 量化; X-ray CT; 三维

# Analysis method of wood cell structure based on high resolution X-ray tomography

Liu Xing, Xia Chong-yang, SHI Jiang-tao\*

(College of Materials Science and Engineering, Nanjing Forestry University, Nanjing 210037, Jiangsu)

**Abstract:** The growth of trees is affected not only by genetic factors, but also by environmental factors. This makes wood contain multicellular species, complex three-dimensional structure and multi-scale structural characteristics. These complex structures are closely related to the physical and mechanical properties of wood. Studying the relationship between wood internal structure and wood properties can provide theoretical support for the fields of wood processing, wood protection, wood identification, wood structure architecture and so on. Nowadays, the study of wood cells mainly depends on the technology of microsection and chemical analysis. However, most of the two-dimensional images obtained by slicing technology can not directly obtain the information of wood cells in the length direction, and the operation is time-consuming and the measurement accuracy is low, which is more difficult to achieve for processed or fragile samples. This also limits the deeper understanding of the relationship between cell structure and wood properties. X-ray tomography (X-ray CT) is a non-destructive X-ray perspective technology. The measured object rotates 360 degrees, and the ray penetrates the measured object through a single axial plane. Collects the penetration image of each angle according to the different absorption and transmittance of the ray of each part of the measured object, and then reconstructs the solid image of the measured object by computer operation. X-ray CT is not limited to two-dimensional scale. It not only has the characteristics of scanning electron microscope, that is, it not only characterizes the internal structure of wood, but also has the characteristics of different attenuation rates of X-rays to different substances without damaging the specimen. The main purpose of this experiment is to explore how to analyze the cell structure of non powdered wood under X-ray tomography, extract the desired data and quantify it. Wood tissue was directly selected and chemically treated from top to bottom, which was established based on synchrotron radiation X-ray  $\mu$ -Data acquisition method of three-dimensional structure of wood tissue based on CT (tomography) technology. At 0.3 for the first time  $\mu$  The 3D visualization model of wood tissue was reconstructed on m high resolution. The construction of lignin 3D visualization model has three steps: 3D data acquisition, image quantitative processing and visualization. 1) Using X-ray  $\mu$ -CT technology directly collects the three-dimensional structure data of lignocellulose (the principle is shown in Figure 2.4), solves the structural deformation or damage caused by traditional two-dimensional observation and sample preparation, and also makes up for the deficiency of model-based prediction. The main parameters of the data acquisition method are: the acceleration voltage is 50kV~60kV, and the voxel resolution is

0.3  $\mu\text{m}$ . The scanning area is  $360^\circ$ , and the exposure time is 2-3 seconds, which takes 3.5-6 hours. About 1000 two-dimensional drawings of a single sample. 2) On the two-dimensional interface, the optimized two-dimensional image is obtained by combining gray level thresholding, histogram and morphological transformation, watershed algorithm analysis, 6 connectivity analysis, Sobel operator edge detection algorithm analysis, etc. The experimental results show that the connection relationship between wood partial or overall structure and cells can be displayed in three-dimensional space, such as tracheids, ducts, the connection mode of wood rays, the spatial distribution and morphology of marginal pits, and the relevant data, such as volume, proportion, porosity, surface area and so on, can be obtained. Realize the research of wood from plane to three-dimensional, from static to dynamic, and from part to whole.

**Keywords:** wood; cells; structure; quantification; X-ray CT; 3D

# 人工倾斜处理对中山杉次生组织分生的影响

勇璐<sup>1</sup> 李茜然<sup>2</sup> 潘彪<sup>2,\*</sup>

(南京林业大学材料科学与工程学院, 南京 210037)

**摘要:** 【目的】中山杉 (*Taxodium hybrid* ‘Zhongshanshan’) 具有早期速生的优良特性, 但出现倾斜、弯曲和偏冠的现象时产生的应力木严重地制约了优质人工林的培育和木材的合理加工利用。本次实验通过研究外加作用力大小对中山杉次生组织分生的影响, 为研究应力木形成机理提供理论支持。

【材料与方法】通过人工施加外力将4组各3棵三年生中山杉分别与垂直方向呈夹角0°、15°、30°、60°, 处理120天(一个生长季)后对其取样研究。将倾斜两侧的中山杉次生组织进行制片观察: 使用光学显微镜、荧光显微镜和环境扫描电镜观察应压区和对应区木质部细胞解剖特征; 使用富兰克林离析法解离应压区和对应区管胞, 每个试样选取30根管胞测定长度、宽度, 并计算其平均值; 使用光学显微镜对传导韧皮部的细胞类型、排列情况进行观察; 使用Image J软件测量10组韧皮部的韧皮纤维组织比量及新分生的木质部和传导韧皮部的宽度和细胞数量。

【结果与分析】1.人工倾斜处理对木质部解剖特征的影响:(1)应压区木质部管胞横截面形态: 相较于0°, 15°时管胞形态略微变圆, 细胞壁未见明显增厚, 可见胞间隙与螺旋裂隙; 30°时管胞横截面明显变圆, 细胞壁显著增厚, 胞间隙增大, 螺旋裂隙显著; 60°时管胞横截面与30°接近但程度略低于30°, 胞间隙与螺旋裂隙显著。对应区木质部管胞横切面与正常材较为接近, 呈多边形, 无胞间隙。(2)不同倾斜角度木质部的管胞形态: 应压区细胞长度与宽度比较为 $30^\circ < 60^\circ < 15^\circ < 0^\circ$ , 双壁厚和圆度值: $30^\circ > 60^\circ > 15^\circ > 0^\circ$ 。对应区细胞长度比较为 $30^\circ > 60^\circ > 15^\circ > 0^\circ$ , 径向直径: $30^\circ < 60^\circ < 15^\circ < 0^\circ$ 。

2.人工倾斜处理对传导韧皮部解剖特征的影响:(1)中山杉韧皮部各细胞呈弦向带交错排列, 正常区与对应区细胞排列多为: “PF(韧皮纤维)-Se(筛胞)-PP(韧皮薄壁细胞)-Se-PF”, 而应压木普遍出现了“PF-Se-PP-Se-PP-Se-PP-Se-PF”的排列方式(如图2), 较正常区增加了一行筛胞和一行韧皮薄壁细胞。(2)应压区传导韧皮部的韧皮纤维组织比量在倾斜角度15°、30°、60°时与0°的比值依次为0.958, 0.810, 0.898; 对应区为: 1.008, 1.256, 1.027。

3.人工倾斜处理对次生组织分生量的影响: 中山杉应压木的形成层径向细胞个数平均3~6个。应压区木质部平均分生细胞数在0°、15°、30°、60°时分别为: 18.1, 22.5, 32.3, 33.8; 传导韧皮部为12.2, 12.7, 13.8, 13.5。对应区木质部平均分生细胞数在0°、15°、30°、60°时分别为: 16.7, 19, 11.3, 8.5; 传导韧皮部为6.8, 7.3, 9.9, 9.75。

【结论】(1)中山杉木质部应压区管胞的典型特征具体表现为管胞壁变厚、管胞横截面近似圆形出现胞间隙和螺旋裂隙、管胞长度变短等。倾斜角度30°时中山杉的应压木特征最明显。

(2)人工倾斜对中山杉应压区和对应区次生木质部的分生能力都具有促进作用。倾斜角度15°的分生数与0°相差不大, 倾斜30°时分生数量明显增多, 60°时与30°相差不大。

(3) 人工倾斜会导致中山杉应压区较对应区分生出更多的传导韧皮部，其中 30°传导韧皮部细胞数量最多。此外人工倾斜会导致中山杉传导韧皮部细胞的径向排列组合发生变化，应压木的传导韧皮部中“PF-Se-PP-Se-PP-Se-PP-Se-PF”排列普遍存在，且韧皮纤维的组织比量减少，即运输和储存营养物质的筛胞和薄壁细胞等占比增加。

**关键词：**中山杉；应压木；管胞形态；次生组织分生



# Effect of artificial tilting treatment on secondary tissue division in *Taxodium* hybrid 'Zhongshanshan'

Yong Lu<sup>1</sup>, Li Xiran<sup>2</sup>, Pan Biao<sup>2,\*</sup>

(College of Materials Science and Engineering, Nanjing Forestry university, Nanjing 210037)

**Abstract:** [objective] *Taxodium* hybrid 'Zhongshanshan' has the excellent trait of early fast-growing, but the stress wood produced when tilting, bending, and crown deviation occur seriously restricts the cultivation of high-quality plantation forests and the rational processing and utilization of wood. In this experiment, we investigated the effect of applied force on the secondary tissue differentiation of Zhongshanshan to provide theoretical support for studying the mechanism of stress wood formation.

[Materials and Methods] Three three-year-old Mesquite trees in each of the four groups were treated with an angle of 0°, 15°, 30°, and 60° to the vertical direction by manual application of external force and sampled after 120 days (one growing season). The secondary tissues of Zhongshanshan on both sides of the inclination were sampled for observation: the anatomical characteristics of xylem cells in the compression wood and the opposite wood were observed using light microscopy, fluorescence microscopy, and environmental scanning electron microscopy; the tracheid in the compression wood and the opposite wood were dissociated using the Franklin dissociation method, and 30 tracheids were selected from each specimen to determine the length and width, and the average value was calculated; The cell type and arrangement of the conduction phloem fibers were observed by light microscopy, and the width and cell number of the newly differentiated xylem and conduction phloem fibers were measured using Image J software.

[Results and Analysis] 1. The effect of artificial tilting treatment on xylem anatomical characteristics: (1) the cross-sectional morphology of xylem cells in the compression wood: compared with 0°, the cell morphology was slightly rounded at 15°, the cell wall was not significantly thickened, and the cell gap and thread fissure were visible; at 30°, the cell cross-section was significantly rounded, the cell wall was significantly thickened, the cell gap increased, and the thread fissure was significant; at 60°, the cell cross-section was close to 30° but to a lesser extent. At 60°, the cell cross-section was similar to that of 30° but slightly lower than that of 30°, and the cell gap and thread fissure were significant. At 60°, the cross-section of the tracheid was close to but slightly lower than 30°, and the cell gap and thread gap were significant. (2) The cell morphology of xylem at different angles of inclination: the comparison of cell length and width in the pressure zone was 30° < 60° < 15° < 0°, and the values of double wall thickness and roundness: 30° > 60° > 15° > 0°. The comparison of cell length in the corresponding area was 30° > 60° > 15° > 0°, radial diameter: 30° < 60° < 15° < 0°.

2. Effects of artificial tilting treatment on the anatomical characteristics of the conducting bast: (1) The cells of the bast of Zhongshanshan were arranged in interlaced chordal bands, and the arrangement of cells in the normal zone and the opposite wood was mostly: "PF (bast fiber)-Se

(sieve cell)-PP (bast thin-walled cell)-Se-PF", while the pressed wood generally showed The arrangement of "PF-Se-PP-Se-PP-Se-PP-Se-PF" (Figure 2), with one more row of sieve cells and one more row of bast thin-walled cells than in the normal zone. (2) The ratio of silique fiber tissue in the conductive phloem fibers of the compression wood was 0.958, 0.810, and 0.898 at tilt angles of 15°, 30°, and 60°, respectively, compared with 0°; the opposite woods were 1.008, 1.256, and 1.027. 3. Effect of artificial tilting treatment on the amount of secondary tissue division: the average number of radial cells in the Zhongshanshan stress wood forming layer was 3-6. The average number of xylem phloem cells in the compression wood was 18.1, 22.5, 32.3, and 33.8 at 0°, 15°, 30°, and 60°, respectively, and 12.2, 12.7, 13.8, and 13.5 in the Conducting phloem. The average number of xylem phloem cells in the opposite wood was 16.7, 19, 11.3, and 8.5 at 0°, 15°, 30°, and 60°, respectively. Conduction phloem fibers were 6.8, 7.3, 9.9, and 9.75.

[Conclusion] (1) The typical characteristics of the tracheid in the compression zone of Zhongshanshan xylem is the thickening of the tubular cell wall, the appearance of cell gaps, and thread fissures in the nearly circular cross-section of the tracheid, and the shortening of the length of the tracheid. The most obvious characteristics of the stress wood of Zhongshanshan were found when the tilt angle was 30°.

(2) Artificial tilting promoted the meristematic ability of secondary xylem in both the compression wood and the opposite wood of Zhongshanshan. The number of phloem at a tilt angle of 15° was not significantly different from that at 0°, and the number of phloems increased significantly at a tilt angle of 30°, which was not significantly different from that at 30° at 60°.

(3) The artificial tilting resulted in more Conducting phloem in the compression wood than in the opposite wood, with the highest number of Conducting phloem cells at 30°. In addition, the radial arrangement of the conduction phloem fibers of Zhongshanshan changed due to artificial tilting, and the arrangement of "PF-Se-PP-Se-PP-Se-PP-Se-PP-PF" was common in the conduction phloem fibers of stressed wood. The tissue ratio of phloem fibers decreased, i.e., the proportion of sieve cells and thin-walled cells for transporting and storing nutrients increased. The proportion of sieve cells and thin-walled cells, which transport and store nutrients, increased.

**Keywords:** Zhongshanshan; Compression wood; Tracheid morphology; Secondary tissue division

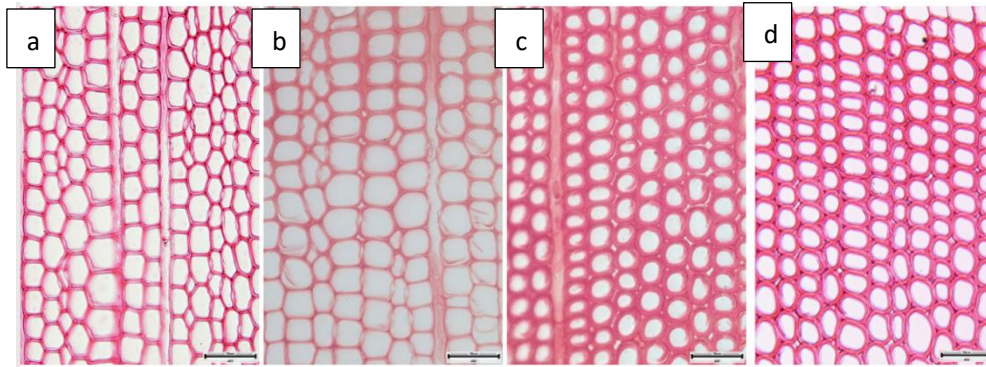


图 1 不同倾斜角度中山杉应压木管胞形态

(a: 倾斜角度为 0°; b: 倾斜角度为 15°; c: 倾斜角度为 30°; d: 倾斜角度为 60°)

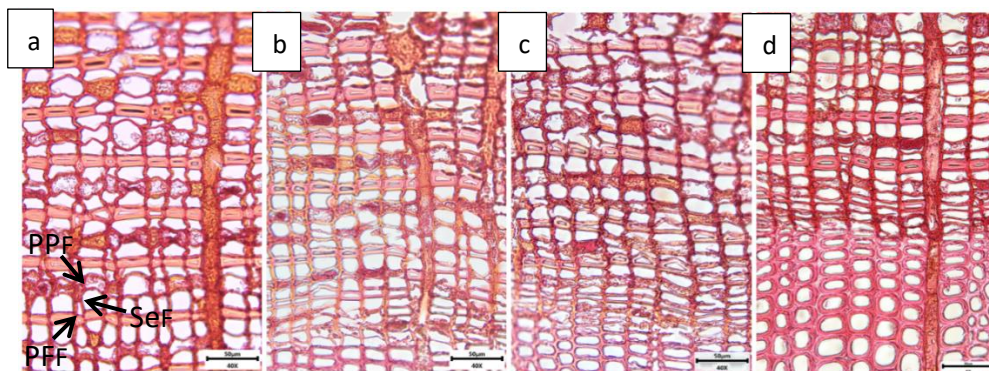


图 2 不同倾斜角度中山杉应压木韧皮部细胞排列

(a: 倾斜角度为 0°, 细胞排列多为“PF-Se-PP-Se-PF”; b-d: 倾斜角度分别为 15°、30°、60°, 细胞排列“PF-Se-PP-Se-PP-Se-PP-Se-PF”普遍)

# “鉴木”APP——海关木材监管的智能化应用

丁志平<sup>1</sup> 王晶晶<sup>1</sup> 王明生<sup>1</sup> 陈旭东<sup>1</sup>

(1 张家港海关)

## 摘要:

木材是国际贸易的大宗商品，是国家重要的进口战略性资源，全国年均进口量超过 1 亿立方米，货值超 190 亿美元。木材及木制品材种是海关进出口监管的重要参数，对 CITES 管制濒危木材的合法监管也离不开对木材材种的验证。由于木材材种鉴别专业性强、技术要求高、归类难度大，目前全国各口岸主要依赖取样送检的方法，存在成本高、周期长、程序复杂等特点。

本课题研发了一款基于安卓系统的 APP（鉴木，WOOD AI）以及配套的图像采集终端，利用木材横截面的识别特征图像，运用人工智能（AI）深度学习技术，可以实现手机/平板端对木材快速而准确的识别。在海关监管一线，可以在 10 分钟内完成对木材样品的处理、拍摄、识别整个流程。目前“鉴木”APP 支持进出口常见的 120 种木材的智能识别，测试识别准确率达 96%。

**关键词：**濒危木材；人工智能；材种鉴定；手机应用

# WOOD AI ——Intelligent mobile APP for customs “Wood Supervision”

Ding Zhiping<sup>1</sup>, Wang Jingjing<sup>1</sup>, Wang Mingsheng<sup>1</sup>, Chen xudong<sup>1</sup>

(1 Zhangjiagang Customs)

## **Abstract:**

Wood is a commodity of international trade and an important import strategic resource of the country. China imports over 100 million M<sup>3</sup> wood per year, which worth over 19 billion US dollars. The identification of wood and wood products is important parameters in customs’ supervision, at the same time is important to the Protection of CITES endangered wood. For wood identification is a highly professional work need high requirements for experience, equipment and personnel technology. At present, most ports of China Customs need to take a wood sample and send it to the wood identify institutions in order to identify the species of woods, which is complicated and high-cost, and need long time.

We have developed an Android system mobil APP (WOOD AI) and the supporting image capture device. WOOD AI developed based on Macroscopic Structural Characteristics Of Wood and deep learning technology. It can identificate wood fastly and accurately by mobile phone/tablet. Users can complete the whole process of processing, image-capture and species-identification of wood samples within 10 minutes. At present, WOOD AI can identificate 120 wood species commonly used in import and export, with a test recognition accuracy of 96%.

**Keywords:** Endangered wood species; AI; Wood identification; Mobile APP

# Ultrastructure of parenchyma cell wall in bamboo

## *(Phyllostachys edulis)* culms

Caiping Lian<sup>1</sup>, Rong Liu<sup>2</sup>, Shuqin Zhang<sup>2</sup>, Jing Yuan<sup>2</sup>, Junji Luo<sup>2</sup>, Feng Yang<sup>3</sup>, Benhua Fei<sup>2,\*</sup>

(1 Nanjing Forestry University, Nanjing 10037, China; 2 Key Laboratory of Bamboo and Rattan Science and Technology of the State Forestry Administration, Department of Bio-materials, International Center for Bamboo and Rattan, Beijing 100102, China; 3 School of Materials Science & Engineering, Beijing Institute of Fashion Technology, Beijing 100029, China; \*Corresponding author e-mail: feibenhua@icbr.ac.cn)

**Abstract:** Parenchyma cell wall structure plays a crucial role in the growth and the mechanical properties of bamboo plants, with the secondary cell wall providing strength and rigidity. However, little is known about the ultrastructure of the parenchyma cell wall. The aim of this study was to characterize the anatomical structure of the parenchyma cell wall and determine how it contributes to great mechanical superiority of bamboo culm. We investigated the ultrastructure of the parenchyma cell wall using transmission electron microscopy and field-emission environmental scanning electron microscopy. The key results show that the secondary cell walls of ground and vascular parenchyma cells exhibited tight-loose (light-dark) alternating layers. The pit membrane of the ground parenchyma cells contained numerous pores, and that of vascular parenchyma cells contained some plasmodesmata. Secondary cell walls of most bamboo parenchyma cells contained seven sub-layers, with a maximum of eleven sub-layers of ground parenchyma cells and nine sub-layers of vascular parenchyma cells. The average thickness of ground parenchyma cell wall sub-layers was higher than that in vascular parenchyma cells. The pit membrane thickness of ground parenchyma cells was also higher than that of vascular parenchyma cells, but the diameter of the ground parenchyma cells was smaller than that of the vascular parenchyma cells. The extremely high flexibility of moso bamboo stem could be the consequence of the presence of secondary cell walls in parenchyma cells, and its ultrastructure.

**Keywords:** moso bamboo; parenchyma cells; cell wall layer; pit membrane; ultrastructure

# 批量木材鉴别抽样检查中样本量的制定

陈松阳<sup>1</sup> 王宪<sup>1</sup> 王辉<sup>2</sup> 邱坚<sup>1</sup>

(1 西南林业大学材料与工程学院; 2 西南林业大学数理学院 云南昆明 650224)

## 摘要:

**【目的】**制定批量木材检查的抽样方案,为国家海关及木材相关行业的原木、锯材及木制品检查提供一个简便的、规范的、标准化的行为方案。

**【方法】**首先确定抽样方案的类型,对以往经验的分析,本方案以检查批的树种信息情况进行分类,又以简单随机抽样方法为基础,结合其他相关因素确定其他抽样方式的样本量。

**【过程】**通过对参考抽样方案的学习和总结,并应用 spss 将参考抽样方案中的样本数据进行汇总,发现样本量的增长随批量增加的规律。通过对本行业抽样检查的历史数据的汇总分析,确定了本方案样本量和批量的区间和范围。通过确定好的批量和样本量之间的关系,使用坐标计算获得了本方案的样本量计算方程式,通过 MATLAB 处理方程式,生成函数图像,再通过函数图像确定了参数区间。根据实际抽样的要求,本方案设置了放宽、正常和加严的抽样方案类别,并依靠不重复抽样样本量的计算公式,确定了三种抽样规格之间的关系。确定好每个抽样方案设定的三种抽样规格后,再以木材信息的关系确定其他抽样方案。

**【结果】**以现场判断检查批中存在多种树种时,且未按照现场初步判断的树种类别将检查批进行分组(多种树种类未分组)的情况为基础,并将多种树种类未分组的简单随机抽样方案设定为基础方案。通过基础方案,设定现场初步判断为检查批样本均为一个树种(单一树种类)以及现场按照初步判断的数种类别将检查批样本进行分组(多种树种类分组)的随机抽样方案,以及现场无法判断样本信息的随机抽样方案。在随机抽样方案的基础上,通过确定与其他抽样方式之间的比例关系从而确定不同抽样方式下的样本量。

**【结论】**将本方案与对其他抽样方案作对比后,本方案的优势在于:1、通过设定抽样比例区间,对于样本量的选取增加了可操作性;2、相邻的批量区间的边界值所对应的样本量更加均匀,消除了批量相差不大而样本量相差很大的缺点;3、放宽、正常、加严的抽样方案,增加了样本量的可选区间长度,对于同一批量样本有了更多的选择方案;4、按照木材样本树种信息的特点,设定不同的抽样方案,对于木材抽样具有更好的适用性;5、本抽样方案可应用于检查批样本之间存在不同属性的样本进行抽样检查判定,即通过对样本的抽样检查结果判定整体的属性信息。

**关键词:**木材检查;批量;区间;抽样方案;样本量

# Formulation of sample size in lot wood identification sampling inspection

Chen Songyang<sup>1</sup>, Wang Xian<sup>1</sup>, Wang Hui<sup>2</sup>, Qiu jian<sup>1</sup>

(1 College of Materials Science and Engineering, Southwest Forestry University; 2 College of Mathematical Statistics, Southwest Forestry University; Yunnan Kunming 6500224)

## Abstract:

[Objective] To develop a sampling plan for lot wood inspection, and provide a simple, standardized and standardized behavior plan for the inspection of logs, sawn timber and wood products of national customs and wood-related industries.

[Methods] Firstly, the type of sampling scheme was determined. Based on the analysis of previous experience, the scheme was classified based on the wood species information of the inspection lot, and the sample size of other sampling methods was determined based on the simple random sampling method and combined with other relevant factors.

[Process] By learning and summarizing the reference sampling plan and using SPSS to summarize the sample data in the reference sampling plan, the law of sample size increasing with lot size was found. By summarizing and analyzing the historical data of sampling inspection in this industry, the interval and scope of sample size and lot of this program are determined. By determining the relationship between lot size and sample size, the sample size calculation equation of this scheme was obtained by coordinate calculation. The equation was processed by MATLAB to generate function images, and then the parameter interval was determined by function images. According to the requirements of actual sampling, the scheme sets up relaxed, normal and strict sampling schemes, and determines the relationship among the three sampling specifications by the calculation formula of non-repeated sample size. After determining the three sampling specifications for each sampling plan, other sampling plans are determined based on the relationship of wood information.

[Result] Based on the situation that there were multiple wood species in the inspection lot and the inspection lot was not divided into groups (multiple wood species were not divided) according to the species category preliminarily judged on site, the simple random sampling scheme with multiple wood species not divided was set as the basic scheme. Through the basic scheme, the field preliminary judgment is set as the random sampling scheme in which the inspection lot samples are all of one wood species (single wood species) and the inspection lot samples are grouped according to several categories of preliminary judgment (multiple wood species), and the random sampling scheme in which the sample information cannot be judged on site. On the basis of random sampling



scheme, the sample size under different sampling methods can be determined by determining the proportional relationship with other sampling methods.

[Conclusion] After comparing this scheme with other sampling schemes, the advantages of this scheme are as follows:1. By setting sampling proportion interval, the selection of sample size increases operability; 2. The sample size corresponding to the boundary value of adjacent lot interval is more uniform, eliminating the defect that the lot size is not very different but the sample size is very different;3. Relaxed, normal and strict sampling scheme increases the selectable length of the sample size and provides more options for the same lot of samples;4. according to the characteristics of wood sample wood species information, set different sampling schemes, for wood sampling has better applicability;5. This sampling scheme can be applied to the sampling inspection and judgment of samples with different attributes among the lot samples, that is, to determine the overall attribute information through the sampling inspection results of the samples.

**Keywords:** Wood inspection; Lot; Interval; Sampling scheme; Sample size

# 木材标本采集与数字标本管理平台的研究

朱培琦<sup>1</sup> 何鑫<sup>2</sup> 孙永科<sup>2</sup> 邱坚<sup>1</sup>

(1 西南林业大学材料科学与工程学院 云南昆明 650224; 2 西南林业大学大数据与智能工程学院 云南昆明 650224)

**摘要:** 木材标本是随着人类文明的进步所出现的, 人类在生产生活实践中, 通过采集自然界野生木本植物资源来满足基本的生活需求, 为了将利用木材资源的知识经验分享和传承下去, 人类将木本植物制作成木材标本进行保存并供今后借鉴和参考。发展到今天, 木材标本作为保藏植物资源和植物信息的一种基本手段, 为国家的植物资源管理和利用提供了科学依据, 并在促进植物信息的利用和提高全民对植物资源重要性的认识等方面发挥着重大的作用。如今, 随着计算机技术的迅速发展, 越来越多的木材标本信息被数字化、管理方式也被信息化管理所取代, 木材标本数字化管理成为了标本馆发展的新趋势, 数字植物标本馆建设已经成为大多数植物标本馆日常工作不可或缺的部分。为了实现木材标本馆木材标本从采集、分类、鉴定等全过程的数字化标准管理和木材标本信息的数字化以及标本数字化管理平台的搭建, 以西南林业大学木材标本馆为例, 对基于网络平台的木材标本采集管理与数字木材标本管理进行研究, 并运用 React+Spring MVC+MySQL 的平台开发技术设计木材标本采集与数字标本管理平台, 开发了西南林业大学木材标本采集与数字标本管理平台作为标本管理、信息查询、科学研究、教学工作、志愿和捐赠服务以及科学普及等公众服务的网络信息平台。该数字标本管理平台建设的研究内容主要包括构建木材标本采集与数字标本网站、设计数字标本数据库、构建木材标本线上采集平台, 在木材标本采集与数字标本管理平台中, 可分别进行标本的在线检索查询、标本信息浏览、线上木材标本采集、线上木材标本捐赠。主要结论如下:

(1) 确定和制定木材标本采集、木材标本数字化和木材标本数字化管理相关的依据以及标准、规范, 实现木材标本全过程的数字化标准管理;

(2) 确定木材标本数字化的基本信息; 改进木材标本数字化的方法和操作流程, 优化标本数字化的工作流程提高标本数字化的工作效率; 开发木材标本的 3D 数字化展示技术, 提升平台用户体验;

(3) 建立木材标本采集与数字标本网站, 实现木材标本的线上数字化展示、木材标本线上采集和线上标本捐赠等服务。

**关键词:** 标本采集; 数字标本管理; 数字化; 标准和规范

# Research on wood specimen collection and digital specimen management platform

Zhu Peiqi<sup>1</sup>, He Xin<sup>2</sup>, Sun Yongke<sup>2</sup>, Qiu Jian<sup>1,\*</sup>

(1 College of Materials Science and Engineering, Southwest Forestry University, Kunming 650224, Yunnan, China; 2 College of Big Data and Intelligent Engineering, Southwest Forestry University, Kunming 6500224, Yunnan, China)

**Abstract:** Wood specimens appear with the progress of human civilization. In the practice of production and life, the human beings for the basic living needs by collecting wild woody plant resources in nature. In order to share and inherit the knowledge and experience of using wood resources, human beings make woody plants into wood specimens for preservation and reference in the future. Today, as a basic means of preserving plant resources and plant information, wood specimens provide a scientific basis for the management and utilization of national plant resources. It play an important role in promoting the utilization of plant information and improving the people's understanding of the importance of plant resources. Nowadays, with the rapid development of computer technology, more and more wood specimen information has been digitized and the management mode has been replaced by information management. The digital management of wood specimens has become the latest trend in the development of Herbarium. The construction of digital herbarium has become an indispensable part of the daily work of most Herbarium. In order to realize the digital standard management of overall process of wood specimens and the digitization of wood specimen information and the construction of specimen digital management platform, this paper studies the construction of wood specimen collection and digital specimen management platform based on the wood specimen museum of Southwest Forestry University. The wood specimen collection and digital specimen management platform is designed by Using the platform development technology of React + Spring MVC + MySQL. The wood specimen collection and digital specimen management platform of Southwest Forestry University is developed as a network information platform for public services such as specimen management, information query, scientific research, teaching, voluntary and donation services and scientific popularization. The construction contents of the digital specimen management platform includes wood specimen collection and digital specimen website, digital specimen database and wood specimen collection and management platform. The platform of wood specimen collection and digital specimen management includes function of online retrieval and query of specimens, browsing of specimen information, online collection and management of wood specimens and online donation of wood specimens can be carried out respectively. The main conclusions are as follows:

(1) Determine and formulate standards and specifications related to wood specimen collection, digitization of wood specimens and digital management of wood specimens in order to realize the

digital standard management of wood specimens;

(2) Determine the basic information of digitization of wood specimens. Improve the method and operation process of wood specimen digitization and optimize the work process of specimen digitization and raise working efficiency of specimen digitization. Develop 3D digital display technology of wood specimens to improve the user experience of the platform;

(3) Establish a website for wood specimen collection and digital specimen and realize online digital display of wood specimens and online collection management of wood specimens and online specimen donation services.

**Keywords:** specimen collection; Digital specimen management; digitization; Standards and specifications

# 白果蒲桃木材基础材性研究

孙明明<sup>1</sup> 徐斌<sup>1,\*</sup> 詹满军<sup>1</sup>

(安徽农业大学 林学与园林学院 安徽 合肥 230026)

## 摘要:

白果蒲桃 (*Syzygium album* Q.F.Zheng) 是桃金娘科 (*Myrtaceae*) 蒲桃属树种, 根据《福建植物志》第四卷记载在 20 世纪 90 年代初才发现、命名, 仅在中国福建省云霄县发现一棵。目前白果蒲桃木材的解剖性质及物理性质尚未见报道。由于该树种资源非常稀有, 本文以中国福建省云霄县恶劣天气下断落的侧枝为对象, 分别从宏观构造特征、微观构造及部分物理性质等方面开展基础材性研究, 以期填补学术空白, 为白果蒲桃的木材识别及后续研究提供理论依据。结果如下:

宏观下, 白果蒲桃木材呈紫红褐色, 结构细腻, 材质致密、较硬, 密度中至重; 材表光滑, 具有光泽, 无特殊气味和滋味; 心边材不明显, 生长轮肉眼下略明显, 在放大镜下较明显, 轮间因早材一列管孔直径稍大、与环管状薄壁组织共同构成一浅色带。散孔材至半散孔材, 管孔小, 在肉眼下不可见、在放大镜下略可见; 早材一列管孔略大于晚材管孔, 在生长轮末端管孔常减少; 以径列为主, 侵填体丰富。轴向薄壁组织环管状。木射线细至极细, 放大镜下略可见, 比管孔细; 在径切面上可见射线斑纹。

利用显微成像系统对其切片观察测量, 可见导管在横切面为圆形及卵圆形, 短径列复管孔 (2-3 个) 为主, 少量单管孔和管孔团; 网状复穿孔, 穿孔板倾斜, 管间纹孔式互列, 系附物纹孔; 导管长度平均为 704.33 $\mu\text{m}$ , 导管弦向直径最大为 127.47 $\mu\text{m}$ , 见于早材起始部位, 最小 43.27 $\mu\text{m}$ , 平均为 79.72 $\mu\text{m}$ , 导管组织比量平均为 22.70%。木纤维胞壁较厚, 直径平均为 20.66 $\mu\text{m}$ , 双壁厚平均为 16.19 $\mu\text{m}$ , 长度平均为 1577.78 $\mu\text{m}$ , 纤维组织比量平均为 53.60%。轴向薄壁组织多, 环管状及星散状; 轴向薄壁细胞间节状加厚略明显; 部分薄壁细胞里填充着砖红色内含物, 可见菱形晶体, 其组织比量平均为 3.44%。木射线非叠生, 射线组织为异形 II 型为主, 少量 I 型和 III 型, 直立或方形射线细胞比横卧射线细胞高或高得多; 射线细胞里填充着丰富的砖红色内含物, 未见晶体, 射线薄壁细胞间节状加厚明显; 单列木射线高度为 247.61 $\mu\text{m}$ ~740.01 $\mu\text{m}$  (5~17 个细胞), 平均 438.88 $\mu\text{m}$ , 宽度为 9.46 $\mu\text{m}$ ~18.97 $\mu\text{m}$ , 平均 12.65 $\mu\text{m}$ ; 多列木射线高度 551.92~900.10 $\mu\text{m}$  (11~37 个细胞), 平均 551.92 $\mu\text{m}$ , 宽度 24.32 $\mu\text{m}$ ~51.42 $\mu\text{m}$  (2~4 个细胞, 以 3 个细胞为主), 平均 36.82 $\mu\text{m}$ ; 射线组织比量平均为 20.30%。

根据国家标准木材物理性质测定方法, 该木材基本密度为 0.62g/cm<sup>3</sup>, 气干密度为 0.78g/cm<sup>3</sup>, 气干含水率为 14.32%; 气干弦向干缩率、气干径向干缩率、气干体积干缩率、全干弦向干缩率、全干径向干缩率、全干体积干缩率分别为 5.73%、3.13%、9.10%、7.88%、4.59%、13.97%; 干缩差异小于 1, 表明该木材干燥处理时性能较好。

**关键词:** 白果蒲桃(*Syzygium album* Q.F.Zheng); 解剖特征; 宏观构造; 物理性质

# 福建特有乡土树种突脉青冈和闽西青冈木材结构特征的分析

吴小莲 李文 黄圣波 关鑫 林金国\*

(福建农林大学材料工程学院, 福建 福州 350002)

**摘要:** 突脉青冈和闽西青冈为福建特有乡土阔叶树种, 本文借助连续变倍体视显微镜、生物数码显微镜和扫描电镜观察了突脉青冈和闽西青冈木材的宏观构造和微观构造特征, 测定分析了木材各种细胞的 36 个形态特征参数, 结果表明: 突脉青冈心边材区别不明显, 为散孔材, 单管孔, 呈溪流状径向排列, 内含侵填体, 管间纹孔互列, 单穿孔, 每平方毫米管孔数量 3.43 个, 管孔平均弦向直径为 172.83 $\mu\text{m}$ , 管孔壁腔比为 10.36, 导管长宽比为 3.67、细胞实质率为 16.71%、组织比量为 5.06%; 木纤维平均长度 1381.4 $\mu\text{m}$ , 长宽比为 57.52, 壁腔比为 1.13, 组织比量为 53.96%, 细胞实质率为 59.20%; 轴向薄壁组织很发达, 为离管带状, 排列规整, 宽 1~7 个细胞, 平均每平方毫米结晶细胞个数为 19 个, 结晶体主要出现在轴向薄壁细胞中且多以结晶细胞链存在; 木射线数量中等, 每毫米 8.47 根, 射线组织同形单列及多列, 窄木射线为同形单列射线, 偶见 2 列或成对, 高 3~23 细胞, 宽木射线少数夹杂着其它轴向分子, 为聚合木射线, 高许多细胞, 往往超出切片范围, 聚合木射线宽 371.61 $\mu\text{m}$ ; 导管与射线间纹孔式为刻痕状和大圆形; 具有环管管胞; 胞间道缺如。闽西青冈心边材区别明显, 为散孔材, 单管孔, 呈溪流状径向排列, 每平方毫米管孔数 6.67 个, 管孔平均弦向直径为 138.51 $\mu\text{m}$ , 壁腔比为 9.66, 实质率为 15.92%, 导管分子长宽比为 3.74, 组织比量为 10.60%, 导管内含侵填体, 管间纹孔互列, 单穿孔; 木纤维平均长度为 1249.63 $\mu\text{m}$ , 长宽比为 66.74, 纤维壁腔比为 3.52, 木纤维细胞实质率为 85.61 $\mu\text{m}$ , 组织比量为 49.85%; 轴向薄壁组织发达, 主要为离管带状, 排列不规整, 宽 1~4 细胞, 结晶细胞主要出现在聚合木射线中, 少见结晶细胞链; 木射线每平方毫米 8.9 条, 组织比量为 31.14%, 射线组织同形单列及多列, 稀异 III 形, 主由横卧细胞组成, 直立和方形细胞间或出现, 窄木射线为同形单列射线, 偶见 2 列, 高 3~19 细胞, 宽木射线多数夹杂着其它轴向分子, 为聚合木射线, 高许多细胞, 往往超出切片范围, 导管-木射线间纹孔式主要为刻痕状, 少数大圆形; 具有环管管胞; 胞间道缺如。

突脉青冈和闽西青冈木材结构特征主要区别在于: 闽西青冈心边材区别较突脉青冈明显; 闽西青冈木材管孔数量明显多于突脉青冈, 每平方毫米管孔数量为突脉青冈的 1.94 倍, 导管组织比量为突脉青冈的 2.09 倍; 突脉青冈木材管孔明显大于突脉青冈, 平均管孔面积为闽西青冈管孔面积的 1.63 倍; 突脉青冈木材轴向薄壁组织较闽西青冈多且排列更规整, 其组织比量为闽西青冈的 2.77 倍; 突脉青冈木材结晶细胞数量明显多于闽西青冈, 每平方毫米结晶细胞个数为闽西青冈的 2.70 倍; 闽西青冈的木纤维壁腔比明显大于突脉青冈, 为突脉青冈的 3.12 倍; 闽西青冈木射线中除横卧细胞外, 偶见直立和方形细胞, 而突脉青冈木射线全部由横卧细胞组成。研究结果可为突脉青冈和闽西青冈木材识别和合理利用提供依据。

**关键词:** 突脉青冈; 闽西青冈; 木材解剖构造; 结构特征参数

# **Anatomical characteristics analysis of *Cyclpbalanopsis elevaticostata* and *Cyclobalanopsis minxiensis* wood as Fujian endemic native species**

Wu Xiaolian, Li Wen, Huang Shengbo, Guan Xin, Lin Jinguo\*

(College of Materials Engineering, Fujian Agriculture and Forestry University, Fuzhou, Fujian 350002)

**Abstract:** Both *Cyclpbalanopsis elevaticostata* and *Cyclobalanopsis minxiensis* wood are unique native broad-leaved tree species in Fujian. In this paper, the macrostructure and microstructure characteristics of *C. elevaticostata* and *C. minxiensis* wood were observed by the means of continuous zoom stereo microscope, bio-digital microscope and scanning electron microscope. 36 morphological characteristic parameters of various wood cells were measured and analyzed. The results showed that the difference between the heart and edge of *C. elevaticostata* wood is not obvious. *C. elevaticostata* belonged to the diffuse-porous wood, and there were solitary pores with radial alignment, tylosis within pores, the intervacular pitting is alternate pitting, with single perforation plates. The number of pores per square millimeter is 3.43, the average string diameter of pore is 172.83 $\mu\text{m}$ , the wall-to-cavity ratio is 10.36, the vessel length-width ratio is 3.67, the cell substance rate is 16.71%, the tissue ratio is 5.06%; the average length of wood fiber is 1381.4 $\mu\text{m}$ , the length-width ratio was 57.52, the wall-to-cavity ratio is 1.13, the tissue ratio is 53.96%, and the solid ratio of wood fiber cells is 59.20%. The axial parenchyma of *C. elevaticostata* wood was very developed, from the vessel banded, with the band width of 1-7 cells, the arrangement is regular. Average number of crystalline cells per millimeter 19, and the crystals mainly appear in the axial parenchyma cells and mostly exist in crystalline cell chains; the number of wood rays is medium, 8.47 per millimeter, the ray tissue is homogeneous ray tissue, and narrow rays are of the same shape Single row of rays, occasionally 2 rows or pairs, The height of uniserial wood ray of was 3 to 19 cells. a few broad wood rays are mixed with other axial molecules, they are polymer wood rays, many cells higher, often beyond the scope of the slice, the polymer wood rays are 371.61 $\mu\text{m}$  wide. The gash-like pitting between vessel and ray, with few large circles. Having an vasicentric tracheid, intercellular canals are absent. The differences between the heart and edge of *Cyclobalanopsis minxiensis* is obvious. *C. minxiensis* belonged to the diffuse-porous wood, and there were solitary pores with radial alignment. The number of pores per square millimeter is 6.67. The average string diameter of pore is 138.51  $\mu\text{m}$ , the wall and cavity ratio is 9.66, the substantive ratio is 15.92%, the vessel length-width ratio is 3.74, the tissue ratio is 10.60%, tylosis within pores, the intervacular pits are alternate pits, with single perforation plates; the average length of wood fiber was 1249.63 $\mu\text{m}$ , the length-width ratio was 66.74, the ratio of fiber wall to cavity was 3.52, the solid

ratio of wood fiber cells is 85.61%, and the tissue ratio is 49.85%; The axial parenchyma of *C. minxiensis* wood was developed, from the vessel banded, with the band width of 1-4 cells, and crystals mainly appear in polymerized wood rays, crystalline cell chains are rarely seen. Wood rays per square millimeter are 8.9 and the tissue ratio is 31.14%. The ray organization is the same shape single row or multiple row, rare and different shape, The main part is composed of horizontal cells, which may appear between upright and square cells. The height of uniserial wood ray of was 3 to 19 cells. Most of the wide wood rays are mixed with other axial molecules, which are polymeric wood rays, high Many cells are often beyond the scope of the slice. The gash-like pitting between vessel and ray, with few large circel. Having an vasicentric tracheid, intercellular canals are absent.

The main difference of wood structure characteristics between *C. elevaticostata* wood and *C. minxiensis* wood is that the difference of heartwood and sapwood of *C. minxiensis* wood is more obvious than that of *C. elevaticostata* wood; the number of pores in the wood of *C. minxiensis* wood is significantly more than that of *C. elevaticostata* wood, which the number of pores per square millimeter was 1.94 times that of *C. elevaticostata* wood, the ratio of vessel tissue is 2.09 times that of *C. elevaticostata* wood. The pores size of *C. elevaticostata* wood is significantly larger than that of *C. minxiensis* wood, which the average pore area is 1.63 times of that of *C. minxiensis* wood. The distribution of axial parenchyma cells of *C. elevaticostata* wood was more regular than that of *C. minxiensis* wood , which its tissue ratio is 2.77 times that of *C. minxiensis* wood. The number of crystalline cells in the wood of *C. elevaticostata* wood is significantly more than *C. minxiensis* wood. The wood fiber wall-to-cavity ratio of *Cyclobalanopsis minxiensis* wood is significantly larger than *C. elevaticostata* wood, which is 3.12 times that of *C. elevaticostata* wood. In addition to horizontal cells, erect and square cells are occasionally seen in the rays of *C. minxiensis* wood. The rays of *C. elevaticostata* wood are all composed of horizontal cells. The results of the study can provide a basis for the identification and rational utilization of the wood of *C. elevaticostata* wood and *C. minxiensis* wood.

**Keywords:** *Cyclpbalanopsis elevaticostata* wood; *Cyclpbalanopsis minxiensis* wood; wood anatomical structure; characteristic structure parameter



# 刚竹属竹材维管束特征结构研究

徐皓诚 张颖 王汉坤\*

(国际竹藤中心 国家林业和草原局/北京市共建竹藤科学与技术重点实验室 北京 100102)

## 摘要:

**【目的】**刚竹属竹材隶属竹亚科,经济价值高、种类多,对其维管束特征结构的全面认识是揭示竹材优良力学性能的关键。

**【方法】**本研究以29种刚竹属竹材胸高部位节间处竹环为研究对象,基于本课题组构建的毛竹维管束识别模型,通过迁移学习等方法,构建刚竹属竹材维管束通用识别模型。在横切面内测量维管束总数量、维管束分布密度、纤维鞘总面积、纤维组织比量以及单个维管束长度、宽度、长宽比、纤维鞘面积等八项维管束特征的均值,并分析维管束特征与竹材壁厚、外周长的关系。根据竹材的壁厚对其横切面进行径向分层处理,计算各层中维管束特征的均值,并对其分布规律进行量化表征。

**【内容】**本研究旨在量化刚竹属竹材维管束特征,揭示其在径向上的梯度分布规律。

**【结果】**(1)本研究构建的维管束通用识别模型对刚竹属竹材维管束的识别精度达96.97%。(2)横切面内维管束总数量、维管束分布密度、纤维鞘总面积、以及单个维管束长度、宽度、纤维鞘面积的均值与竹材壁厚、外周长呈显著的线性相关。(3)横切面内纤维组织比量( $25.50 \pm 3.51\%$ )以及单个维管束长宽比的均值( $1.226 \pm 0.091$ )在不同竹种间差别很小。(4)沿竹材径向,从竹青到竹黄纤维组织比量呈指数型下降( $R^2=0.95$ ),维管束长宽比呈二次函数型下降( $R^2=0.87$ ),维管束宽度呈线型增加( $R^2=0.93$ )。

**【结论】**本研究所得模型可高效、准确识别刚竹属竹材维管束;刚竹属竹材维管束特征与竹材壁厚、外周长相关性高,并且维管束特征的径向梯度分布规律高度一致。

**关键词:**刚竹属;维管束;径向分布

# Research on the characteristics of vascular bundle in *Phyllostachys*

Haocheng Xu, Ying Zhang, Hankun Wang\*

(International Center for Bamboo and Rattan; Key Laboratory of National Forestry and Grassland Administration/Beijing for Bamboo & Rattan Science and Technology, Beijing, 100102, China)

## Abstract:

[Objective] Bamboos of the genus *Phyllostachys* are one of the most economically valuable and numerous species in the Chinese bamboo subfamily. A comprehensive understanding of vascular bundles is the key to elucidate the excellent intrinsic mechanical properties of bamboos.

[Method] In this study, twenty-nine kinds of *Phyllostachys* species at the breast height of the internode bamboo ring as the object, based on the detection model for vascular bundle of Moso bamboo constructed by our research group, through transfer learning and other methods, a universal detection model for vascular bundle of *Phyllostachys* was constructed. The total number of vascular bundles, the distribution density of vascular bundles, the total area of fiber sheath, the fiber volume fraction, the mean value of single fiber sheath area, the mean value of the length of vascular bundle, the mean value of the width of the vascular bundle and the mean value of the length-to-width ratio of vascular bundle were measured. In addition, the relationship between the characteristics of vascular bundle and the outer circumference and the wall thickness of bamboo was also discussed. Furthermore, the radial changes in fiber volume fraction and the shape (the length, the width and the length-to-width ratio) of vascular bundle were studied.

[Content] This study aims to quantify the characteristics of the vascular bundle of *Phyllostachys* and its gradient distribution in the radial direction.

[Result] (1) The universal detection model of vascular bundles constructed in this study has an accuracy of 96.97% for the recognition of vascular bundles. (2) The total number of vascular bundles, the distribution density of vascular bundles, the total area of fiber sheath, the mean value of single fiber sheath area, the mean value of the length of vascular bundle and the mean value of the width of the vascular bundle are significantly linearly correlated with bamboo wall thickness and outer circumference. (3) The fiber volume fraction ( $25.50 \pm 3.51\%$ ) in the cross section and the mean value of the length-to-width ratio of a single vascular bundle ( $1.226 \pm 0.091$ ) had very little difference among different bamboo species. (4) Along the radial direction of the bamboo, the fiber volume fraction from the outer skin of bamboo to the inner skin decreased exponentially ( $R^2=0.95$ ), the length-to-width ratio of vascular bundle decreased quadratically ( $R^2=0.87$ ), and the width of vascular bundle increased linearly ( $R^2=0.93$ ).

[Conclusion] The model obtained in this study can efficiently and accurately identify the vascular bundles of *Phyllostachys*. The characteristics of vascular bundle of *Phyllostachys* have a

large relationship with the bamboo wall thickness and outer circumference, and the radial gradient distribution of vascular bundle characteristics is highly consistent.

**Keywords:** *Phyllostachys*; vascular bundle; radial distribution

# 斜叶黄檀降真香的描述及其与海南黄檀木和降香黄檀木的区分

李浩杰<sup>1</sup> 宁莉萍<sup>1,2,\*</sup> 李英健<sup>3</sup> 何奕霖<sup>1</sup> 赵文琦<sup>1</sup> 刘芷妍<sup>1</sup>

(1 四川农业大学 林学院; 2 四川农业大学 林学院, 木材工业与家具工程高校重点实验室; 3 广西大学)

**摘要:** 斜叶黄檀(*Dalbergia pinnata*)、海南黄檀(*Dalbergia hainanensis*)和降香黄檀(*Dalbergia odorifera*)是同为属的三个易混淆树种。这三个树种都已被列入《濒危野生动植物种国际贸易公约》(CITES)的附录 II。降真香是源自于斜叶黄檀的一种传统香料。本研究中对这些树种的木材解剖构造特征进行了描述, 并使用 GC-MS 进行化学鉴定分析。结果表明, 斜叶黄檀在管孔的数量和大小以及木射线的类型上与其他两个树种相比具有显著差异, 可以作为木材识别的依据。此外, 降真香不同样品的挥发性物质化学成分中含有 11 种共同成分, 其中榄香素的相对含量最高(67%)。降真香的各样品的挥发性物质化学成分呈高度相关( $r > 0.9$ ), 而各树种间挥发性物质化学成分呈不相关( $r < 0.1$ )。假如未知样品的挥发性物质化学成分中榄香素的相对含量超过 66%, 且与降真香标准样品呈高度相关( $r > 0.8$ ), 则可鉴定为降真香。

**关键词:** 斜叶黄檀; 木材构造; 木材识别; GC-MS; 榄香素。

# Description of the wood of *jiangzhenxiang* from *Dalbergia pinnata* and its separation from *Dalbergia hainanensis* and *Dalbergia odorifera*

Haojie Li<sup>1</sup>, Liping Ning<sup>1,2,\*</sup>, Yingjian Li<sup>3</sup>, Yilin He<sup>1</sup>, Wenqi Zhao<sup>1</sup>, and Zhiyan Liu<sup>1</sup>

(1 College of Forestry, Sichuan Agricultural University, Chengdu 611130, PR China; 2 Key Laboratory of Wood Industry and Furniture Engineering, Sichuan Agricultural University, Chengdu 611130, PR China; 3 Guangxi University, Nanning 530004, PR China)

**Abstract:** *Dalbergia pinnata*, *Dalbergia hainanensis* and *Dalbergia odorifera* are three easily confused species. These three species included in CITES Appendix II. *Jiangzhenxiang* is a traditional fragrance derived from *D. pinnata*. This study reports the wood anatomy of these species, and GC-MS was used for chemical identification analysis. The results show that *D. pinnata* has significant differences in the number and size of the pores and the type of the wood rays compared with the other two species, which can be used as identification. In addition, the volatile substances composition of different samples of *jiangzhenxiang* contain 11 common components, among which the relative content of elemicin was the highest (67%). The volatile substances composition of *jiangzhenxiang* is highly correlated ( $r > 0.9$ ), and the volatile substances composition among these species was uncorrelated ( $r < 0.1$ ). If the relative content of elemicin in the volatile substances composition of unknown sample exceeds 66% and is highly correlated ( $r > 0.8$ ) with *jiangzhenxiang* standard sample, it can be identified as *jiangzhenxiang*.

**Keywords:** *Dalbergia pinnata*; wood structure; wood identification; GC-MS; elemicin.

# 黄杨木特性及木雕应用

石兰兰 汪睿 王玉荣\*

(中国林业科学研究院木材工业研究所, 北京 100091)

**摘要:** 黄杨木 (*Buxus spp.*) 为黄杨科黄杨属植物, 是一种四时不凋的常绿灌木或小乔木。我国分布广泛, 除东北外, 全国各省区均有自然分布或栽培。黄杨木为散孔材, 生长轮不显至略显明、宽度不均匀、甚窄, 木射线极细至略细, 材质坚韧细密、纹理细致均匀、略重硬、色彩黄亮。具有较强的抗虫耐腐性、易锯解、握钉力优良。研究表明, 黄杨木是用于雕刻的上等木料。其含有蜡质, 经精雕细刻磨光后能同象牙雕相媲美, 被世人称为“木中象牙”。黄杨树的树干、树冠和树根, 均可用于雕刻。其中, 树干利用率最高; 树冠分主枝、侧枝, 适合制作体积较小的雕刻品; 树根可被根雕艺人依材立意进行局部雕刻创作。黄杨木具有生长慢、大料难得的特点。黄杨木的生长特性及其适合雕刻的优良品质, 决定了其多用于制作文玩陈设、印章或镶嵌装饰材料等。用黄杨木雕刻形成的木雕艺术和产业, 为历史朝代发展、人们生活方式及样貌等留下了无数珍贵的文化记忆。早在西汉时, 黄杨木已被用来制作精美梳篦。唐宋时期, 黄杨木常被用来雕刻印刷中的精细文字和插图的雕版。元代黄杨木雕《铁拐李》为我国现存年代最为久远的黄杨木雕人物像。明清时期, 黄杨木雕形成了独特的艺术表现风格, 并以刻画形神兼备的中国民间神话传说等人物形象而受到人们的喜爱。清晚期至民国, 是我国黄杨木雕最为成熟和鼎盛的时期。近当代黄杨木雕更多地是以体现地域文化特征, 出现了各具特色风格的不同地方流派。其中浙江的乐清黄杨木雕与上海的海派黄杨木雕是两个典型代表。浙江乐清黄杨木雕现已入选国家级非遗名录, 与浙江东阳木雕、潮州金漆木雕和福建龙眼木雕并称为中国四大木雕。黄杨木雕具有艺术欣赏、文化研究以及收藏价值, 在我国得到了很好的传承与发展, 特别是其承载的文化研究价值及国家对非遗传承产业的重视, 使黄杨木雕市场潜力巨大。目前关于黄杨木资源特性、在雕刻作品方面的应用以及黄杨木雕历史文化演变未有较全面的文献资料。本文旨在通过介绍黄杨木及其木雕方面的利用, 让更多人了解黄杨木及其雕刻文化, 从而促进黄杨木高效利用以及黄杨木雕艺术的传承与发展。

**关键词:** 黄杨木; 资源特性; 黄杨木雕; 历史文化

# Characteristics of boxwood and its utilization in woodcarving

Lanlan Shi, Rui Wang, Yurong Wang\*

(Research Institute of Wood Industry, Chinese Academy of Forestry, Beijing 100091, China)

**Abstract:** Boxwood (*Buxus* spp.) is a plant of the genus *Buxus* in the Buxaceae family. It is an evergreen shrub or small tree that does not wither all the time, widely naturally distributed or cultivated in all provinces of China except Northeast China. Boxwood is diffuse porous wood, and the width of the growth ring is uneven and very narrow, not obvious to slightly visible. What's more, the wood rays are extremely thin to slightly thin, and the material is tough and dense. The texture is fine and uniform, slightly heavy and hard, and the color is yellow and bright. It has strong resistance to insects and corrosion, easy to saw, and excellent nail-holding power. Studies have shown that boxwood is the finest wood for carving. It is called "ivory in wood" by the world for wax-like qualities, which can be comparable to ivory carving after being finely carved and polished. The trunk, crown and roots of boxwood trees can all be used for carving. Among them, the utilization rate of the trunk is the highest; the crown has main branches and side branches, suitable for making smaller carvings; and the roots can be carved locally by root carving artists according to the material. Boxwood has the characteristics of slow growth and rare anecdote. Because of the growth characteristics of boxwood and its good quality suitable for carving, it is mostly used for making cultural and play furnishings, seals or inlaid decorative materials. The wood carving art and industry formed from boxwood carvings have left countless precious cultural memories for the development of historical dynasties, people's lifestyles and appearances. As early as the Western Han Dynasty, boxwood had been used to make exquisite combs. In the Tang and Song dynasties, boxwood was often used to engrave fine text and illustrations in printing. The boxwood carving "Tieguai Li" in Yuan Dynasty is the oldest existing boxwood carving figure in our country. During the Ming and Qing Dynasties, boxwood carvings formed a unique style of artistic expression, and were loved by people for portraying characters such as Chinese folk myths and legends with both form and spirit. From the late Qing Dynasty to the Republic of China, it was the most mature and prosperous period of boxwood carving in China. Modern and contemporary boxwood carvings more reflect regional cultural characteristics, and distinctive styles have appeared in many places. Among them, the Yueqing boxwood carvings in Zhejiang and the Shanghai style boxwood carvings are two typical representatives. Zhejiang Yueqing boxwood carving has been selected as a national intangible cultural heritage. It is now known as the four famous Chinese woodcarvings along with Zhejiang Dongyang woodcarving, Chaozhou gold lacquered woodcarving and Fujian longan woodcarving. Boxwood carving has artistic appreciation, cultural research and collection value, and has been well inherited and developed in our country. Especially its cultural research value and the country's

emphasis on non-genetic inheritance industries make the boxwood carving market huge potential. At present, there is no comprehensive literature on the characteristics of boxwood resources, its application in carving works, and the historical and cultural evolution of boxwood carvings. This article aims to introduce boxwood and its use in wood carving, so that more people understand boxwood and its carving culture, so as to promote the efficient use of boxwood and the inheritance and development of boxwood wood carving art.

**Keywords:** boxwood; resource characteristics; boxwood carvings; history and culture



# 竹节维管束数量与形态特征研究

张颖 徐皓诚 王汉坤\*

(国际竹藤中心 国家林业和草原局/北京市共建竹藤科学与技术重点实验室 北京 100102)

## 摘要:

**【目的】**竹节对竹材横向运输物质、抵御横向载荷具有关键作用。通过竹节时，维管束发生弯曲、盘绕、分叉行为。全面研究竹节结构有利于充分理解、发挥竹材的天然优势，推动竹材与仿生材料、智能材料的有机结合。

**【方法】**本研究以毛竹 (*Phyllostachys edulis* (Carr)H. de Lebaie) 的无侧枝竹节为研究对象，截取箨环两侧 1 cm 范围内的竹环，沿轴向劈制成条状样品。对样品横切面进行连续砂光与扫描，运用本课题组自主研发的维管束检测模型统计轴向维管束数量；通过平板式影像扫描仪和电子显微镜，结合人工标定维管束群，对轴向维管束的相对位置、排列分布进行进一步定量与定性表征。

**【内容】**连续采集竹节处横切面图像，对横切面内的轴向维管束数量、形态结构与排列分布进行全面分析。

**【结果】**(1) 节部竹条试样自下向上，维管束数量呈现先减少、再增加、再减少的变化趋势：箨环下 10 mm 处维管束数量为 213 个；至箨环下 6 mm 处，维管束数量逐渐减少，直至达到最小值 197 个，减少幅度为 7.51%；至箨环下 3 mm 处，维管束数量逐渐增加，达到峰值 264 个，增加幅度达 34.0%；至箨环处，维管束数量逐渐减少，最后趋于稳定值 214 个，减小幅度为 18.94%；维管束的数量变化主要由竹青侧引起，竹青侧维管束分生引起数量的大幅增加，竹青侧大量维管束随箨鞘脱落形成封闭末端引起数量的大幅减少；(2) 节部竹条试样自下向上，维管束形态逐渐发生不同的变化：箨环下 7 mm 处，开始出现膨大维管束；沿轴向往上，膨大形态进一步扩展，主要为指向竹青侧的径向延展，延展中可见轴向维管束的再生与逐渐偏移，并对邻近维管束造成影响，使其发生变形、偏移；箨环附近，存在大量横向维管束；经过箨环后，维管束的形态开始与节间处相近。

**【主要结论】**竹节中，自箨环下 7 mm 至箨环之间维管束数量、形态、排列分布发生连续、复杂的变化，数量的变化主要是由竹青侧维管束引起的，形态、排列分布的变化则与膨大维管束相关。

**关键词：**毛竹竹节；维管束；数量；形态；排列分布

# Study on the number and morphological characteristics of vascular bundles at Moso bamboo nodes

Ying Zhang, Haocheng Xu, Hankun Wang\*

(International Center for Bamboo and Rattan; Key Laboratory of National Forestry and Grassland Administration/Beijing for Bamboo & Rattan Science and Technology, Beijing, 100102, China)

## Abstract:

[Objective] The nodes play a key role in the transverse transportation of materials and resisting the transverse load in Moso bamboo. When passing through node, vascular bundles bend, wind and bifurcate. A comprehensive study of the structure of bamboo nodes is conducive to fully understand and give full play to the natural advantages of bamboo, as well as promote the organic combination of bamboo with bionic materials and intelligent materials.

[Method] In this study, the non-branching bamboo nodes of Moso bamboo were taken as the research object. The bamboo rings within 1 cm on both sides of the sheath ring were cut from bamboo stem and split into strip samples along the axis. Continuous sanding and scanning were performed on the cross section of the sample, and the number of axial vascular bundles was counted by using the vascular bundle detection model independently developed by our research group. The relative position, arrangement and distribution of axial vascular bundles were further quantitatively and qualitatively characterized by flat plate image scanner and electron microscope, combined with manual calibration of vascular bundle group.

[Content] Collect cross-sectional images of bamboo nodes, and the number, morphological structure, arrangement and distribution of axial vascular bundles in the cross section were comprehensively analyzed.

[Result] (1) From bottom to top, the number of vascular bundles decreased first, then increased and then decreased. The number of vascular bundles 10 mm below the sheath ring was 213. To 6 mm below the sheath ring, the number of vascular bundles decreased gradually until it reached the minimum of 197, with a reduction range of 7.51%. To 3 mm below sheath ring, the number of vascular bundles increased gradually, reaching a peak of 264, with an increase of 34.0%. To the sheath ring, the number of vascular bundles decreased gradually, and finally reached a stable value of 214, with a decrease range of 18.94%. The number change of vascular bundles was mainly caused by the bamboo green side. The number of vascular bundles increased significantly because of the bifurcation. A large number of vascular bundles in the bamboo green side formed closed ends with sheath falling off, resulting in a significant decrease in the number. (2) The shape of vascular bundles gradually changed from bottom to top in the bamboo node sample. The swollen vascular bundles began to appear at 7 mm below the sheath ring. Along the axis, the expanded shape expanded further,

mainly radial extension to the bamboo green side. In the extension, the regeneration and gradual offset of axial vascular bundles could be seen. The expanded shape also affected the adjacent vascular bundles, made them deform and offset. There are a large number of transverse vascular bundles near the sheath ring. After passing through the sheath ring, the morphology of vascular bundle began to be similar to that of internode.

[Conclusion] In the bamboo node, the number, morphology, arrangement and distribution of vascular bundles from 7 mm below the sheath ring to the sheath ring had continuous and complex changes. The changes in number were mainly caused by the vascular bundles on the green side of bamboo, and the changes in morphology, arrangement and distribution were related to the enlarged vascular bundles.

**Keywords:** Moso bamboo nodes; vascular bundles; number; morphology; arrangement and distribution

# 等离子体处理对热处理木材表面特性及渗透性能的影响

黄雅茜<sup>1</sup> 石江涛<sup>1</sup> 冷魏祺<sup>1</sup> 李万兆<sup>1</sup> 王新洲\*

(1 南京林业大学材料科学与工程学院 南京 210037)

**摘要:** 热处理技术可显著降低木材中碳水化合物和羟基的含量,从而提高木制品的生物耐久性和尺寸稳定性,作为一种环保的改性技术已被广泛应用于木材工业中。然而,在热处理过程中,半纤维素的降解会导致木材表面脆性增加及润湿性降低,进而对热处理木材胶合产品的粘接性能产生不利影响。近年来,等离子体处理作为一种环保、高效的改性方法被应用于提高生物复合材料表面润湿性进而提高界面结合强度。因此,本文采用高温饱和蒸汽对火炬松木材进行热处理,再通过大气介质阻挡放电(DBD)等离子体对热处理材(HTW)的界面性能进行改性,并运用扫描电子显微镜、压汞仪、红外光谱、X射线光电子能谱及荧光示踪技术研究木材微观结构、化学结构、润湿性等表面特征及胶黏剂渗透性的变化,评价等离子体对热处理材的改性效果。研究结果表明:热处理后早材与晚材的平均孔隙率从49.69%降低至38.33%,材料表面润湿性下降;而经等离子体处理后,热处理材的表面粗糙度略有增加,细胞壁表面可见蚀刻痕迹,同时亲水性基团和含氧官能团均略有增加,水及酚醛树脂胶粘剂(PF)在热处理材表面的润湿性得到显著改善。例如,未处理材的早材水接触角在10s内从72.9°急剧下降到0°;而在相同条件下,热处理材的早材水接触角从95.3°缓慢下降到54.08°,然后逐渐趋于稳定;经过等离子体处理后,其早材水接触角以较快的速率从33.47°下降到1.47°。同时经等离子体处理后,酚醛胶粘剂在热处理材中的平均渗透深度(AP)和有效渗透面积(EP)有所提升。在早材与早材胶接的试样中,热处理材经等离子处理后,胶粘剂平均渗透深度(AP)和有效渗透面积(EP)分别从909.5 μm和59.5 μm提升至1674.2 μm和183.2 μm。本文举例分析了等离子体处理对热处理材表面的物理及化学性能变化的影响,以证DBD等离子体处理是一种很有前途的提高HTW产品粘接性能的方法。

**关键词:** 木材; 热处理; 微观结构; 化学性质; 润湿性; 渗透性

# Effect of plasma treatment on the surface characteristics and penetration performance of heat-treated wood

Huang Yaqian<sup>1</sup>, Shi Jiangtao<sup>1</sup>, Leng Weiqi<sup>1</sup>, Li Wanzhao<sup>1</sup>, Wang Xinzhou<sup>1,\*</sup>

(1 College of Materials Science and Engineering, Nanjing Forestry University, Nanjing 210037)

**Abstract:** It is well known that heat treatment (HT) can significantly reduce the content of carbohydrates and hydroxyl in wood, thereby the biological durability and dimensional stability of wood products can be improved. In the past decades, as an environmental-friendly technology, HT has been widely used to modify the wood on the industrial scale. However, the degradation of hemicellulose during the heat treatment resulted in the increased surface brittleness and the decreased surface wettability of wood, which could produce negative effects on the bonding properties of the glued HT wood products. In recent years, plasma treatment has been proved as an eco-friendly and effective method to improve the surface wettability and then to increase the adhesion strength of biocomposites. Therefore, the atmospheric dielectric barrier discharge (DBD) plasma treatment was attempted to modify the interfacial properties of heat-treated wood (HTW) in this work. The changes in the wood surface characteristics such as the microstructure, chemical structure, and wettability were investigated by using scanning electron microscope (SEM), mercury intrusion porosimeter (MIP), FTIR spectroscopy, and X-ray photoelectron spectroscopy (XPS). The adhesive penetration performance was finally analyzed by the means of fluorescent tracer technique to evaluate the modification effect of plasma treatment. Results indicated that the mean porosity of both earlywood and latewood was decreased from 49.69% to 38.33% after heat treatment to some extent. However, the roughness of HTW surfaces is increased slightly after plasma treatment and etching traces are marginally visible on the cell wall surfaces of HTW. After being treated with plasma, the wettability of both water and phenolic formaldehyde adhesive on the surface of HTW is improved significantly, which can be mainly attributed to the increasing the hydrophilic groups and the oxygen-containing functional groups induced by plasma treatment. For example, the WCA on untreated pine's earlywood decreased sharply from 72.9° to 0° within 10s. However, the WCA on HTW's earlywood decreased slowly from 95.3° to 54.08° at the same condition, and then gradually tended to be stabilized. However, after plasma treatment, the WCA on PHW's earlywood decreased from 33.47° to 1.47° with a higher speed. Meanwhile, the average penetration (AP) and effective penetration (EP) of phenolic adhesive into heat-treated wood increased significantly, e.g., the AP and EP values of E-E bonded samples (earlywood to earlywood) of HTW increased from 909.5 and 59.5 μm to 1674.2 and 183.2 μm after plasma treatment, respectively, which indicated the DBD plasma treatment is a promising method to improve bonding properties of the glued HTW products.

**Keywords:** wood; heat treatment; microstructure; chemical properties; wettability; adhesive

penetration

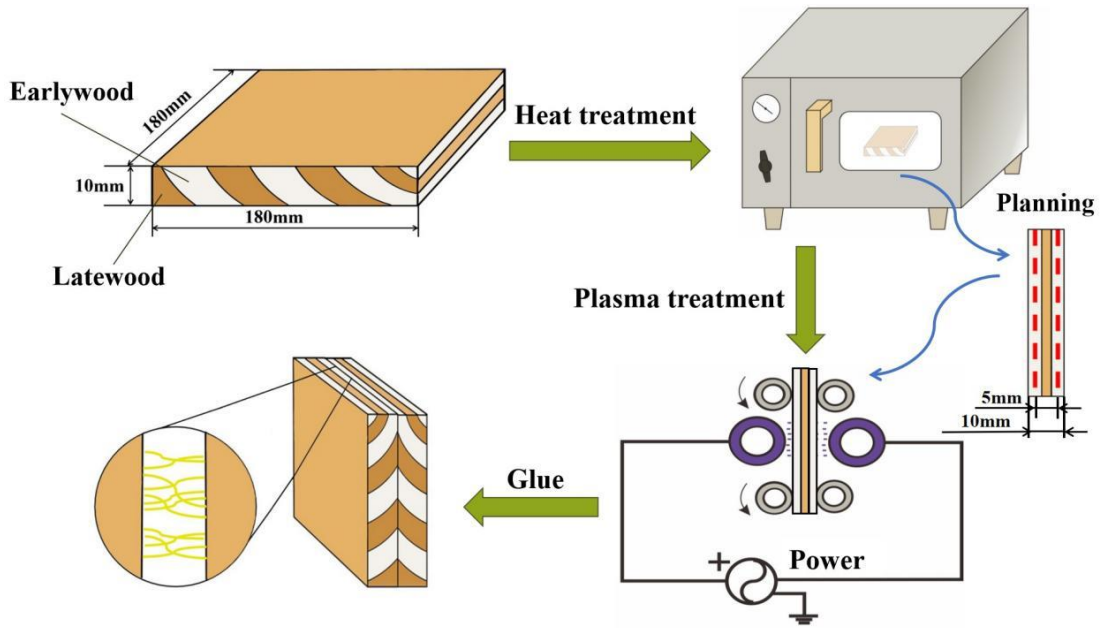


图 1 等离子体处理热处理木材的工艺流程示意图

Fig.1. The preparation processing of the plasma-treated HTW samples.

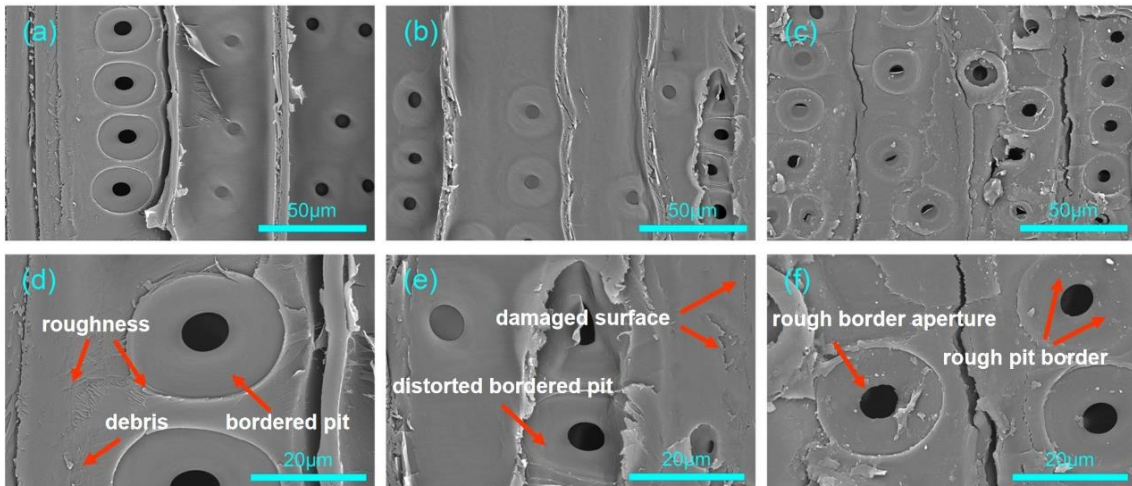


图 2 木材在不同处理状态下径切面的扫描电镜图像 (a, d: 未处理材; b, e: 热处理材; c, f: 经等离子体处理的热处理材)

Fig.2. SEM images of wood with different treatments along the tangential section (a, d: CW; b, e: HTW; c, f: PHTW).

# 橡胶木菌纹薄板的制备

闫妍 秦磊\* 张玲梅 邱坚

(西南林业大学云南省木材胶黏剂及胶合制品重点实验室, 云南 昆明 650224)

**摘要:** 菌纹薄板是真菌作用于木材薄板上产生美丽花纹的一种板材。真菌依靠木材上的营养物质生长形成菌纹线、染色及漂白现象。为了把菌纹木运用于家具行业, 本文以橡胶木薄板为研究对象, 通过人工分离、纯化野生花斑真菌和人工培育制备菌纹木薄板, 并对培育成功的菌纹木进行切片拍偏光及荧光图像来分析木质素和纤维素的降解程度。实验表明: 菌株 ZHX63-4 及菌株 ZHX18-6 培育形成的菌纹木, 用偏光和荧光显微镜观察, 它们和橡胶木正常材比较观察不到明显变化, 菌纹木薄板的腐朽程度比较小并不影响木材本身的性能, 因此在严格控制木材含水率和时间的前提下能满足家具等装饰行业的使用要求。

**关键词:** 菌纹薄板; 人工培育; 降解程度

# Preparation of rubberwood spatled veneer

Yan Yan, Qin Lei\*, Zhang Lin-mei, Qiu Jian

(Yunnan Provincial Key Laboratory of Wood Adhesives and Glued Products, Southwest Forestry University, Kunming 650224, Yunnan, China)

**Abstract:** Spatled veneer is a type of veneer in which fungi act on the wood veneer to produce a beautiful pattern. The fungus grows on the nutrients on the wood to form zone lines, staining and bleaching. In order to apply spatled wood to the furniture industry. In this paper, we prepared spatled wood veneers by artificially isolating and purifying wild fungus and artificially cultivating spatled wood veneers, and analyzed the degradation of lignin and cellulose by taking polarized light and fluorescence images of the successfully cultivated spatled wood sections. The experiments showed that the decay level of spatled wood veneers was relatively small and did not affect the performance of the wood itself, so it could meet the requirements of furniture and other decorative industries.

**Keywords:** Spatled veneer; artificial cultivation; the degree of degradation



# 心材型花斑木解剖构造特征分析

贾慧文<sup>1</sup> 李智<sup>1</sup> 郑平<sup>1</sup> 杨蕊<sup>2</sup> 邱坚<sup>1</sup>

(1 西南林业大学材料科学与工程学院, 云南 昆明 650233; 2 西南林业大学生物多样性保护学院, 云南 昆明 650233)

**摘要:** 花斑木(spalted wood)是指由微生物染色而形成美丽花纹的一类木材的统称, 最初从自然中发现, 主要发生在砍伐后的木材上或生长在环境条件恶劣下的活立木上。通过微生物在木材上着色, 从而使木材呈现独一无二的美感。心材型花斑木(heartwood spalted wood)是在探究花斑木形成机理时发现的一种与原有花斑木在花斑分布区域、颜色和形状上有很大区别的木材。笔者将对该心材型花斑木进行探究, 确定易产生心材型花斑的树种, 并进一步探索花斑的存在对木材宏观微观的影响, 为后续心材型花斑木形成机理的研究提供理论依据。通过观察法和木材解剖学方法对具有心材型花斑的木材进行观察研究; 采用体视数码显微镜、生物数码显微镜和扫描电子显微镜, 对有无花斑部位进行对比分析。取现有心材型花斑木, 由西南林业大学木材标本馆提供, 对木材的宏观微观结构进行分析, 木材在宏观下心材部位有明显的黑色纹路, 黑色花斑部位颜色有明显的深浅不同, 可以看到明显的颜色变化, 但木材触感没有影响, 没有明显的过渡, 产生花斑的木材密度很大。木材材色黄褐色, 有光泽, 无特殊气味和滋味。生长轮界明显但心边材区别不明显, 薄壁组织在放大镜下略见, 主要为细弦线; 木射线在放大镜下略见(见图1), 甚窄。

微观情况下, 具有与宏观完全一致的明显黑色纹路, 花斑覆盖木材结构, 花斑较深部位完全看不到结构, 较浅部位可以看到部分。黑色花斑形似油脂或色素(见图2), 材色黄褐色, 散孔材, 径列或斜列管孔, 主为单管孔, 少数径列复管孔2-4个, 管孔平均弦径 $98.8\mu\text{m}$ ; 导管分子长度平均 $530\mu\text{m}$ ; 木纤维壁厚平均 $15.3\mu\text{m}$ , 平均长度 $1251.9\mu\text{m}$ 。心材导管内含树脂, 单穿孔, 管间纹孔式互列。导管射线间纹孔式与管间纹孔式相同状, 轴向薄壁组织离管带状(多为单列, 少数两列), 木射线非叠生。多数单列, 偶见两列, 木射线平均高度 $281.7\mu\text{m}$ 。在荧光、偏光下(见图4、5), 整体亮度木射线细胞壁>木纤维组织>黑色花斑部位, 花斑部分由于黑色类油脂色素不会产生偏光荧光, 所以亮度最暗。扫描电镜下(见图6), 花斑部位没有任何结构的破坏, 证明花斑并不会造成内部结构的变化。得出结果: 该木材为柿科柿属缅甸垂枝柿(*Diospyros* spp.), 经过大量的心材型花斑木探究, 易产生花斑的木材树种主要为柿科柿属, 花斑没有造成宏观微观结构的影响, 没有腐朽产生。结论: 心材型花斑木的花斑存在并不会影响木材材性。

**关键词:** 心材型花斑木; 宏观; 微观; 荧光; 偏光; 扫描电镜

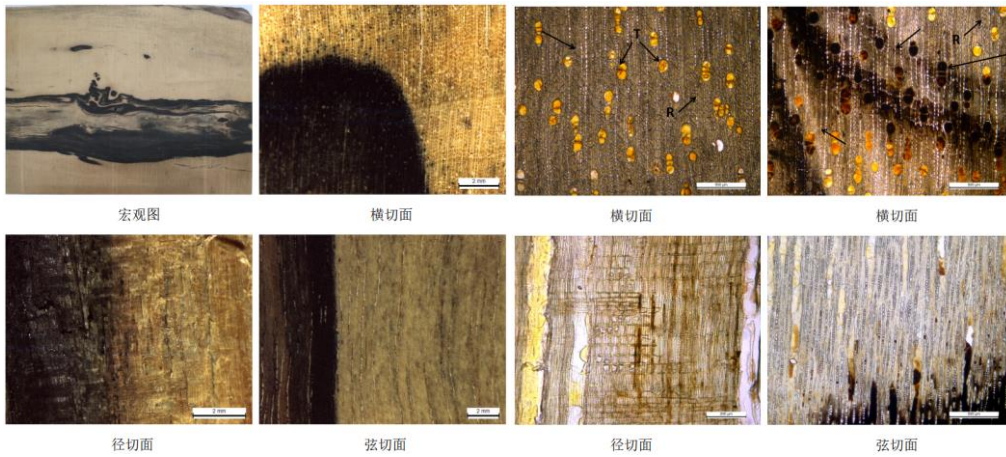


图 1 心材型花斑木宏观图片

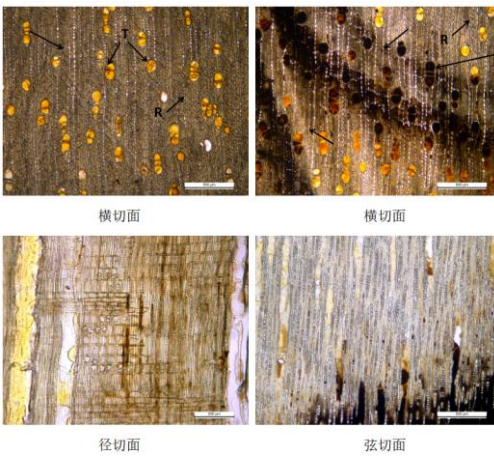


图 2 心材型花斑木微观图片

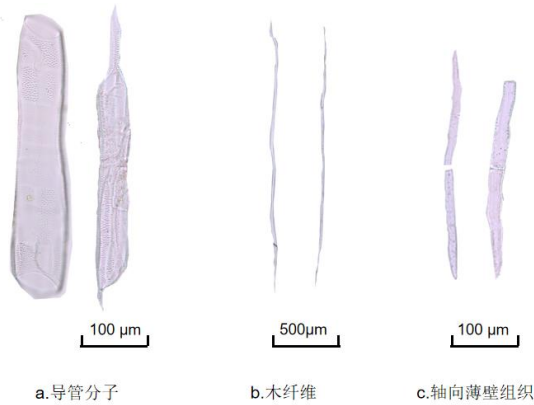


图 3 心材型花斑木离析图片

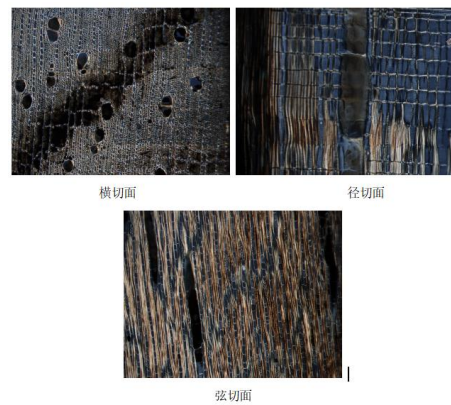


图 4 心材型花斑木偏光图片

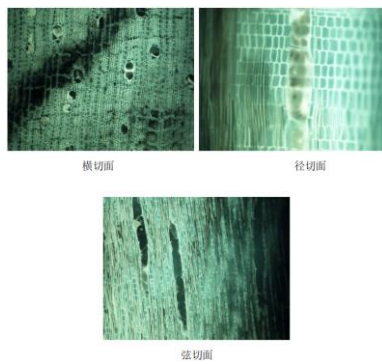


图 5 心材型花斑木荧光图片

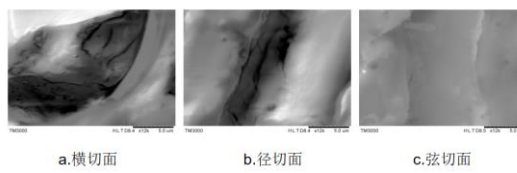


图 6 心材型花斑木 SEM 图片

# Analysis of anatomical structure characteristics of heartwood spalted wood

**Abstract:** Spalted wood is a general name for a kind of wood dyed by microorganisms to form beautiful patterns. It was first found in nature, and mainly occurred on felled wood or on standing trees under harsh environmental conditions. Wood is colored by microorganisms, so that it presents a unique aesthetic feeling. Heartwood spalted wood is a kind of wood which is found to be quite different from the original spalted wood in the distribution area, color and shape. In this paper, the author will explore the heartwood spalted wood, identify the tree species which are easy to produce heartwood spalted wood, and further explore the influence of the existence of spalted wood on the macroscopic and microscopic aspects of wood, so as to provide theoretical basis for the subsequent research on the formation mechanism of heartwood spalted wood. The wood with heartwood spalted was observed and studied by observation and wood anatomy. Stereoscopic digital microscope, biological digital microscope and scanning electron microscope were used to compare and analyze the spalted. The existing heartwood spalted wood is provided by the Wood Specimen Museum of Southwest Forestry University. The macroscopic and microscopic structure of wood was analyzed, On the macro level and it was found that the wood had obvious black lines in the heartwood and the color of black spalted was obviously different in depth. We can see the obvious color change, but the touch of wood has no effect, and there is no obvious transition. The density of wood that produces spalted is very high. Wood is yellow-brown and shiny, without special smell and taste. The growth ring boundary is obvious, but the difference between heartwood and sapwood is not obvious. The parenchyma is slightly seen under a magnifying glass, and it is mainly thin strings. Wood rays are slightly seen under a magnifying glass ( fig. 1), which is very narrow.

Microscopically, it has obvious black lines which are completely consistent with macroscopic. The spalted cover the wood structure, and the structure can not be seen at the deeper part of the spalted, while the part can be seen at the shallower part. Black spalted are similar to oil or pigment (fig. 2), and the color of wood is yellow-brown, Wood diffuse-porous, Vessels in diagonal or radial pattern, Vessels exclusively solitary, Vessels in radial multiples of 2-4, The average chord diameter of the pipe is  $98.8 \mu\text{m}$ ; The average length of vessel molecules is  $530 \mu\text{m}$ ; The average wall thickness of wood fiber is  $15.3\mu\text{m}$  and the average length is  $1251.9 \mu\text{m}$ . Heartwood spalted wood duct contains gum, Simple perforation plates, Intervessel pits alternate, The inter-ray groove type is the same as the inter-tube groove type, Axial parenchyma is separated from the tube (mostly single column, a few two columns). Wood rays are not storied. Rays exclusively uniseriate, occasionally width 2 cells, The average ray height of wood is  $281.7 \mu\text{m}$ . Under fluorescence and polarized light ( fig. 4 and fig. 5), the overall brightness of wood ray cell wall > wood fiber tissue > black spot part,

and the spot part is the darkest because black grease pigment does not produce polarized fluorescence. Under the scanning electron microscope ( fig. 6), there is no structural damage in the spot, which proves that the spot will not change the internal structure. Results: The wood is *Diospyros spp.* After a lot of exploration of heartwood spalted wood, it is found that the main wood species prone to mottling are *Diospyros* of Ebenaceae. Spalted have no influence on macro and micro structures, and there is no decay. Conclusion: The existence of mottle in heartwood spalted wood does not affect the wood properties.

**Keywords:** heartwood spalted wood; Macroscopic; Microscopic; Fluorescence; Polarized light; scanning electron microscope

# 人工林杨树吸收土壤中重金属 Cd 的累积规律研究

戎恭<sup>1,2</sup> 储茵<sup>2,\*</sup> 刘盛全<sup>1,\*</sup>

(1 安徽农业大学林学与园林学院, 合肥 230036; 2 安徽农业大学资源与环境学院, 合肥 230036)

**摘要:** 为探究杨树对土壤重金属 Cd 胁迫的响应, Cd 进入杨树体内后的分布、转运、动态累积规律和累积机制以及杨树对 Cd 的提取修复潜能。以人工林 69 杨(*Populus deltoids* Bartr. cv. 'Lux' I-69/55)为研究对象, 通过添加 5、20、50、100 mg·kg<sup>-1</sup> Cd(NO<sub>3</sub>)<sub>2</sub> 处理土壤进行盆栽试验, 同时设置未施加 Cd 土壤作为对照组。通过连续三年跟踪测定不同浓度 Cd 污染下杨树的生长量, 在收获时测量不同部位、树干和树皮不同高度下的 Cd 含量、计算生物富集系数和转运系数来分析比较杨树对重金属 Cd 的富集、转运能力。结果表明, 杨树在 Cd 胁迫下均能随着生长季不断增长, 树高在第二年和第三年分别比第一年增加了 16.1%和 26.4%, 地径分别增加了 32.8%和 82.1%, 表明杨树对 Cd 有较强的耐受性。杨树各部位 Cd 含量均随着处理浓度的增加而显著增加, 不同部位对 Cd 的吸收和富集能力总体表现为树叶>树皮>树枝>树根>树干。随着生长季的延长, Cd 在地上各部位逐年累积, 各生长季地上部分 Cd 含量均表现出从树干基部、中部、顶部、树枝到树叶逐渐增加的趋势, 表明 Cd 从根部进入杨树后, 沿着导管经过树干、树枝从底部向上转运最终在树叶中累积。杨树因其强大的生物量和转运能力, 可以将土壤中的 Cd 转移至地上部分并在树叶中积累下来。

**关键词:** 重金属 Cd; 植物提取; 直立生长; 69 杨; 树木修复

# Study on the accumulation of heavy metal Cd in soil absorbed by poplar plantation

Rong Gong<sup>1,2</sup>, Chu Yin<sup>2,\*</sup>, Liu Sheng-quan<sup>1,\*</sup>

(1 College of Forestry and Landscape Architecture, Anhui Agricultural University, Hefei 230036; 2 College of Resources and Environment, Anhui Agricultural University, Hefei 230036)

**Abstract:** In order to explore the response of poplar to soil heavy metal Cd stress, the distribution, transport, dynamic accumulation laws and accumulation mechanism of Cd after entering poplar, as well as the extraction and repair potential of poplar to Cd. Taking the artificial forest poplar 69(*Populus deltoids* Bartr. cv. 'Lux' I-69/55) as the research object, the pot experiment was carried out by adding 5, 20, 50, 100 mg·kg<sup>-1</sup> Cd(NO<sub>3</sub>)<sub>2</sub> to the soil treated, and the soil without Cd was set as the control group. By tracking and measuring the growth of poplar under different concentrations of Cd pollution for three consecutive years, measuring the Cd content in different parts, trunk and bark at different heights at harvest, and calculating the bioconcentration coefficient and transport coefficient, the enrichment and transport capacity of poplar to heavy metal Cd were analyzed and compared. The results showed that poplars can grow with the growing season under Cd stress. The height of the trees increased by 16.1% and 26.4% in the second year and the third year, and the ground diameter increased by 32.8% and 82.1% respectively, indicating that poplar has a strong tolerance to Cd. The Cd content of each part of the poplar increased significantly with the increase of the treatment concentration. The overall performance of the Cd absorption and enrichment capacity of different parts of the poplar was leaf>bark>branch>root>trunk. With the extension of the growing season, Cd accumulates in various parts of the ground year by year. The Cd content of the above-ground part of each growing season shows a gradual increase from the base, middle, top of the tree trunk, branches to leaves, indicating that Cd enters the poplar from the root and along the vessels through the trunk and branches are transported from the bottom up and finally accumulated in the leaves. Poplar trees can transfer Cd in the soil to the above-ground part and accumulate in the leaves due to their strong biomass and transport capacity.

**Keywords:** heavy metal Cd; Phytoextraction; Upright growing; Poplar 69; Dendroremediation

# 钝叶黄檀和斜叶黄檀新鲜叶片 DNA 提取方法的研究

曹秀龙<sup>1</sup> 甘昌涛<sup>2</sup> 邱坚<sup>1</sup>

(1 西南林业大学材料科学与工程学院 云南昆明 650224; 2 西南林业大学艺术与设计学院 云南昆明 650224)

## 摘要:

【背景】相较于传统形态学分类, DNA 条形码不受组织部位、发育时期和样品状态等因素的限制, 可以直接鉴别到物种的水平。

【目的】为了探寻钝叶黄檀 (*Dalbergia obtusifolia*) 与斜叶黄檀 (*Dalbergia pinnata*) 新鲜叶片 DNA 的最佳提取方法。

【方法】本研究以两个树种的新鲜叶片为研究对象, 分别用 CTAB 植物基因组 DNA 快速提取试剂盒、植物基因组 DNA 提取试剂盒 (通用型) (Trelife™ Plant Genomic DNA Kit)、自行改良的 CTAB 植物基因组 DNA 提取试剂盒以及 Ezup 柱式植物基因组 DNA 抽提试剂盒对两个树种新鲜叶片 DNA 进行提取, 并通过 NanoDropND-2000 超微量分光光度计检测 DNA 样品的浓度与质量、用 3.0% 琼脂糖凝胶电泳检测 DNA 样品的完整性和降解程度、设计 15 条引物对 DNA 样本进行 PCR 扩增以及用 3.5% 琼脂糖凝胶电泳检测扩增效果; 从而对钝叶黄檀 (*Dalbergia obtusifolia*) 与斜叶黄檀 (*Dalbergia pinnata*) 新鲜叶片 DNA 的提取方法进行研究。

【结论】研究表明: (1) 除植物基因组 DNA 提取试剂盒 (通用型) 法以外的其他 3 种方法提取的边叶片基因组虽然都存在微量的 RNA 污染或者碳水化合物 (糖类) 污染, 但其提取浓度与纯度均能满足后续的 PCR 扩增反应要求; (2) 对于同一树种叶片而言, CTAB 植物基因组 DNA 快速提取试剂盒法提取的叶片 DNA 虽然浓度最低, 但纯度最高 (平均浓度: 钝叶黄檀为  $171.1\text{ng}\cdot\mu\text{L}^{-1}$ ; 斜叶黄檀为  $42.5\text{ng}\cdot\mu\text{L}^{-1}$ ); 自行改良的 CTAB 植物基因组 DNA 提取试剂盒法的提取效果恰好与之相反 (平均浓度: 钝叶黄檀为  $628.5\text{ng}\cdot\mu\text{L}^{-1}$ ; 斜叶黄檀为  $299.4\text{ng}\cdot\mu\text{L}^{-1}$ ); 而 Ezup 柱式植物基因组 DNA 抽提试剂盒法所提 DNA 的浓度和纯度皆介于二者之间 (平均浓度: 钝叶黄檀为  $212.6\text{ng}\cdot\mu\text{L}^{-1}$ ; 斜叶黄檀为  $58.2\text{ng}\cdot\mu\text{L}^{-1}$ ); (3) 从凝胶电泳图中可以看出, 三种提取方法所得 DNA 均有降解, 其中自行改良的 CTAB 植物基因组 DNA 提取试剂盒法对应的 DNA 样本降解最为严重, 但是均满足后续分子实验要求; (4) PCR 扩增产物凝胶电泳结果显示, 第 2、3、6、7 号引物不适于对这两种木材 DNA 进行扩增, 可能是因为引物本身设计不当或者是退火温度太高所导致的, 同时, 该凝胶电泳结果也说明高纯度低浓度的 DNA 能够满足 DNA 分子实验要求; (5) 新鲜叶片 DNA 的提取效果与叶片本身的碳水化合物 (糖类)、盐类等含量有关, 本研究中同一种方法提取的 DNA 样品浓度和质量, 斜叶黄檀较钝叶黄檀要差些, 原因在于斜叶黄檀叶片中含有大量的多糖多酚等物质, 使提取液更加粘稠, 影响 DNA 提取效果。

**关键词:** 钝叶黄檀; 斜叶黄檀; CTAB; 试剂盒; DNA 提取方法

# Study on Methods of DNA extraction from fresh leaves of *Dalbergia obtusifolia* and *Dalbergia pinnata*

Cao Xiulong<sup>1</sup>, Gan Changtao<sup>2</sup>, Qiu Jian<sup>1</sup>

(1 Southwest Forestry University Materials Science and Engineering College Kunming, Yunnan Province, 650224;

2 Southwest Forestry University Materials Art and Designing College Kunming, Yunnan Province, 650224)

## Abstract:

[Background] Compared with traditional morphological classifications, DNA barcodes are not limited by factors like tissue site, developmental period, and sample status, and can be directly identified to the sample level.

[Objective] To explore the best extraction method of DNA from fresh leaves of *Dalbergia obtusifolia* and *Dalbergia pinnata*.

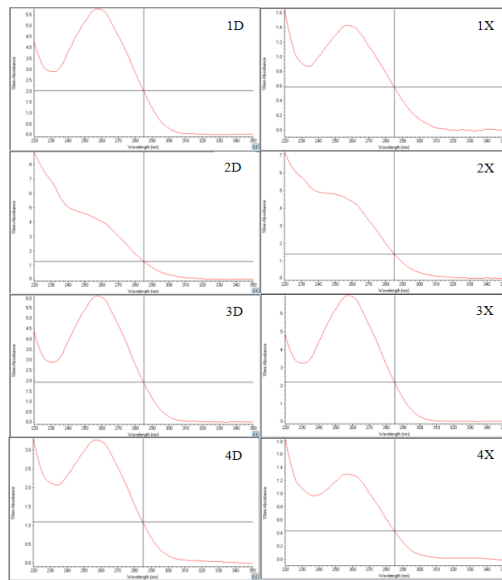
[Methods] In this study, fresh leaves of two tree species were taken as research objects. CTAB Rapid extraction kit for Plant Genomic DNA, Trelife™ Plant Genomic DNA extraction Kit (General type), self-improved CTAB Plant Genomic DNA Extraction Kit and Ezup Column Plant Genomic DNA extraction Kit were used respectively to extract DNA from fresh leaves of two tree species. The concentration and quality of DNA samples were detected by NanoDropND-2000 ultrafine spectrophotometer, the integrity and degradation degree of DNA samples were detected by 3.0% agarose gel electrophoresis, 15 primers were designed for PCR amplification of DNA samples, and the amplification effect was detected by 3.5% agarose gel electrophoresis. Thus, the methods of DNA extraction from fresh leaves of *Dalbergia obtusifolia* and *Dalbergia pinnata* were studied.

[conclusion] the results showed that: (1) Although the genomes extracted by the other three methods except the Trelife™ Plant Genomic DNA Kit (General type) were contaminated with trace amounts of RNA or carbohydrates (carbohydrates), their extraction concentration and purity could meet the requirements of subsequent PCR amplification reaction; (2) For the leaves of the same tree species, the leaf DNA extracted by CTAB rapid extraction kit had the lowest concentration but the highest purity (Average concentration: *Dalbergia obtusifolia* is 171.1ng·μL<sup>-1</sup>; *Dalbergia pinnata* is 42.5ng·μL<sup>-1</sup>); The extraction effect of CTAB plant genome DNA extraction kit was just the opposite (Average concentration: *Dalbergia obtusifolia* is 628.5ng·μL<sup>-1</sup>; *Dalbergia pinnata* is 299.4ng·μL<sup>-1</sup>). The concentration and purity of DNA extracted by Ezup column plant genomic DNA extraction kit were between the two methods (Average concentration: *Dalbergia obtusifolia* is 212.6ng·μL<sup>-1</sup>; *Dalbergia pinnata* is 58.2ng·μL<sup>-1</sup>); (3) As can be seen from the gel electrophoresis diagram, DNA obtained by the three extraction methods were degraded, among which the DNA samples corresponding to the self-improved CTAB plant genomic DNA extraction kit method were the most degraded, but all met the requirements of subsequent molecular experiments. (4) The



products of the PCR amplification gel electrophoresis results showed that 2, 3, 6, 7 primers is not suitable for DNA amplification of the two kinds of wood, probably because the primer itself caused by improper design or the annealing temperature is too high, at the same time, the gel electrophoresis results also suggests that low concentration of DNA with high purity can meet the requirements of the DNA molecule experiments; (5) The extraction effect of DNA from fresh leaves was related to the contents of carbohydrates (sugars) and salts in leaves. In this study, *Dalbergia pinnata* was inferior to *Dalbergia obtusifolia* in the concentration and quality of DNA samples extracted by the same method. The reason is that *Dalbergia pinnata* leaves contain a lot of polysaccharide polyphenols and other substances, which make the extract more viscous and affect the DNA extraction effect.

**Keywords:** *Dalbergia obtusifolia*; *Dalbergia pinnata*; CTAB; Kit; DNA extraction methods

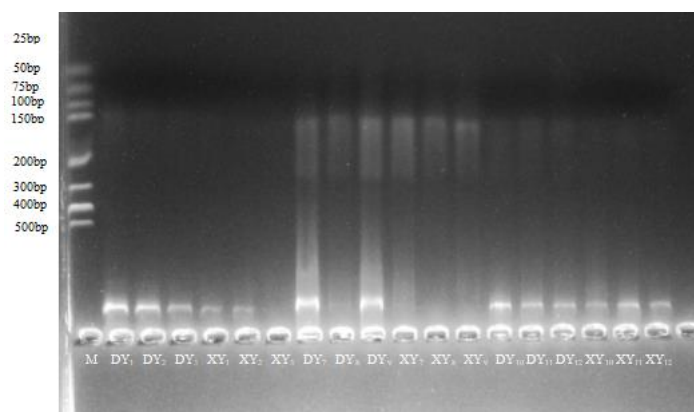


1: CTAB 植物基因组 DNA 快速提取试剂盒法; 2: 植物基因组 DNA 提取试剂盒 (通用型) 法; 3: 自行改良的 CTAB 植物基因组 DNA 提取试剂盒法; 4: Ezup 柱式植物基因组 DNA 抽提试剂盒法; D: 钝叶黄檀 (*Dalbergia obtusifolia*) 新鲜叶片; X: 斜叶黄檀 (*Dalbergia pinnata*) 新鲜叶片

1: CTAB Plant Genomic DNA rapid extraction kit; 2: Plant Genomic DNA extraction kit (general type) method; 3: self-modified CTAB Plant Genome DNA extraction kit; 4: Ezup column Plant Genome DNA extraction kit; D: blunt leaf sandalwood (*Dalbergia obtusifolia*) fresh leaves; X: oblique leaf sandalwood (*Dalbergia pinnata*) fresh leaves

图 1-1 DNA 吸光度曲线图

Figure 1-1 Plot of the absorbance of DNA

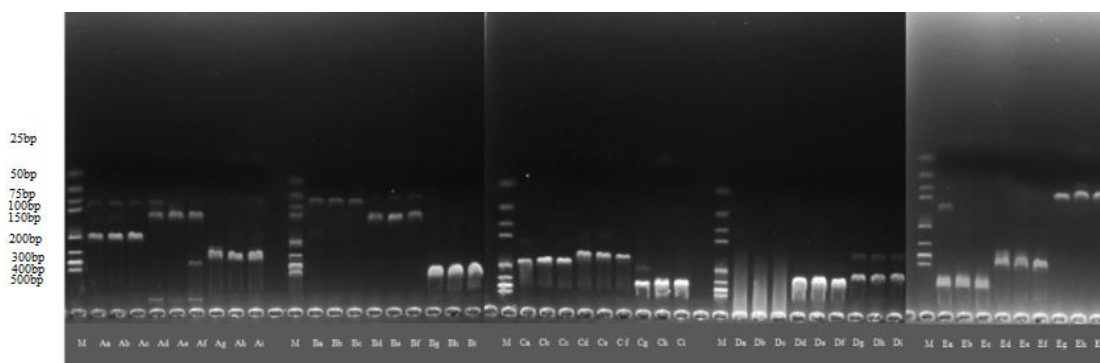


M: DNA 分子量标准 Marker A(25~500bp); DY: 钝叶黄檀; XY: 斜叶黄檀; 1~3: CTAB 植物基因组 DNA 快速提取试剂盒; 7~9: 自行改良的 CTAB 植物基因组 DNA 提取试剂盒法; 10~12: Ezup 柱式植物基因组 DNA 抽提试剂盒

M: DNA Molecular weight standard Marker A (25~500bp); DY: blunt leaf sandalwood; XY: oblique leaf sandalwood; 1~3: CTAB Plant Genome DNA rapid extraction kit; 7~9: Self-modified CTAB Plant Genomic DNA extraction kit; 10~12: Ezup column Plant Genomic DNA extraction kit

图 1-2 3 种 DNA 提取方法所得 DNA 样品凝胶电泳图

Figure 1-2 Gel electrophoresis plot of DNA samples obtained from the 3 DNA extraction methods

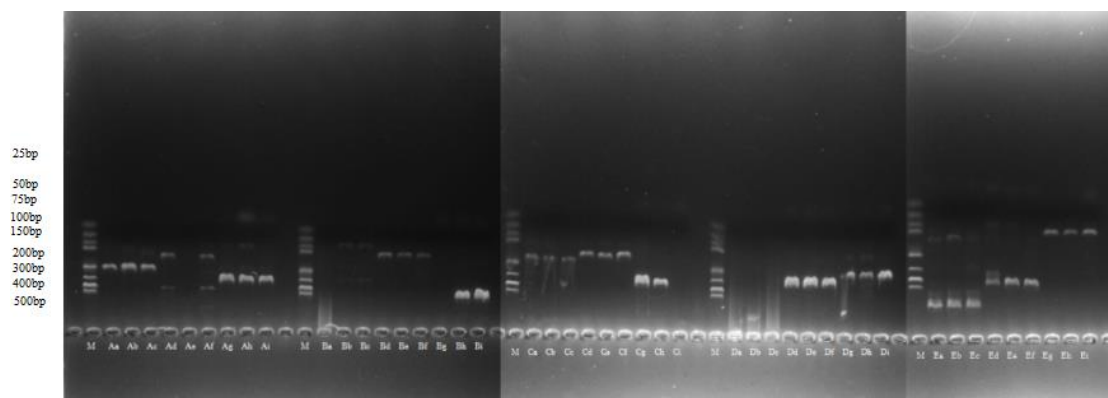


M: DNA 分子量标准 Marker A(25~500bp); A: *psbA-trnH*; B: *rbcL*; C: *matK*; D: ITS2、ITS1、ITS2; E: *trnL*。每一种引物从左往右按照引物编号从小到大排列。

M: DNA Molecular Weight Standard Marker A (25~500bp); A: *psbA-trnH*; B: *rbcL*; C: *matK*; D: ITS2, ITS1, ITS2; E: *trnL*. Each primer was arranged from left to right according to primer numbers from small to large.

图 1-3 钝叶黄檀 DNA 样品 PCR 产物凝胶电泳图

Figure 1-3 Gel electrophoresis plot of PCR products of *Dalbergia obtusifolia* DNA samples



M: DNA 分子量标准 Marker A(25~500bp); A: *psbA-trnH*; B: *rbcL*; C: *matK*; D: ITS2、ITS1、ITS2; E: *trnL*。每一种引物从左往右按照引物编号从小到大排列。

M: DNA Molecular Weight Standard Marker A (25~500bp); A: *psbA-trnH*; B: *rbcL*; C: *matK*; D: ITS2, ITS1, ITS2; E: *trnL*. Each primer was arranged from left to right according to primer numbers from small to large.

图 1-4 斜叶黄檀 DNA 样品 PCR 产物凝胶电泳图

Figure 1-4 Gel electrophoresis plot of PCR products of *Dalbergia pinnata* DNA samples

# 碳酸钙原位增强热改性杨木热稳定性研究

梁殿恩 杨子 李龙浩 王健博 孙玉 姚涛 丁振浩 刘盛全 储德森\*

(国家林草局重点实验室“林木材质改良与高效利用”, 安徽农业大学林学与园林学院, 合肥 230036)

**摘要:** 为了提高热处理杨木的热稳定性和拓展其使用范围, 实现速生材的高质利用。本研究利用绿色环保无机物  $\text{CaCO}_3$ , 采用原位改性方法对  $200^\circ\text{C}$ 、1.5hr/3hr 蒸汽热处理的热改性杨木进行填充增强处理。首先, 在真空条件下将浓度比为 1:1 的  $\text{CaCl}_2$  和  $\text{Na}_2\text{CO}_3$  溶液先后导入木材中, 使  $\text{CaCO}_3$  晶体原位生成于热改性材内部以得到  $\text{CaCO}_3$ -热改性材复合材料。然后筛选出最佳填充效果的浸渍液浓度, 并着重分析热改性材内部原位形成的  $\text{CaCO}_3$  阻隔层对热改性材热稳定性的影响。研究发现浸渍液浓度为  $1.2\text{mol/L}$  时木材中  $\text{CaCO}_3$  的填充效果最佳, SEM 显示  $\text{CaCO}_3$  生成在热改性材细胞腔、附于并嵌入细胞壁中。热重分析表明, 由于碳酸钙的引入, 素材、 $200^\circ\text{C}$  热处理 1.5hr 和 3hr 杨木试样的残碳率依次增高 8.96%、9.37% 和 9.62%, 最大失重速率依次降低 11.48%、19.75% 和 17.74%, 热稳定性明显提升。碳酸钙原位填充可有效提升热处理材的热稳定性, 对于热改性材应用的拓展具有一定意义。

**关键词:** 高温热处理; 碳酸钙; 杨木; 原位合成; 复合材料; 热稳定性

# Study on the thermal stabilization of heat-treated poplar wood enhanced by in-situ synthesis of CaCO<sub>3</sub>

Liang D E, Yang Z, Li L H, Wang J B, Sun Y, Yao T, Ding Z H, Liu S Q, Chu D M\*

(Key Lab of State Forest and Grassland Administration on "Wood Quality Improvement & High Efficient Utilization", School of Forestry & Landscape Architecture, Anhui Agricultural University, Hefei 230036)

**Abstract:** In order to enhance the thermal stabilization of high temperature heat treated wood and expand its application range, achieving high-quality utilization of the fast-growing wood. In this study, CaCO<sub>3</sub>, which is thought to be an environmental-friendly inorganic substance, was in-situ synthesized into the poplar after high temperature heat treatment under 200°C for 1.5hr/3hr with steam. The CaCl<sub>2</sub> and Na<sub>2</sub>CO<sub>3</sub> solutions with a concentration ratio of 1:1 was successively introduced into the thermal modified wood at vacuum condition, so that CaCO<sub>3</sub> crystals could generated in-situ in the wood structure, and the CaCO<sub>3</sub> thermal modified material composite material was obtained. The concentration of the impregnation solution with the best filling effect was selected, and the thermal stability of the CaCO<sub>3</sub> in-situ treated thermal modified wood was analyzed. The results showed that the solution concentration of 1.2 mol/L has the best impregnation effect, and CaCO<sub>3</sub> is generated in the cell cavity of thermal modified wood, some of them are embedded in the cell wall. The thermogravimetric analysis shows that the residual mass rate of the untreated wood, and samples treated at 200°C for 1.5hr and 3hr were increased by 8.96%, 9.37% and 9.62% due to the synthesis of CaCO<sub>3</sub>, and the maximum of the pyrolysis rate of them were decreased by 11.48%, 19.75% and 17.74%, correspondingly. The CaCO<sub>3</sub> in-situ modification resulted in the enhancement of wood thermal stabilization on the heat-treated wood. Therefore, CaCO<sub>3</sub> filling could be a reference for the application of thermal modified wood. The CaCO<sub>3</sub> in-situ can effectively improve the thermal stability of heat-treated wood, which is of great importance for the expansion of the application.

**Keywords:** CaCO<sub>3</sub>; Heat treatment; Poplar wood; In-situ synthesis; Composite materials; Thermal stabilization

# 毛白杨不同冠层枝条木质部水力功能性状对水氮添加的响应

章毓文<sup>1</sup> 刘岩<sup>1</sup> 李姍<sup>2</sup> 席本野<sup>1</sup> 段劼<sup>1,\*</sup>

(1 北京林业大学林学院, 北京 100083; 2 陕西科技大学环境科学与工程学院, 西安 710021)

## 摘要:

**【目的】**杨树是一种速生、环境敏感型树种, 合理的灌溉和施氮可以有效提升杨树的吸水量和生长量, 但木质部输水结构在这些处理下的变化还不明确。本文旨在探索长期水氮处理下, 毛白杨枝条木质部解剖结构、导水率、木材密度等水力功能性状在冠层间的变异规律及可塑性差异, 为加深树种生理学认知, 改善人工林水养管理策略提供依据。

**【方法】**以六年生三倍体毛白杨无性系 S86 [*Populus tomentosa* × *P. bolleana*) × (*P. alba* × *P. glandulosa*)] 为研究对象, 在大田环境下设置长期的灌溉、施氮和水氮耦合处理。从各处理林木中选取 3 株平均木, 从上、中、下冠层内分别剪取 6 根二至三年生枝条, 测定木材密度, 并制作木质部横切显微切片。利用光学显微镜观察导管和纤维的解剖结构指标, 并推算导水率和导管加固系数。通过方差分析检验冠层、灌溉和施肥三类因子对木质部水力功能性状的影响, 通过相关性分析检验性状间的相关性。

**【结果】**(1) 冠层高度对毛白杨木质部水力性状的影响最为广泛, 导管水力直径 ( $D_h$ )、单管孔比重 (SVD) 和纤维腔径 ( $D_f$ ) 随冠层高度的上升而下降, 导管密度 (VD)、导管腔占比 (VF)、导管加固系数 ( $(t/b)^2$ )、纤维壁腔比 ( $(L/D)_f$ ) 和木材密度 (WD) 随冠层高度的上升而上升, 导管双壁厚 ( $t$ )、纤维双壁厚 ( $L_f$ ) 和理论导水率 ( $K_p$ ) 则在不同冠层间无显著差异; (2) 长期的水氮处理改变了枝条木质部的 SVD、 $D_f$ 、 $L_f$ 、 $(L/D)_f$ 、 $K_p$  等一系列指标, 但各冠层的响应规律不完全相同, 相比上冠层, 中下冠层受水氮添加的影响更显著; (3) 木质部各类功能性状之间存在复杂的关联, 纤维结构和导管结构间、木材密度和解剖指标间均存在良好的相关性。

**【结论】**随着冠层高度的上升, 毛白杨枝条木质部的水力结构呈现出显著的轴向变异。下冠层枝条呈现高效、高风险型策略, 而上冠层枝条则呈现保守、安全型结构策略, 这样的差异可能源于不同树高上的水力风险。结构策略的差异还影响了枝条木质部对水氮处理的响应, 尽管水氮处理改变了一系列水力性状, 但各冠层的响应规律和敏感程度均不相同, 中下冠层的枝条木质部对土壤水肥环境更敏感。同时, 研究还发现了枝条木材密度与解剖结构、水力功能之间复杂的相关关系, 高密度木材往往具有更安全、但也更低效的水力构造。表明即使在被子植物复杂的木质部构成下, 木材密度这类传统指标仍旧具有良好的水力学指示意义。

**关键词:** 木质部结构; 水力功能; 可塑性; 毛白杨; 木材密度

# Response of xylem hydraulic function traits to water and nitrogen addition in different canopy height of *Populus tomentosa*

Zhang Yuwen<sup>1</sup>, Liu Yan<sup>1</sup>, Li Shan<sup>2</sup>, Xi Benye<sup>1</sup>, Duan Jie<sup>1</sup>

(1 School of Forestry, Beijing Forestry University, Beijing 100083, China; 2 School of Environmental Science and Engineering, Shaanxi University of Science and Technology, Xi'an 710021)

## Abstract:

[Objective] *Populus* is a fast-growing species that is also very sensitive to the environment. Therefore, irrigation and nitrogen addition can significantly improve water absorption and growth of poplars. However, the changes of the xylem transport structure under these treatments are still unclear. This study investigated the variety and plasticity of xylem hydraulic function traits, including xylem anatomical structure, hydraulic conductivity, and wood density of *Populus tomentosa* branches treated with long-term water and nitrogen treatment. As a result, we better understand the physiological characteristics, which can also be used to guide future *Populus* plantation and management.

[Method] 6-year-old triploid *Populus tomentosa* clone S86 [*(Populus tomentosa* × *P. bolleana*) × (*P. alba* × *P. glandulosa*)] were taken as the research object, long-term irrigation, nitrogen, and fertigation treatment were applied in the field. Three mean sample trees of each treatment were selected, and six 2 to 3 years old branches were cut from the upper, middle, and lower canopy to measure wood density and xylem anatomical traits. The vessel and fiber structure were observed using a light microscope, and theoretical hydraulic traits, including hydraulic conductivity and vessel wall reinforcement, were calculated from previous equations. Kolmogorov–Smirnov test, analysis of variance (ANOVA) and Pearson correlations were used for data analysis.

[Result] (1) Canopy position had the most significant effect on xylem hydraulic traits. Vessel hydraulic diameter ( $D_h$ ), single vessel density (SVD), fiber lumen diameter ( $D_f$ ) increased with canopy height. In contrast, vessel density (VD), vessel fraction (VF), vessel wall reinforcement  $(t/b)^2$ , fiber wall to lumen ratio  $(L/D)_f$ , wood density (WD) changed inversely. And the wall thickness of vessels and fibers ( $t$ ,  $L_f$ ), potential hydraulic conductivity ( $K_p$ ) had no significant differences among canopy layers. (2) Three years of irrigation and fertilization altered some xylem traits, such as SVD,  $D_f$ ,  $L_f$ ,  $(L/D)_f$ ,  $K_p$ , but the response of xylem differed between different canopy layers. The xylem of the middle and lower canopy was more sensitive to water and nitrogen addition than the upper canopy. (3) Correlations between xylem hydraulic functional traits were complex, vessel structure and fiber structure, wood density and anatomical traits were all found to be closely related.

[Conclusion] The xylem structure of *Populus tomentosa* varied significantly axially within the

canopy. Branches in the lower canopy were constructed in an efficient but risky strategy, whilst the upper canopy branches were built in a conservative and safe strategy. The change in strategy may be due to the hydraulic risk associated with height. The difference in xylem structure also affected the xylem plasticity to water and nitrogen addition; branches from three canopy layers respond differently. The middle and lower canopy were more responsive to the environment. Additionally, this study discovered a strong correlation between wood density and anatomical structure, hydraulic function. Denser wood tended to have a safer but less efficient hydraulic structure. This finding demonstrated that, despite its complicated structure, angiosperm wood density is still a useful indicator of plant hydraulics, at least at the intra-specific level.

**Keywords:** xylem structure; hydraulic function; xylem plasticity; *Populus tomentosa*; wood density



# 基于 BP 神经网络的木材解剖特征的树种识别

陈博文 詹伟辉 黄圣波 李文 林金国 关鑫

(福建农林大学材料工程学院, 福建 福州 350002)

**摘要:** 本研究利用三种青冈属的木材解剖特征数据, 借助 BP 神经网络建立树种识别模型。首先借助连续变倍体显微镜, 生物数码显微镜观察了福建青冈、赤皮青冈与青冈栎的微观构造, 并利用 Leica Application Suite 软件提取管孔的弦向直径、壁厚、腔径、管孔面积、腔面积、管孔周长、腔周长和实质率与木纤维的细胞面积、腔面积、实质率等解剖特征数据, 并将管孔解剖特征数据与木纤维解剖特征数据相互组合, 将数据增强至 16000 组, 接下来采用后向传播 (BackPropagation, BP) 算法, 按 80%数据作为训练集, 5%作为验证集, 15%作为测试集, 进行神经网络训练。结果表明利用 BP 神经网络方法对木材解剖特征进行树种识别, 最终平均识别率可达 93.9%, 其中该识别模型对赤皮青冈的识别效果最好, 识别率达 100%, 对福建青冈与青冈栎的识别率分别达到 92.4%与 88.6%。研究结果可为计算机识别同属的树种提供依据。

**关键词:** BP 神经网络; 木材解剖特征; 树种识别; 青冈属

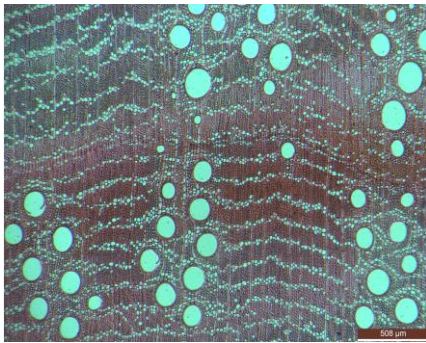
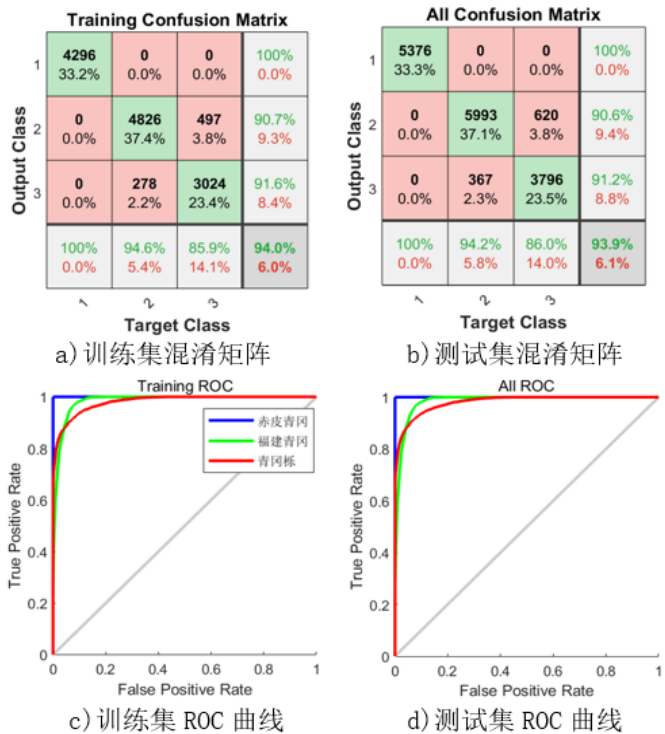


图 1 福建青冈导管显微构造



图 2 福建青冈木纤维显微构造



a) 训练集混淆矩阵

b) 测试集混淆矩阵

c) 训练集 ROC 曲线

d) 测试集 ROC 曲线

图 3 BP 网络树种识别结果

# Tree species identification of wood anatomical features based on BP neural Network

Chen Bowen, Zhan Weihui, Huang Shengbo, Li Wen, Lin Jinguo, Guan Xin

(College of Materials Engineering, Fujian Agriculture and Forestry University, Fuzhou, Fujian 350002)

**Abstract:** In this study, the anatomical data of three species of *Cyclobalanopsis* were used to establish tree species identification models with the help of BP neural network. Firstly, the microstructures of *Cyclobalanopsis chungii*, *Cyclobalanopsis glauca* and *Cyclobalanopsis* were observed with the help of continuous ploydy microscope and biological digital microscope. The chord diameter, wall thickness, cavity diameter, cavity area, cavity area, cavity circumference, cavity circumference and parenchyma rate of the tube holes were extracted with Leica Application Suite software, and the cell area, cavity area and parenchyma rate of wood fibers were also extracted Anatomic characteristic data. The data were enhanced to 16000 groups by combining the data of anatomical features of tube holes and wood fibers. Then, the neural network training was carried out by using the (BackPropagation, BP) algorithm, 80% of the data as training set, 5% as verification set and 15% as test set. The results showed that the average recognition rate of BP neural network was up to 93.9%, and the recognition rate of This model was the best for *Cyclobalanopsis*, with 100% recognition rate, and 92.4% and 88.6% recognition rates for *Cyclobalanopsis* and *Cyclobalanopsis chungii*, respectively. The results can provide a basis for computer identification of tree species of the same genus.

**Keywords:** BP neural network; wood anatomical characteristics; tree species recognition; *Cyclobalanopsis*

# 苯丙素生物合成途径响应方竹茎秆变异的研究

蒋倩倩<sup>1,2</sup> 周亮<sup>1</sup> 刘盛全<sup>1,3,\*</sup>

(1 安徽农业大学; 2 亳州学院; 3 林木材质改良与高效利用国家林业与草原局重点实验室)

**摘要:** 本研究以金佛山方竹 (*Chimonobambusa utilis*) 为材料, 将横截面区分为周向的“角”和“边”, 利用显微技术、光谱学技术和非靶向代谢组学方法, 结合笋节的表型特征、微观构造、和化学组分的分布, 挖掘关键代谢通路中代谢物表达模式在不同周向组织部位的差异。方形竹作为特异性一类竹种, 其共同的形态特点是节间竹竿呈现出近方形而非通常所见的圆形。金佛山方竹为我国独有的节间呈方形的稀有竹种, 其特异性方形节间形态的形成机理仍不清楚。

我们利用显微技术观测维管束微观结构, 发现纤维细胞细胞壁厚度及维管束尺寸在周向上差异显著 ( $p < 0.001$ ), 借助傅立叶变换红外光谱法 (FTIR) 测定“角”部位的木质素相对含量高于“边”, 但是这些差异与细胞壁形成过程的分子和代谢机制之间的关联尚不明确。为此, 我们进一步利用先进的代谢组学技术, 分析差异表达的代谢物及其调控模式, 揭示关键代谢通路—苯丙素合成通路中差异代谢物对秆形变异的响应机制。基于非靶向代谢组学, 利用液质联用 (LC-MS) 技术, 在三组样本中共定性到 531 种代谢物, 82 种差异代谢物。为了进一步了解关键差异代谢物的功能和途径, 进行了 KEGG 分类和富集分析 ( $FDR > 0.5$ )。结果表明, 苯丙素生物合成途径中差异表达的代谢物共 17 个, 其中关键差异代谢物反式-2-羟基肉桂酸和芥子醛水平显著上调。表明这两种关键差异代谢物是方秆性状形成的关键物质基础。

本研究既可对稀有竹种方竹秆形变异的机理研究提供学术价值, 同时对竹类发育的分子生物学研究提供理论借鉴, 最终为多组学的研究提供参考价值。

**关键词:** 金佛山方竹; 秆形变异; 非靶向代谢组学; 苯丙素生物合成途径

# The responses of the phenylpropanoid biosynthesis pathway upon culm variation of square bamboo (*Chimonobambusa utilis*)

Qianqian Jiang<sup>1,2</sup>, Liang Zhou<sup>1</sup>, Shengquan Liu<sup>1,3,\*</sup>

(1 Anhui Agriculture University; 2 Bozhou University; 3 Key Lab of State Forest and Grassland Administration on "Wood Quality Improvement & High Efficient Utilization")

**Abstract:** Diversity of morphological variability in the plant kingdom, mainly expressed in flower, fruit, seed, leaf, and root, are fields of active discussion. The square bamboo presents an unusual 'four-angled culm', which belongs to *Chimonobambusa*, showed a formidable talent for square morphology controlling. How such a square externally and round internally construction emerges from developmental mechanisms has remained elusive. To reveal the relevance between the core differential metabolites and the variant culm, we selected bamboo shoots of three groups (H30, H50, and H70) for sample preparation. Variations of anatomical characteristics were observed in cell wall thickness of fiber ( $p < 0.001$ ), the tangential diameter of vascular bundles ( $p < 0.001$ ) by histoanatomic method; differences in chemical composition were detected with Fourier transform infrared spectroscopy, the result showed relative content of lignin was higher in the corner parts; differentially expressed metabolites (DEMs) and the regulation patterns were revealed using the modern metabolomics technology.

The result showed a total of 531 metabolites were identified, 82 DEMs were identified. To further understand the functions and pathways of core DEMs, KEGG classification and enrichment analysis were performed for the DEMs. The results showed that 17 DEMs were detected in phenylpropanoid biosynthesis, in which levels of Trans-2-Hydroxycinnamate and sinapaldehyde were up-regulated. Comprehensive analysis of phenotype with metabolomics, accumulation of Sinapaldehyde, which would, in turn, leading to the variation in lignin biosynthesis with different cell wall-thickness in various circumferential directions of culm.

**Keywords:** *Chimonobambusa utilis*; stalk malformation; untargeted metabolomics; phenylpropanoid biosynthesis pathway

# Physical and mechanical properties of *Catalpa bungei* clones and estimation of the properties by near-infrared spectroscopy

Rui Wang, Lanlan Shi, Yurong Wang\*

(Research Institute of Wood Industry, Chinese Academy of Forestry, Beijing 100091, China)

**Abstract:** *Catalpa bungei* has the advantages of excellent material, straight and dense texture, and versatility characteristics, is a precious wood species unique to China. To provide scientific basis and theoretical guidance for the genetic improvement and utilization of *C. bungei*, the physical and mechanical quality characteristics and the best modeling methods for each performance were explored. Taking three *C. bungei* clones, “Luoqiu 2”, “Luoqiu 3”, and “Luoqiu 5”, as the research objects, the air-dry density, modulus of rupture (MOR), modulus of elasticity (MOE), compressive strength parallel to grain, and hardness of the three clones were measured by the national standards of physical and mechanical properties testing. The study compared the physical and mechanical properties between different positions in the radial direction and systematically analyzed the correlation between the physical properties and mechanical properties of 3 clones by one-way variance analysis and Pearson's correlation test. Near-infrared (NIR) coupled with partial least squares (PLS) regression were used to investigate the feasibility of predicting physical and mechanical properties quickly. The results showed that air-dry density of three clones ranged from 0.492 to 0.537 g·cm<sup>-3</sup>, MOR, MOE, compressive strength parallel to grain, and hardness ranged from 82.2 to 94.2 MPa, 10.7 to 12.0 GPa, 56.5 to 62.0 MPa, and 2804 to 3603 N respectively. Their values from near the pith were all less than near the bark. There were positive correlations between the air-dry density and the four mechanical properties, and also positive correlations among different mechanical properties. The correlation coefficient was above 0.90. The NIR-based PLS models for predicting air-dry density, MOR, MOE, compressive strength parallel to grain, and hardness were established. The R<sub>p</sub><sup>2</sup> were above 0.7, while exceeding 0.76 for some of the NIR models. Compressive strength parallel to grain and harness models constructed with spectra collected from cross section had better accuracy due to higher absorbance of cross section. The bending performance model based on the average spectra of radial and tangential sections was the best. The results showed that PLS based on NIR spectra pretreated by MSC + S-G smoothing method to evaluate air-dry density and mechanical properties of *C. bungei* clones were promising. Compared with five-point sampling methods, the model using the three-point sampling method was less effective, but it can also complete the preliminary prediction. In summary, the 13-year-old *C. bungei* wood has high-grade compressive strength parallel to grain, medium-grade MOR, and low-grade

MOE and hardness. According to the material properties of each clone, “Luoqiu 3” was an excellent clone for promotion and application. The physical and mechanical properties of outerwood samples were higher than those of corewood samples. There were extremely significant positive correlations between the air-dry density and various mechanical properties of wood at the level of  $p < 0.01$ . NIRs can be used as a high throughput method to non-destructively estimate important wood traits for rare *C. bungei* clones. When different pretreatment methods, spectra of different sections, and number of spectra collection were used, the effects of NIR prediction models on the wood density and mechanical properties exhibited differences. The study explored the prediction models of the physical and mechanical properties of 3 clones with the highest accuracy by NIR.

**Keywords:** *Catalpa bungei*; clone; wood density; mechanical properties; Near-infrared Spectroscopy

# 在线测量木材颜色的智能传感检测系统设计

席靖宇<sup>1</sup> 徐兆军<sup>1</sup> 王新洲<sup>1</sup>

(1 南京林业大学材料科学与工程学院 南京 210037)

**摘要:** 木材颜色检测是木材工业中十分重要的环节, 本系统基于色度学的基本理论和颜色传感器的应用方法, 设计了一套利用颜色传感器读取木材表面颜色以快速评估样品色度的在线检测设备。该系统具备高动态性能, 其颜色分析精度远远高于传统的测色方法。由于该系统不易准测量, 从而有利于大幅提升木材颜色检测精度及木材工业颜色监测环节效率。受到外界环境影响, 因此在弱光和强光条件下均可进行在线检测。该系统首先通过稳定色温 5700k 的 LED 灯为待测物体提供恒定的照明环境, 再经过颜色传感器 AS73211, 将选择的光谱分离成三个分别配有对应光电二极管且安装了 X、Y 和 Z 信号滤光片的光谱通道, 以代表红绿蓝三种波长光的强度。随后通过光电二极管将光信号转换为数字结果以实现连续或触发测量。待颜色识别系统将实时检测出的各个波段的数据信息通过 IIC 总线传输给控制器后, 控制器采用配置好的数据处理算法对检测结果进行分析处理。所得结果上传至上位机与标准值进行比值处理即可得到反射率。

结果表明: 同种树种不同部位的颜色深浅存在差异。通过颜色的检测可找出木材中颜色差异较大的部位, 进行筛选、剔除, 进而提高木材的总体质量。不同树种的 XYZ 值多位于某个固定区间内, 可借此作为一种树种鉴定的辅助工具来区别不同的树种。其中, 差异较大的树种其图中点的距离较大, 而图中点的距离较小则通常代表着为同一类别的树种。同时, 从 XYZ 值树种的区间分布中可以看出: 绝大多数树种的在 XYZ 三维图中的分布区间差异较明显, 但刺猬紫檀、大果紫檀等花梨木类树种及巴里黄檀、交趾黄檀等红酸枝木类的树种, 木材由于其表面颜色较浅, 因此在 XYZ 三维图中的分布区间极为相似; 鸡翅木类的卢氏黑黄檀以及黑酸枝木类的乌木由于颜色较深也难区分。为此这部分的树种将进一步通过其他途径辅助来进行鉴别。综上所述, 基于 AS73211 传感器和 stm32 芯片所设计的木材颜色检测仪器通过三个通道快速的将光源转换为数字信号, 对木材颜色的在线检测及木材材色测量的专用化具有重要意义。

**关键词:** 木材颜色; 颜色传感器; AS73211

# Design of intelligent sensing detection system for online wood color measurement

Xi jingyu, Xu zhaojun, Wang xinzhou

(1 College of Materials Science and Engineering, Nanjing Forestry University, Nanjing 210037)

**Abstract:** Wood color detection plays an important role in in the wood industry. This system has designed a set of equipment to detect the color of wood surface online based on the basic theories of colorimetry and the application method of color sensors, which could evaluate sample color directly through the color sensor. The color analysis accuracy of the system with high dynamic performance was much higher than the traditional methods of color measurement. Because the system was not easily affected by external environmental conditions, it can accurately measure on-line under both weak and strong light conditions to improve the accuracy of wood color detection and the efficiency of color monitoring in the wood industry effectively. Firstly, the system provided a constant lighting environment for the object to be measured through LED lights with a stable color temperature of 5700k. And then separated the selected spectrum into three different spectral channels through the color sensor AS73211, which represented the intensity of the red, green and blue wavelengths equipping with corresponding photodiodes and installed filters for X, Y and Z signals, respectively. The continuous or trigger measurements were achieved by the digital results, which were converted by the photodiode. The data information of each band detected in real time was transmitted to the controller through the IIC bus by the color recognition system subsequently. Finally, the test results were analyzed by the controller equipping with the configured data processing algorithm, and the reflectivity was acquired by the comparison between the test results and the standard values. The results indicated that the color depth of different parts of the same tree species was different. Through the color detection, the parts with significant color differences of wood could be found, screened and eliminated, and the overall quality of the wood can be improved. The X, Y, and Z values of different tree species were mostly located in a certain fixed interval, which can be used as an auxiliary tool for tree species identification to distinguish different tree species. And the tree species with an obvious distinguish will have a farther distance of points in the figure, while a close distance of points in the figure were mostly presented the same type of tree species.

the distribution intervals of most tree species in the three-dimensional map (X, Y, and Z) were quite different. Notably, the rosewood species, such as the Hedgehog red sandalwood and the *Pterocarpus macrocarpus*, and the red acid mahogany species, such as the *Dalbergia cochinchinensis* and the *Dalbergia bariensis*, with the light color were indistinguishable due to the similarly distribution intervals in the three-dimensional graph. And the same situation was occurred in the *Dalbergia louvellii* and the *Diospyros ebenum*, which was due to the dark color of them. Therefore, this part of the tree species will be further assisted by other means for identification. In



summary, wood color detection instrument realized the online detection of wood color and the specialization of color measurement by converting the light source into a digital signal, which was design based on the AS73211 sensor and the stm32 chip.

**Keywords:** wood color; color sensor; AS73211

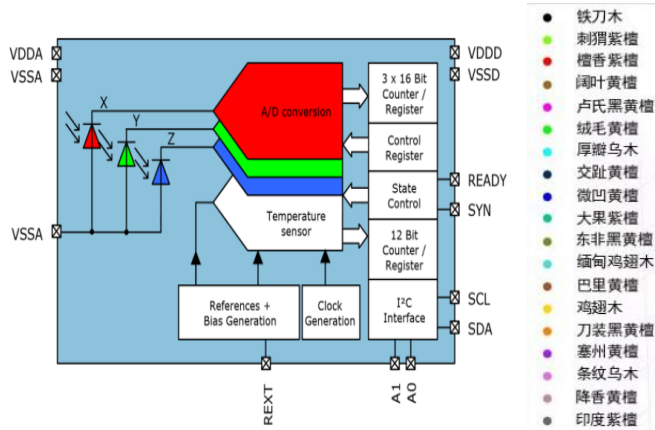


图 1 AS73211 原理图

Fig.1 AS73211 schematic

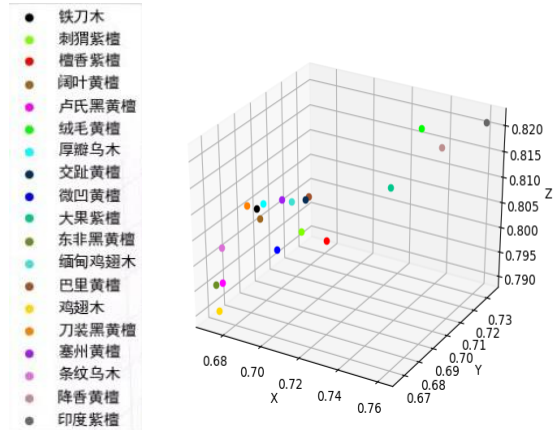


图 2 常见红木的 XYZ 值空间分布三维图

Fig.2 Three-dimensional map of XYZ value spatial distribution of common mahogany

# 酚醛树脂浸渍-机械压缩处理对杉木木材细胞尺寸稳定性的影响

姚艳<sup>1</sup> 马英杰<sup>1</sup> 潘彪<sup>1</sup> 冷魏祺<sup>1</sup> 王新洲\*

(1 南京林业大学材料科学与工程学院 南京 210037)

**摘要:** 为系统化研究树脂对压缩木材细胞的固定机理,采用酚醛树脂以真空加压浸渍法对速生杉木木材进行改性处理,再对未浸渍材和浸渍处理材沿径向机械压缩至压缩率分别为10%、20%及30%。运用光学显微镜采集改性木材显微构造图像,通过图像软件处理分析获得树脂在木材中的分布情况。再对绝干的未处理材、浸渍处理材和压缩处理材调湿处理,计算宏观木材的线吸湿膨胀率和体积吸湿膨胀率;同时对木材细胞构造切片进行调湿处理,计算细胞的线吸湿膨胀率。运用扫描电镜和拉曼光谱观察分析细胞腔中填充的树脂和细胞壁与树脂的物理化学作用,揭示浸渍压缩改性机理。研究表明:浸渍增重率与浸渍压力和时间呈正相关,较低的浸渍压力无法使树脂渗入芯部,而较高的压力下较短时间内即可达到良好浸渍效果。更高的浸渍压力也能使细胞中树脂填充量更多,提高浸渍压力和时间使更多木材细胞被树脂填充。树脂浸渍处理显著降低木材线吸湿膨胀率和体积膨胀率,吸湿膨胀率随浸渍压力和时间增加而减少,高湿度时水分子对木材组织的进一步润胀作用使90%湿度环境下的木材线性膨胀率普遍高于60%湿度下木材膨胀率。另外,同一湿度条件下所有弦向膨胀率均大于径向膨胀率。树脂在细胞中的填充对木材细胞的吸湿膨胀有抑制作用,随着浸渍压力和时间增加,树脂填充的细胞数量增多,木材细胞尺寸稳定性越高。浸渍压力对细胞尺寸稳定性的影响高于浸渍时间,且木材弦向吸湿膨胀率为径向膨胀率的1.5倍至3倍。浸渍处理后,部分木材细胞腔被树脂填充与内壁结合紧密,管胞壁上的开放的纹孔也被树脂填充,这阻碍了水分子的进入,且对细胞具有良好的充胀作用,进而固定了细胞,使得细胞在湿度环境下有更好的尺寸稳定性。树脂不仅可以简单填充细胞腔,同时也能渗透进细胞壁并与其发生一定的化学作用,使得填充的细胞腔不易发生形变。本文分析探究了树脂浸渍和机械压缩联合作用下树脂对速生杉木木材细胞的固定机理,即树脂对被压缩变形的木材细胞具有固定作用,使细胞具有良好的尺寸稳定性,这种作用在高湿度环境下也依然存在,并且随浸渍压力和时间增大而增大。

**关键字:** 杉木; 浸渍; 压缩; 木材细胞; 尺寸稳定性

# Study on dimensional stability of phenolic resin pretreated Chinese fir by co-compression

Yao Yan<sup>1</sup>, Ma Yingjie<sup>1</sup>, Pan Biao<sup>1</sup>, Leng Wei<sup>1</sup>, Wang Xinzhou<sup>1,\*</sup>

(1 College of Materials Science and Engineering, Nanjing Forestry University, Nanjing 210037)

**Abstract:** In order to study the fixation mechanism of resin on compressed wood cells systematically, phenolic resin was used to modify the fast-growing Chinese fir wood with vacuum pressure impregnation method, and then the control wood and impregnated wood were mechanically compressed along the radial direction until the compression rate reached to 10%, 20% and 30%, respectively. The optical microscope and the image software were used to collect and analyze the microscopic structure images of modified wood. Moisture conditioning treatment was performed on the control wood, the impregnated treated wood and the compressed treated wood, which were absolutely dry. And then the linear moisture swelling rate and volume moisture swelling rate of macroscopic wood were calculated subsequently. At the same time, the wood cell structure sections were processed for humidity control and the linear soaking swell rate of cells was calculated as well. In order to reveal the modification mechanism of impregnation compression, the resin filled in the cell cavity and the physical and chemical interaction between the cell wall and resin were observed and analyzed by SEM and Raman spectroscopy. The results show that the increased weight percent of impregnation was positively correlated to the pressure and time. The resin could not penetrate into the core section of samples with the low-pressure in impregnation, while the excellent impregnation results could be achieved in a short time with the low-pressure in impregnation. The high pressure and the long processing time of impregnation presents a mass of the resin filling in the cells. Resin impregnation significantly reduced the linear soaking swell rate and volume soaking swell rate of wood, and the soaking swell rate decreased with the increase of impregnation pressure and time. The further swelling effect of water molecules on wood tissue at high humidity condition could made the linear soaking swell rate of wood at 90% humidity generally higher than that of 60% humidity. In addition, under the same humidity condition, all tangential swell rates were greater than radial swell rates. The filling of resin in wood cells has an inhibitory effect on the hygroscopic expansion of wood cells. With the increase of impregnation pressure and time, the number of resin-filled cells and the dimensional stability of wood cells was elevated. The influence of impregnation pressure on cell dimensional stability was higher than that of the impregnation time, and the soaking swell rate in tangential direction was 1.5 to 3 times that of the radial direction. After impregnation treatment, some wood cell cavities were filled with resin and bonded tightly with the inner wall. And the open pits on the tracheid walls were also filled with resin, which impedes the entry of water molecules and has a good swelling effect on the cells. This made the cells had a better dimensional stability in a

humid environment. The resin could fill the cell cavity and have a chemical interaction with the cell walls to make the filled cell cavity less prone to deformation. The fixation mechanism of the resin on the fast-growing Chinese fir wood cells, which were under the combination of resin impregnation, and the mechanical compression were explored in this work. The fixation effect of the resin on the compression and deformed wood cells made the cell had a good dimensional stability, which was also existed in high humidity environments and increased with the increase of immersion pressure and time.

**Keywords:** Chinese fir; impregnation; compression; wood cell; dimensional stability

# 植物激素诱导杨树应拉木形成和负向地性生长的转录组分析

余敏<sup>1,2</sup> 魏宇创<sup>1,2</sup> 张浩<sup>1,2</sup> 张彭俐<sup>1,2</sup> 刘盛全<sup>1,2,\*</sup> 高俊兰<sup>3,\*</sup>

(1 “林木材质改良与高效利用”国家林业和草原局重点实验室; 2 安徽农业大学林学与园林学院; 3 安徽省农业科学研究院农业工程研究所)

**摘要:** 油菜素内酯和赤霉素在应拉木形成中起着重要的调控作用, 但它们在应力木形成和响应重力刺激的作用机制尚不明确。本研究以人工倾斜杨树苗木为研究对象, 比较油菜素内酯和赤霉素对倾斜杨树苗木生长性状、木质部细胞发育和转录组差异表达的影响。研究表明, 赤霉素对倾斜杨树苗木负向地性生长有明显的促进作用。RNA-seq 分析结果显示, 油菜素内酯处理组应拉木中参与木质素和半纤维素合成的 *FLA* 和 *XET* 基因显著下调, 而赤霉素处理组应拉木中的大部分纤维素、木质素和半纤维素的合成基因显著上调。KEGG 分析表明, 赤霉素处理后倾斜杨树应拉木中编码糖类代谢、生长素响应通路的基因转录丰度发生了显著变化。

**关键词:** 胶质层; 转录组; 纤维素生物合成; 负向地性

# Effect of plant hormone on tension wood formation and negative gravitropism by RNA-Seq analysis in poplar seedlings

Min Yu<sup>1,2</sup>, Yuchuang Wei<sup>1,2</sup>, Hao Zhang<sup>1,2</sup>, Pengli Zhang<sup>1,2</sup>, Shengquan Liu<sup>1,2,\*</sup>, Junlan Gao<sup>3,\*</sup>

(1 Key Laboratory of State Forestry and Grassland Administration on “Wood Quality Improvement & High Efficient Utilization”; 2 School of Forestry & Landscape Architecture, Anhui Agricultural University; 3 Institute of Agricultural Engineering, Anhui Academy of Agricultural Sciences)

**Abstract:** Brassinolide (BR) and gibberellic acid (GA) play an important role in regulation of the reaction wood formation. However, the effects of BR and GA in tension wood formation and negative gravitropism of a woody species have not been demonstrated. The artificially inclined poplar seedlings were treated by two different kinds of exogenous hormones (BR and GA). The morphology of artificially inclined seedlings, xylem cell development and transcriptome differential expression were analyzed. The artificially inclined seedlings showed dramatically negative gravitropic bending by exogenous GA treatment. RNA-Seq analysis of several lignin and hemicellulose biosynthetic genes indicated that genes (*FLA* and *XET*) were significantly down-regulated in BR-treated stems compared to that in control stems. Most genes involved in cellulose, lignin and hemicellulose biosynthesis were significantly upregulated in GA-treated stems compared with control stems. In addition, KEGG pathway analysis showed that the transcription levels of many genes involved in the carbohydrate metabolic pathway and the auxin response pathway were significantly changed during the tension wood formation in GA-treated stems.

**Keywords:** Gelatinous layer; Transcriptome; Cellulose biosynthesis; Negative Gravitropism

# 13年生楸树无性系材性径向遗传变异研究

张浩<sup>1,2</sup> 魏宇创<sup>1,2</sup> 张彭俐<sup>1,2</sup> 刘盛全<sup>1,2,\*</sup> 余敏<sup>1,2,\*</sup>

(1“林木材质改良与高效利用”国家林业和草原局重点实验室; 2 安徽农业大学林学与园林学院)

**摘要:** 通过对6个13年生楸树无性系的28个材性性状进行遗传变异研究, 比较楸树无性系材性性状的径向变异, 并估算无性系重复力、遗传变异系数和表型变异系数等遗传参数, 采用聚类分析和主成分分析方法对楸树无性系进行分类和初步评价。结果表明, 18个材性性状在不同无性系及年轮间差异达到显著或极显著差异水平, 不同无性系与年轮交互效应中苯醇抽提物含量达到极显著差异水平。性状变异系数中各性状表型变异系数均大于遗传变异系数, 其中13个材性性状在年轮间平均重复力大于0.5。聚类分析可将6个楸树无性系分为3类, 主成分分析可将28个材性性状分为5个主成分。6个楸树无性系在13个材性性状上存在遗传差异并受较强遗传控制, 具备遗传改良条件。

**关键词:** 楸树无性系; 木材材性; 径向变异; 遗传变异

# Radial Genetic Variation Analysis of Wood Properties among Thirteen-year-old *Catalpa bungei* Clones

Hao Zhang<sup>1,2</sup>, Yuchuang Wei<sup>1,2</sup>, Pengli Zhang<sup>1,2</sup>, Shengquan Liu<sup>1,2,\*</sup>, Min Yu<sup>1,2,\*</sup>

(1 Key Laboratory of State Forestry and Grassland Administration on “Wood Quality Improvement & High Efficient Utilization”; 2 School of Forestry & Landscape Architecture, Anhui Agricultural University)

**Abstract:** Radial genetic variation of 28 wood properties among six new 13-year-old *Catalpa bungei* clones were analyzed. The genetic parameters such as repeatability of clones, coefficient of genetic variation and coefficient of phenotypic variation were estimated. *C. bungei* clones were then classified and preliminarily evaluated using clustering analysis and principal component analysis. Eighteen wood properties of *C. bungei* clones showed significant or extremely differences on different clones and annual rings. The content of benzene alcohol extract showed extremely differences on interaction between clones and annual rings. The phenotypic variation of clones was greater than the genetic variation, and the average repeatability of 13 wood properties was greater than 0.5 on different annual rings. Clones were divided into three categories by cluster analysis, and 28 wood properties were divided into 5 principal components by principal component analysis. Six *Catalpa bungei* clones showed genetic differences in 13 wood properties, which were under strong genetic control and possessed the conditions of genetic improvement.

**Keywords:** *Catalpa bungei* clones; Wood properties; Radial variation; Genetic variation





## 2021 木材解剖学国际青年论坛

2021' International Youth Forum for Wood Anatomy

Meeting Agenda

论  
文  
摘  
要

四川 成都

2021年11月13日-14日

Chengdu

November 13-14th, 2021, UTC+8, Beijing Time Zone

# Comparison of vessel traits for plantation grown teak wood of different ages from the wet zone of Ghana.

James Govina<sup>1,3</sup>, Robert Németh<sup>1</sup>, Martin Amoah<sup>2</sup>

(1 Department of Wood Science, University of Sopron, Hungary; 2 College of technology Education, University of Education-Winneba, Kumasi, Ghana; 3 CSIR-Forestry Research Institute of Ghana, Kumasi, Ghana.)

**Abstract:** Wood vessel traits are important anatomical features for relating wood's formation and growth to a tree's present and past growing conditions. Vessels are constituents of the xylem, used as channels for water and mineral transport from tree roots to the leaves. The density of vessels, their sizes and distribution in living trees are central to ecological and environmental studies. Equally for processed timber, vessels traits are important for efficient wood utilization. This study looked at the vessels' area sizes and density (count) for *Tectona grandis* (teak) trees of ages 10, 15 and 20 years, with attention to their axial positions (base and top). Teak remains the premier plantation species for many countries across Africa including Ghana. Wood samples from top and base positions of randomly selected trees were softened, sectioned with sledge microtome, stained with 1% safranin, dehydrated using decreasing grades of ethanol, dipped in xylene, and mounted on a slide with Canada balsam. The prepared slides were observed under a digital microscope. Images were taken with the aid of the Motic Image Plus Software. The transverse images were processed with imagej software for data on vessel traits. The data was analyzed using R statistical software, with ANOVA adopted to test for differences between mean values. Overall, the minimum and maximum vessel area size were 0.004 and 0.1 mm<sup>2</sup>. Both age and axial position had significant influence on vessel area size. Contrary, age and axial position had no significant influence on vessel frequency with mean values ranging from 17 to 23 counts per mm<sup>2</sup>. The observed variability in vessel area sizes could influence other wood and wood products properties such as wood lustre (optical), permeability and retention of preservatives, drying, application of finishes.

**Keywords:** Vessel; *Tectona grandis*; pores, microscope; microtome.

# From herbs to trees and back again: changes in the degree of woodiness among carrots

Kamil E. Frankiewicz

(Institute of Evolutionary Biology, Faculty of Biology, University of Warsaw Żwirki i Wigury, 101, 02-089 Warsaw, Poland)

**Abstract:** The most striking features of angiosperms is their wealth of growth forms: from herbaceous annuals to woody perennials with innumerable intermediates. In fact, it probably was the occurrence of short-lived, minimally woody herbs in the Cretaceous that spurred angiosperms diversification. The habit shifts from herbaceous ancestors to woody descendants are known as secondary (derived) woodiness. The phenomenon was already noticed by Darwin and has been extensively studied since the seminal works of Carlquist in the 60s.

We investigated wood anatomy of over 150 representatives of the carrot family (Apiaceae) in relation to their stem architecture and reproductive strategy (mono- or polycarpic), and reconstructed evolutionary changes of life form in selected clades.

We found that species with monocarpic strategy and/or long internodes deposited fibrous wood, while polycarpic species with shortened internodes produced parenchymatous wood (i.e. xylem with parenchyma in place of fibres) at first, and fibrous wood later in their ontogeny. We hypothesise that this correlation is governed by the dual effect of gibberellic acid which affects flowering and maturation of cambial derivatives. At the same time, we found no evidence for a direct interdependence between wood structure and life form. We also showed that secondarily woody habit may evolve readily (six times in studied groups) and rapidly (within 130 thousand years) in response to different environmental cues. Our results clarify how nonanatomical traits affect wood structure and reinforce the notion how important for plant adaptive strategy habit lability is.

# Stem anatomy of the South African genera of Gnaphalieae (Asteraceae) with emphasis on the evolution of interxylary phloem

Milan Gavrilović<sup>1,2,\*</sup>, Pedja Janačković<sup>1</sup>, Alexei Oskolski<sup>2,3</sup>

(1 University of Belgrade - Faculty of Biology, Department of Morphology and Systematics of Plants, Studentski trg 16, 11000 Belgrade, Serbia; 2 Department of Botany and Plant Biotechnology, University of Johannesburg, Johannesburg, South Africa; 3 Botanical Museum, Komarov Botanical Institute, St. Petersburg, Russia; \*Corresponding author: mgavrilovic@bio.bg.ac.rs; Studentski trg 16, 11000 Belgrade, Serbia; mobile phone: +381638889696)

**Abstract:** The Gnaphalieae are a large tribe of Asteraceae with ca. 2100 species in 178 genera. The basal lineages of this tribe (subtribe Relhaniinae, *Ifloga* clade, *Metalasia* clade or grade, and *Stoebe* clade) are mostly confined to southern Africa. The aim of this research was to clarify the stem anatomical diversity within South African Gnaphalieae. Wood structure in 20 genera as well as the stem development in six genera was examined. Our observations suggest that all Gnaphalieae species lack the periderm. Also, almost all genera share the wide sheaths of thick-walled sclereids associated with the conductive elements of secondary phloem. *Helichrysum*, as well as *Anaxeton* and *Syncarpha* share the persistence of fascicular and interfascicular portions in their vascular cambia. The fascicular portions produce the plates of secondary xylem with vessels, and the clusters of secondary phloem with sieve elements and sclereids, whereas the interfascicular portions give rise to the zones of parenchyma or sclerenchyma located coradially with the medulary rays. The species of Relhaniinae and the *Ifloga* clade have similar groundplan of secondary tissues, but the portions of their cambia can temporarily switch between fascicular and interfascicular modes. As a result, the clusters of conductive elements separated by tangential bands of parenchyma or sclerenchyma are formed to inside and outside of the cambium. The *Metalasia* clade and the *Stoebe* clade are distinctive from other Gnaphalieae in having interxylary phloem. In the members of *Stoebe* clade, the strands of secondary phloem are initiated externally of cambium whereas the secondary xylem strands bearing clusters of vessels are differentiated internally of it. Later, the phloem and xylem increments with the portion of fascicular cambium bend off the cambial zone to the inside, and arcs of coalescent cambia is formed external to it. Unlike that, in the species of *Metalasia* clade, the entire bundles with phloem and xylem are formed in the inner regions of cambial zone from the cambial derivatives, but the cambium is not immediately involved in this process. Such a deep difference in the ways of formation of conductive tissues between two clades must be taxonomically important. The shifts from the phloem located outside of the cambium to the interxylary phloem in

the *Metalasia* clade and the *Stoebe* clade are thought to be associated with the gains to the ericoid leaves driven by their adaptation to the summer-arid fynbos biome in the course of their late Miocene radiation in the Cape region.

**Keywords:** cambial variants; Cape Floristic Region; fascicular cambium; interfascicular cambium

# Wood anatomy of the tribe Diosmeae, a large Cape lineage of Rutaceae

FM Akinlabi<sup>1,\*</sup>, EL Kotina<sup>2</sup>, AA Oskolski<sup>1,2</sup>

(1 Department of Botany and Plant Biotechnology, University of Johannesburg, Johannesburg, South Africa; 2 Botanical Museum, Komarov Botanical Institute, St. Petersburg, Russia; \*Corresponding author: funmilad@gmail.com)

**Abstract:** The tribe Diosmeae comprise ten shrubby genera which are endemic to the Cape Floristic Region in South Africa, and the genus *Calodendrum* with two species of trees ranged from the southern Africa to Tanzania. We examined wood structure of nine Diosmeae genera, in order to elucidate their systematic and ecological significance. It was shown that the investigated species share the combination of wood traits characteristic for Rutaceae: radial vessels multiple, exclusive simple perforation plate and alternate intervessel pits. The occurrence of the vested intervessel pits found in *Adenandra*, *Calodendrum* and *Macrostylis* that is the first record of this trait in Rutaceae. In contrast to other examined genera, the canopy tree *Calodendrum capense* is distinctive in many wood traits which are characteristic of the large trunk: relative wide vessels, longer libriform fibers and vasicentric to winged-aliform and confluent parenchyma, mostly multiseriate rays with common occurrence of prismatic crystals in ray cells, while *Empleurum unicapsulare* lacks marginal bands of axial parenchyma. The rest of the studied species are very similar in wood structure showing mainly weak quantitative differences. The pattern of wood structure diversity within the shrubby Diosmeae is related more to their plant stature and climatic factors than to their taxonomy or phylogenetic relationships. Particularly, the vessel grouping increases with increasing water limitation along the gradient from a semi-arid winter-dry climate to a Mediterranean winter-wet climate found in the Cape Floristic Region. The significant correlations of vessel frequency, vessel diameter, and the frequency of multiseriate rays with some bioclimatic variables are thought to be underpinned by the plant stature. The presence of spherocrystals and acicular crystals in the axial parenchyma and rays in *Adenandra*, *Agathosma*, *Coleonema*, *Diosma* and *Macrostylis* represent indirect evidence of the presence of flavonoids which might have important pharmacological effects.

**Keywords:** *Calodendrum*; *Agathosma*; buchu; axial parenchyma; vested pits; spherocrystals; acicular crystals; ecological trends; Cape floral clades

# Adaptation of different tree species to increasing autumn temperatures

Weiwei Huang<sup>1,2</sup>, Jørgen Bo Larsen<sup>2</sup>, Jon Kehlet Hansen<sup>2</sup>, Patrick Fonti<sup>3</sup>, Anders Ræbild<sup>2</sup>

(1 Bamboo Research Institute, Nanjing Forestry University, Nanjing 210037, China; 2 Department of Geosciences and Natural Resource Management, The University of Copenhagen, Rolighedsvej 23, DK-1958 Frederiksberg C, Denmark; 3 Swiss Federal Institute for Forest, Snow and Landscape Research WSL, Zürcherstrasse 111, CH-8903 Birmensdorf, Switzerland \*Presenter email: huangww36@gmail.com)

Climate-growth relationships are an important tool to investigate tree growth responses under changing climatic conditions, and provide a scientific basis for the selection of species and provenances for future forests.

Our recent study of tree ring data from a Danish common garden experiment revealed that warm August-October in previous-year significantly reduced the growth of *Picea abies* (L.) Karst. and *Abies grandis* Lindl. in the current-year. Our hypothesis is that the negative growth response was due to combined effects of high evapotranspiration, poor soil water availability occurring at the end of the growing season and high respiration, which combined leads to a negative carbon balance. However, *Pseudotsuga menziesii* (Mirb.) Franco, *Quercus robur* L. and *Fagus sylvatica* L. did not show a negative growth response to warm autumn temperatures, and *Q. robur* even seemed to benefit from previous autumn warming. It was thus hypothesized that the previous warm autumn conditions promote carbon assimilation and storage in *Q. robur* which is then used to sustain next year growth.

A temperature-free-air-controlled enhancement (T-FACE) facility was used in current study to experimentally expose seedlings of five tree species to normal and elevated autumn temperatures to study their physiological, phenological, wood anatomical and growth responses. This project aimed at addressing the questions about why warm autumns challenge the growth performance of some species more than others, and thus contribute to the identification of species with sufficient adaptive potential to perform well under future warm climates.

Our preliminary results suggest that autumn warming influence the length of current-year growing period and affect timing of spring flushing and xylogenesis differently next year. The experimental results will deepen our understanding of the effects of warm autumn on the growth and physiology of trees, and provide a scientific basis for forest management under uncertain climatic conditions in the future.

# Addressing controversies in safety - vessel diameter relationships

Emilie Isasa<sup>1</sup>, Roman Mathias Link<sup>1</sup>, Steven Jansen<sup>2</sup>, Juliano Sarmiento Cabral<sup>3</sup>,  
Bernhard Schuldt<sup>1</sup>

(1 Ecophysiology and Vegetation Ecology, Julius-von-Sachs-Institute of Biological Sciences, University of Würzburg, Julius-von-Sachs-Platz, 97082 Würzburg, Germany; 2 Institute of Systematic Botany and Ecology, Albert-Einstein-Allee 11, Ulm University, D89081 Ulm, Germany; 3 Ecosystem Modeling Group, Center for Computational and Theoretical Biology, University of Würzburg, Würzburg, Germany)

**Abstract:** Xylem embolism formation is a key process during drought-induced tree mortality, but its relationship to wood anatomical properties is debated. While the classical assumption is that larger vessels provoke a higher embolism risk, the evidence is mixed, and recent studies show that differences in embolism resistance are rather driven by pit membrane characteristics. Based on data from 20 temperate broad-leaved tree species, we identify a strong across-species relationship between water potential at 50% loss of conductivity ( $P_{50}$ ) and hydraulically weighted vessel diameter ( $D_h$ ), but no clear within-species patterns. We further show that while  $D_h$  and pit membrane thickness ( $T_{pm}$ ) are associated, this is insufficient to explain the specieslevel link between  $P_{50}$  and  $D_h$ , as a large  $D_h$  effect remains after accounting for  $T_{pm}$ . Our results indicate that controversies about xylem safety – vessel size relationships may largely be explained by the species sample and the scale on which they are studied.

**Keywords:** Angiosperm xylem; drought stress; embolism resistance; hydraulic conductivity; vessel diameter; pit membrane



# Ontogeny of divided vascular cylinders in *Serjania*: the rise of a novel vascular architecture in Sapindaceae

Yanã C. Rizzieri<sup>1,\*</sup>, Arno F.N. Brandes<sup>1</sup>, Israel L. Cunha Neto<sup>2</sup>, Genise V. Somner<sup>3</sup>,  
Michaela J.N. Lima<sup>4</sup>, André Pereira<sup>5</sup>, and Neusa Tamaio<sup>4</sup>

(1 Universidade Federal Fluminense, Instituto de Biologia, Departamento de Biologia Geral, Rua Professor Marco Waldemar de Freitas Reis, s/n, 24210-201 Rio de Janeiro, Niterói, Brazil; 2 Universidade de São Paulo, Instituto de Biociências, Departamento de Botânica, Rua do Matão, 277, Cidade Universitária, CEP 05508-090 São Paulo, SP, Brazil; 3 Universidade Federal Rural do Rio de Janeiro, Instituto de Ciências Biológicas e da Saúde, Departamento de Botânica, CP. 74582, 23851-970 Rio de Janeiro, RJ, Brazil; 4 Instituto de Pesquisas Jardim Botânico do Rio de Janeiro, Diretoria de Pesquisa Científica, Rua Pacheco Leão, 915, 222460-030 Rio de Janeiro, RJ, Brazil; 5 Universidade Federal Fluminense, Instituto de Computação, Departamento de Ciência da Computação, Rua Passo da Pátria 156, 24210-240 Rio de Janeiro, Niterói, Brazil; \*Corresponding author: yana.rizzieri@gmail.com)

**Abstract:** Sapindaceae lianas are remarkable for the diversity of cambial variants found in their stems. One of the family's exclusive cambial variant is the divided vascular cylinder, which occurs in eight species of the genus *Serjania*. This cambial variant is marked by 5 peripheral vascular cylinders around a large pith. We performed a comparative developmental analysis, integrating traditional plant anatomy techniques with high-resolution X-ray micro-computed tomography to investigate the structure and development of the stems of three species with divided vascular cylinder. Our observations showed that the initial stages of stem development were similar to those described in the literature, however, on later developmental stages a central vascular cylinder appears in all species. The ontogeny of these stems are marked by three main processes: (i) dissection of vascular tissue from the peripheral vascular cylinders; (ii) development of new cambial arcs through the redifferentiation of pith cells; and (iii) recruitment of cambial cells from the inner portions of the vascular cambium of the peripheral vascular cylinders, forming a novel central vascular cylinder where the pith was, surrounded by five initial peripheral cylinders. As an ulterior developmental stage, some older stems also develop neoformations and connections between the different vascular cylinders. While our findings support previous descriptions of divided vascular cylinders, this is the first study illustrating the formation of the central vascular cylinder in this cambial variant. Our observations further corroborate that *Serjania* is the lineage with the highest and some of the most complex forms of cambial variants among all vascular plants.

**Keywords:** Anastomosis; cambial variants; climbing plants; secondary growth; stem anatomy; development.

# An introduction to quantitative wood anatomy using ROXAS

Jingshu Wei<sup>1,2,3</sup>, Georg von Arx<sup>2</sup>, Zexin Fan<sup>3</sup>, Flurin Babst<sup>4</sup>

(1 W. Szafer Institute of Botany, Polish Academy of Sciences, ul. Lubicz 46, 31-512 Kraków, Poland; 2 Swiss Federal Research Institute WSL, Zuercherstrasse 111, CH-8903, Birmensdorf, Switzerland; 3 Key Laboratory of Tropical Forest Ecology, Xishuangbanna Tropical Botanical Garden, Chinese Academy of Sciences, Menglun Town, Mengla County, Yunnan Province 666303, China; 4 Laboratory of Tree-Ring Research, University of Arizona, 1215 E Lowell Street, Tucson, AZ 85721, USA)

**Abstract:** Quantitative wood anatomy (QWA) is a growing field that links tree physiological processes with environmental change based on xylem cell structure. Technically, there are still some difficulties in quantifying the anatomical features of wood, such as how to obtain high-quality sections/images, and how to batch analyze a huge number of cells within the analyzed images. Here, we present the procedure of wood anatomical analysis including paraffin embedding and thin sectioning of wood samples, followed by quantification of a large number of wood anatomical parameters using the image analysis tool ROXAS. Some outstanding characters of the tool include automatic identification of tree-ring borders and up to 1,000,000 cells especially for conifer species. With ROXAS, more than 120 output parameters are automatically produced. Finally, several case studies of dendro-anatomy exemplify that ROXAS is an ideal tool for reaching the need of efficiently processing the wood anatomical sections and for further research applications.

**Keywords:** QWA; tree-ring anatomy; wood section; wood anatomical features; dendrochronology; image analysis

# Anatomical structure of three lesser-used wood species grown in Indonesia

Sarah Augustina<sup>1</sup>, Imam Wahyudi<sup>2,\*</sup>, I Wayan Darmawan<sup>2</sup>, Jamaludin Malik<sup>3</sup>

(1 Forest Products Science and Technology Study Program, IPB University, Bogor 16680; 2 Department of Forest Products, Faculty of Forestry & Environment, IPB University, Bogor 16680; 3 Forest Products Research and Development Center, Bogor 16610; \*Corresponding author: imyudarw16@yahoo.com)

**Abstract:** Anatomical structure of three lesser-used wood species grown in North Kalimantan Province, Indonesia namely nyatoh (*Palaquium* spp.), sepetir (*Sindora* spp.) and pisang putih (*Mezzettia* spp.) has been studied following the IAWA's List. The results showed that anatomical characteristics of nyatoh wood are as follows: vessels predominantly in radial multiples of 2–4, 6 cell per mm<sup>2</sup>, maximum tangential diameter 100–235 µm, perforation simple, intervessel pits alternate to slightly opposite, vessel-ray pits simple, tyloses common; rays mostly uniseriate with a maximum height of 1800 µm and coloured materials, while axial parenchyma in regularly and closely spaced narrow tangential bands. Crystal and silica grains in axial parenchyma, but resin canals absent. For pisang putih wood, the vessels are exclusively solitary, perforation simple, intervessel pits alternate, vessel-ray pits simple, tyloses absent; rays two distinct sizes, up to 3000 µm high, while axial parenchyma in scalariform tangential bands with irregularly spaced. Oil cells present in rays, but crystal and silica grains absent. In case of sepetir wood, vessels solitary and in radial multiples of 2–3, 3–8 per mm<sup>2</sup>, maximum tangential diameter 120–220 µm, perforation simple, intervessel pits alternate, vessel-ray pits simple, tyloses rather rare; rays with a tendency to 2 sizes, 450–1000 µm high, while axial parenchyma vasicentric to aliform. Crystals in chambered axial and ray parenchyma cells, but silica grains absent. Axial resin canals are found in continuous tangential bands.

**Keywords:** Anatomical structure; lesser-used wood species; *Mezzettia* spp.; *Palaquium* spp.; *Sindora* spp.

# **Anatomical identification of charcoal and briquettes - developments in the international charcoal trade and the increasing use of substitutes from NTFPs**

Volker Haag<sup>1</sup>, Valentina Zemke<sup>1</sup>, Simon Zabler<sup>2</sup>, Stephanie Helmling<sup>1</sup>, Tim L.  
Lewandrowski<sup>1</sup>, Andrea Olbrich<sup>1</sup>, Johannes Zahnen<sup>3</sup>, Peter Hirschberger<sup>4</sup>

(1 Thünen Institute of Wood Research, Hamburg, Germany; 2 Fraunhofer Development Center X-ray Technology EZRT, Fürth, Germany; 3 WWF, World Wide Fund For Nature, Germany; 4 4con forestconsulting, Bernau a. Chiemsee, Germany)

**Abstract:** The Thünen Institute of Wood Research has been routinely conducting wood species identifications for charcoal and briquettes since 2016. These anatomical examinations are used to determine if the product declarations included on a sample's packaging are correct. They also provide additional information on the origin of certain taxa (especially tropical vs. non-tropical). The studies, often carried out in cooperation with environmental protection organizations such as the WWF, support product producers and traders with quality assurance and contribute to consumer protection. Furthermore, they generate important data for understanding the trade flows of the international charcoal business. In context of the studies, it was also observed that an increasing number of charcoal substitutes made from more environmentally compatible raw and residual materials such as "non-timber forest products" (NTFPs) are steadily becoming established on the charcoal market. In cooperation with the Fraunhofer Development Center X-Ray Technology EZRT, anatomical studies are currently being carried out to characterize the structure of important NTFPs, such as coconut shells and olive or mango kernels, in order to describe the anatomical structure and be able to reliably identify the organic material in practical applications for market analyses.

**Keywords:** Anthracology; wood anatomy; NTFPs; Ecology;  $\mu$ -CT; wood identification

# **Anatomical structure of benuang (*Octomeles sumatrana*) wood and its fiber quality assessment for pulp and paper manufacturing**

Sari Delviana Marbun<sup>1</sup>, Imam Wahyudi<sup>2,\*</sup>, Jajang Suryana<sup>2</sup>, Deded Sarip Nawawi<sup>2</sup>

(1 Forest Products Science and Technology Study Program, IPB University, Bogor 16680, Indonesia; 2 Faculty of Forestry and Environment, IPB University, Bogor 16680, Indonesia; \*Corresponding author: imyudarw16@yahoo.com)

**Abstract:** Since the last two decades, timber industries in Indonesia, which play an important role in the Indonesian economy, have been replaced by the pulp and paper industry. Promoting new wood resources, i.e. benuang (*Octomeles sumatrana*) a member of lesser-used wood species, is one way to address the wood demand challenges faced by pulp and paper industry. Therefore, the aim of this study was to investigate the anatomical structure of this wood and to evaluate the suitability of its fibers as raw material for pulp and paper manufacturing. Anatomical structure was observed macro- and microscopically following standard procedures, while fiber quality class was analyzed following the Rachman and Siagian's method. Result showed that vessels mostly solitary, sometimes in radial multiples of 2, diffuse porous, tangential diameter of solitary vessels 142–232  $\mu\text{m}$ , frequency 2–7 per  $\text{mm}^2$ , perforations simple, intervessel pits alternate, while vessel-ray pits simple. The rays 1–3 to 1–4-seriate, sometimes with dark-brown contents, and average height of rays 738.10  $\mu\text{m}$ . Axial parenchyma vasicentric to weakly aliform. Crystal sand sometimes found in rays and axial parenchyma cells, but silica grains absent. Fibers non-septate, with average fiber length, fiber diameter, lumen diameter, and fiber wall thickness are 1763.80  $\mu\text{m}$ , 38.47  $\mu\text{m}$ , 33.32  $\mu\text{m}$ , 2.57  $\mu\text{m}$ , respectively. Based on fiber quality assessment, benuang wood has great potential to be utilized as raw material for pulp and paper manufacturing.

**Keywords:** Anatomical structure; benuang; fiber quality class; *Octomeles sumatrana*; pulp and paper.

# Wood Species Identification by Using Two-Electrode Capacitive-Based Spectroscopy

Harisma Nugraha<sup>1\*</sup>, Rohmadi Rohmadi<sup>1</sup>, Mahfudz Al-Huda<sup>1,2</sup>, Citra Oktapiani<sup>3</sup>, Annisa Nur Fitria<sup>1</sup>, Panji Nursetia Darma<sup>1</sup>, Marlin Ramadhan Baidillah<sup>1</sup>, Warsito Purwo Taruno<sup>1</sup>, Ratih Damayanti<sup>3</sup>, G Pari<sup>3</sup>, Djarwanto<sup>3</sup>, Lina Karlinasari<sup>4</sup>, LM Dewi<sup>3</sup>, Krisdianto<sup>3</sup>, Yulianti Bramasto<sup>5</sup>, Aam Aminah<sup>5</sup>, Eka Novriyanti<sup>6</sup>, IZ Siregar<sup>4</sup>, RGH Rahmanto<sup>3</sup>, ER Satiti<sup>3</sup>, Andianto<sup>3</sup>, S.atria Astana<sup>7</sup>, Indah Bangsawan<sup>7</sup>, Mohamad Iqbal<sup>7</sup>, Michael C. Wiemann<sup>8</sup>, John C. Hermanson<sup>9</sup>

(<sup>1</sup>Center for Innovation and Products Development, C-Tech Labs Edwar Technology, 15235, Jalan Jalur Sutera Kav. Spektra Blok 23 BC No. 10-12, Alam Sutera, Tangerang, 15320, Banten, Indonesia; <sup>2</sup>Research Organization for Assessment and Application of Technology, National Research and Innovation Agency, Technology 2 Building 2nd fl., PUSPIPTEK, Tangerang Selatan, BANTEN; <sup>3</sup>Forest Products Research and Development Center, Jl. Gunung Batu No. 5, Bogor, 16610, West Java, Indonesia; <sup>4</sup>Forestry Faculty, IPB University, Jl. Lingkar Akademik Kampus IPB, Dramaga, Bogor, 16680, West Java, Indonesia <sup>5</sup>Research and Development Center for Forest Plant Seed Technology, Jl. Pakuan Cihuleut, Tegallega, Bogor, 16129, West Java, Indonesia; <sup>6</sup>Research and Development Center for Forest Plant Fiber Technology, Jl. Raya Riau-Bangkinang. Kuok 28294, Riau Province, Indonesia; <sup>7</sup>Center for Research and Development on Social, Economy, Policy and Climate Change, Jl Gunung Batu No. 5, Bogor, 16610, West Java, Indonesia; <sup>8</sup>USDA Forest Service, Center for Wood Anatomy Research Forest Products Laboratory, Madison, USA; <sup>9</sup>University of Washington/University of Wisconsin–Madison, USA; \*Corresponding author: nugraha.harism@gmail.com)

## Abstract

The wood samples from some species were studied by using capacitive-based spectroscopy. The purposes of this study were to characterize and to identify the wood species based on the measured capacitive signals. Experiments were performed using two-electrode capacitive sensor with the frequencies ranging from 250 kHz to 60 MHz on 5 wood species with a dimensions of 4 cm x 1 cm x 10 cm. The wood samples studied were *Canarium sp.*, *Dracontomelon dao*, *Endospermum sp.*, *Koordersiodendron pinnatum* and *Pterygota sp.* The results showed that the signal characteristics were different corresponding to their wood species. In frequencies below and above 5 MHz, the signal characteristics were similar and different respectively. It was believed that the signals above 5 MHz have unique information correlating with the physical and chemical structures of wood. Moreover, the wood species could be identified with the accuracy of 91% based on the signal information and the k-nearest neighbors algorithm for machine learning modeling.

**Keywords:** capacitive-based spectroscopy, wood species identification, machine learning

# Spatial distribution of chemical components in the phellem of *Cerasus jamasakura* (Siebold ex Koidz.) H. Ohba

H. Saito<sup>1,\*</sup>, T. Nakai<sup>1</sup>, H. Aiso<sup>2</sup>, K. Toba<sup>1,3</sup>, T. Kanbayashi<sup>3</sup>, H. Abe<sup>1,3</sup>

(1 Mie University, Tsu, Mie, Japan; 2 Shizuoka Professional University of Agriculture; 3 Forestry and Forest Products Research Institute; \*Corresponding author: 520m107@m.mie-u.ac.jp)

Bark is an important woody bioresource that has been utilized as a material for forest products. In Japan, the phellem of *Cerasus jamasakura* (Siebold ex Koidz.) H. Ohba has traditionally been used to connect wood pieces in various articles such as tableware, lunch boxes, tea canisters, etc. Suberin, lignin, and polysaccharides are the major chemical components of the phellem of *C. jamasakura*. Among these substances, suberin, a complex biopolymer, is the most characteristic chemical component of the phellem in bark. However, there have been few studies examining the mechanical role of this waxy substance in the phellem. Our previous research on the relationship between the anatomical and mechanical properties of the phellem of *C. jamasakura* showed 200µm long fibers oriented to the tangential direction of the stem, and that the phellem has the property of extending in the same direction. Furthermore, from the results of a tensile test of the phellem treated with successive removals of chemical components, it was found that each component has a different effect on the mechanical properties of the phellem. Based on these results, we have focused on obtaining information on the spatial distribution of chemical components in the phellem in this study.

Sample pieces of phellem (7 mm (L) × 30 mm (T) × 0.3~0.6 mm (R)) were taken from branches of *C. jamasakura*. These were treated for the successive removal of suberin, lignin, and hemicellulose. After the treatments, a glass knife was used to cut 2-µm-thick radial sections were cut from the samples embedded in epoxy resin. The sections were stained with phloroglucinol, safranin, and toluidine blue, and observed by fluorescence and light microscopy. To confirm the remaining chemical composition after the removals, the treated samples were analyzed using Fourier-transform infrared spectroscopy.

With microscopic observation, lignin autofluorescence was observed in the cell corners and the middle lamellas of fibers of the phellem, which is similar to what can be observed with xylem fibers. On the other hand, phloroglucinol fluorescence indicating the existing of suberin was observed in the cell walls, except for the cell corners and middle lamella.

# Blue intensity as climate proxy: Application on black spruce in the eastern Canadian taiga

Feng Wang<sup>1</sup>, Dominique Arseneault<sup>1</sup>, Étienne Boucher<sup>2</sup>, Shulong Yu<sup>3</sup>

(1 Département de Biologie, Chimie et Géographie, Centre d'Études Nordiques, Université du Québec à Rimouski; Rimouski, G5L 3A1, Canada; 2 Département de Géoscience, GEOTOP, and Centre d'Études Nordiques, Université du Québec à Montréal, Montréal, H3A 0B9, Canada; 3 Key Laboratory of Tree-ring Ecology of Uigur Autonomous Region, Key Laboratory of Tree-ring Physical and Chemical Research, Institute of Desert Meteorology, China Meteorological Administration, Urumqi, 830002, China)

**Abstract:** Tree-ring traits, such as ring width, latewood density, and cellulose stable isotopes, are important proxies to reconstruct past climate change over centuries to millennia. Although maximum latewood density of high-latitude conifers is the most temperature sensitive tree-ring traits, its use has been hampered by the high costs of X-ray densitometric facilities. Over the last two decades, the relatively cheap optical-based blue intensity (BI) technique has been progressively recognized as a promising surrogate to tree-ring density. However, the application of the BI technique is limited due to its sensitivity to various color biases on wood surface, such as the sapwood-heartwood color difference as well as various wood stains. Here, we investigated whether BI measurements from two types of black spruce (*Picea mariana*) samples (unstained living trees and iron-stained subfossil wood) from the eastern Canadian taiga are reliable proxies for long-term summer temperature reconstructions. Two BI measurements, i.e., the latewood BI values and delta BI (DBI, BI measurements corrected using earlywood BI values), were compared to the conventional X-ray maximum latewood density (MXD). We found that LBI and DBI of living black spruce trees highly resembled MXD in recording summer temperature signal during the 20<sup>th</sup> century, although the signal was slightly weaker in LBI, likely due to the sensitivity of LBI to color biases and measurement resolution. These potential color biases were significantly amplified when LBI were measured from stained subfossil wood, yielding a bias of about +4 °C in a ~360-yr LBI-based temperature reconstruction compared to the same reconstruction based on MXD data. DBI was surprisingly not affected by the iron-staining issue and compared well with MXD across the frequency spectrum. Our results thus highlight the high potential of DBI as a climate proxy for reconstructing long-term summer temperatures in the eastern Canadian taiga.



# Hygroscopic swelling of moso bamboo cells

Qi Chen<sup>1</sup>

(1 College of Forestry, Sichuan Agricultural University, Chengdu, Sichuan, 611130, PR China)

**Abstract:** Bamboo is a natural cellulosic material which is strongly reactive to water. Its hygroscopic behavior affects almost all other physical and mechanical properties of bamboo. This study investigated the hygroscopic swelling of moso bamboo (*Phyllostachys edulis*) cells in response to changes in environmental humidity using a confocal laser scanning microscope. The swelling strains of fiber, vessel and parenchyma cells were obtained and compared. The interactions between adjacent cells were also analyzed. The results demonstrated that the swelling strain of cell wall increased with the increase of relative humidity (RH), and was independent of its location and orientation, but dependent on the cell type. The absolute swelling of cell wall was positively influenced by the cell wall thickness and was about 56 nm for every percentage of moisture content (MC) increase for fiber cells, 44 nm for parenchyma cells and 11 nm for vessel cells. On the other hand, due to constraint of its adjacent fibers, the relative swelling of fiber cell wall was 0.53% for every percentage of MC increase. This value was almost of half of 1.1% relative swelling for parenchyma and vessel cells. The deformation and movement of cell lumens of parenchyma and vessel cells were influenced by their geometric positions in relation to fiber bundles. The cell lumen increased with RH when it was parallel to the fibers, and decreased when it was perpendicular to the fibers. In contrast to wood, there was a lack of differential swelling in bamboo in the tangential and radial directions, due to the similar microfibril angle in both directions, the circular cellular shape and the random embedment of vascular bundles. While the numerical results found in this study may vary depending on species and age of bamboo, the general swelling mechanisms and relationships should be applicable to all bamboo fibers.

**Keywords:** Bamboo; Hygroscopic swelling; Cell wall; Cell lumen; Moisture adsorption; Dimensional stability

# Performance of low molecular weight of phenol formaldehyde-impregnated woods on dimensional stability and durability against termites

Sarah Augustina<sup>1</sup>, Imam Wahyudi<sup>2,\*</sup>, I Wayan Darmawan<sup>2</sup>, Jamaludin Malik<sup>3</sup>

(1 Forest Products Science and Technology Study Program, IPB University, Bogor 16680; 2 Department of Forest Products, Faculty of Forestry & Environment, IPB University, Bogor 16680; 3 Forest Products Research and Development Center, Bogor 16610; \*Corresponding author: imyudarw16@yahoo.com)

**Abstract:** Performance of low molecular weight of phenol formaldehyde (LmwPF) as impregnating agent on dimensional stability and durability of three lesser-used wood species grown in North Kalimantan Province namely nyatoh (*Palaquium* spp.), sepetir (*Sindora* spp.) and pisang putih (*Mezzettia* spp.) has been studied and analyzed. Impregnation process was initiated by soaking the samples in LmwPF solutions of 7, 8, 9, 10 and 11% concentration (w/w), continued by vacuuming at -98 kPa for 15 minutes, followed by applying 350 kPa of pressure for 4 hours, then immersing in each impregnating solution at 80 °C for 3 hours. Results showed that dimensional stability and durability of LmwPF-impregnated wood had significantly improved compared to untreated (control) wood. Sepetir wood impregnated by LmwPF had a higher WPG value, which resulted in better improvement on dimensional stability and durability against termites than nyatoh- and pisang putih-impregnated wood. LmwPF-impregnated woods tended to increase in durability class as concentration increased, becoming durable class II for 7% concentration and durable class I for 11% concentration.

**Keyword:** dimensional stability; durability against termites; impregnation; lesser-used wood species; low molecular weight of phenol formaldehyde.